1958

A study of adsorption processes occurring at an ideally polarizable electrode-solution interphase

Donald Andrew Hickson
Iowa State College

A STUDY OF ADSORPTION PROCESSES OCCURRING AT AN IDEALLY POLARIZABLE ELECTRODE-SOLUTION INTERPHASE

by

Donald Andrew Hickson

A Dissertation Submitted to the
Graduate Faculty in Partial Fulfillment of
The Requirements for the Degree of
DOCTOR OF PHILOSOPHY

Major Subject: Physical Chemistry

Approved:

Signature was redacted for privacy.

In Charge of Major Work

Signature was redacted for privacy.

Head of Major Department

Signature was redacted for privacy.

Dean of Graduate College

Iowa State College
Ames, Iowa
1958

TABLE OF CONTENTS

INTRODUCTION

Recent advances in the field of electrode kinetics have served to illustrate the prominent role played by adsorption in influencing the character of electrode processes. The addition of very small amounts of capillary active materials to the bulk solution can produce a pronounced change in the properties of the electrode-solution interphase which subsequently influences the character of the overall electrode reaction. The use of maximum suppressors to alter the shape of polarographic waves in polarography, the pronounced effect of proprietary brighteners upon the nature of metallic deposits in electroplating, and the inhibition of galvanic action by organic films in corrosion control are common examples of this phenomenon. Until quite recently very few electrochemical investigations have seriously considered the pronounced effects of surface active non-electrolytes upon the behavior of electrode reactions as anything but unfortunate. However, it is now becoming apparent that the profound alteration of the properties of the electrode-solution interphase following the adsorption of capillary active materials may be a powerful tool for the investigation of adsorption from solution upon adsorbents of very small surface area and for inferring adsorption isotherms at solid-solution interphases.

The application of this phenomenon to the investigation of adsorption at metal-solution interphases is particularly promising since the usual methods of investigating adsorption on these adsorbents have been notoriously unsuccessful. The possibility of developing a new method of investigating adsorption in these instances is particularly intriguing and it is with this subject that the present investigation is concerned.

LITERATURE SURVEY

The Inference of Adsorption from Solution by Electrochemical Measurements

Adsorption data can be obtained from either electrokinetic or electrocapillary measurements. The former technique involves measurements in the presence of a sol with a non-polarizable electrode or an electrode which behaves reversibly to one of the components of the system. An infinitesmal variation of the electrode potential results in the transfer of charge across the electrode interphase during the re-establishment of equilibrium and, consequently, the equilibrium potential is determined by the concentration of the ion to which the electrode acts reversibly. Adsorption density vs. log concentration of potential determining ion curves can be used within limitations as an index of the adsorption of organic adsorbates by the sol particles (1). Unfortunately, the inference of adsorption from electrokinetic data is complicated by ignorance of the total surface area of the sol particles and by uncertainties regarding the potential of zero charge as well as the tenuous assumption of the identification of surface excesses with surface concentrations. Nevertheless, an attempt has been recently made to infer the adsorption of acetone molecules at silver iodide interphases from electrokinetic data (2).

Electrocapillary measurements, however, deal with measurements made at an ideally polarized electrode. The latter class of electrodes is not too familiar to chemists and requires some elaboration. An ideally polarized electrode is defined to be an electrode system in which at equilibrium the concentration of all charged components remains finite in one phase only (3), i.e., no Faradaic reaction occurs on polarization. This definition implies that the potential of such an electrode can be varied at will without the passage of charge across the interphase. Thus, at equilibrium, charges may approach and recede from the interphase but do not cross it. Such an electrode is blocking to a direct current flow and experimentally behaves like a condenser of large specific capacity. In actual practice such conditions cannot be fully realized. However, a close approximation to ideality is possible within the hydrogen over-voltage region of many metals. Due to the irreversible nature of the hydrogen discharge reaction which permits the passage of a Faradaic current, equilibrium at the metal interphase with the ionic charges in the solution occurs more rapidly than the attainment of overall equilibrium for the depolarizing reactions. Consequently, within the hydrogen overvoltage region, the electrode behaves as if it were ideally polarized.

Generally speaking, almost all investigations of electrocapillary phenomena are conducted at mercury-solution interphases. This is due mainly to the fact that mercury

electrodes in inert solutions of electrolytes may be polarized as much as one volt with negligible hydrogen evolution. This offers a wide range of potentials over which ideally polarizable behavior can be approximated. In addition, mercury can be easily purified and forms strain-free surfaces of easily measured area and interfacial tension. These latter properties make mercury a particularly attractive choice for adsorbent in this and most electrocapillary investigations.

If the interfacial tension of an ideally polarizable electrode immersed in a solution of inert electrolyte is measured as a function of the polarizing potential, an electrocapillary curve is obtained. This curve which is roughly parabolic in shape increases with increasing cathodic polarization relative to some reference electrode until a maximum value for the interfacial tension is obtained and, thereafter, continuously decreases with further polarization. The potential at which the maximum interfacial tension occurs is called the potential of the electrocapillary maximum. The thermodynamic relationship between the interfacial tension, polarizing potential, and solution composition is given by the Gibbs adsorption equation modified to include the electrical work:

$$d\gamma = -\sigma\, dE - RT \sum_i \Gamma_i\, d\ln a_i \qquad (1)$$

where γ is the interfacial tension, E is the polarizing

potential, a_i the activity of component i, and σ is the surface charge density. Consequently, it is seen that σ is equal to the slope of the electrocapillary curve at constant composition. At the potential of the electrocapillary maximum the slope is zero. This potential is of particular significance for it represents the point of zero change on the electrode and, since it is characteristic of the particular electrode-solution system, furnishes a convenient reference potential. As the potential recedes from the electrocapillary maximum, the surface charge density increases. The mutual electrostatic repulsion of like charges in the interphase results in a lowering of the interfacial free energy which is manifested as a depression of the interfacial tension.

If a capillary-active material is added to the solution, the electrocapillary curve will become truncated in the region of the electrocapillary maximum due to a decrease in the interfacial tension resulting from the adsorption of the material at the interphase. Consequently, adsorption isotherms may be inferred by measuring the decrease in interfacial tension as a function of adsorbate activity at constant polarization. The surface excess of the adsorbate is thus

$$\Gamma_i = - 1/RT(\partial \gamma / \partial \ln a_i)_E \quad . \qquad (2)$$

Information regarding the surface charge density at any point of the electrocapillary curve, amount of adsorbed material, variation of amount of other constituents present at the interphase, orientation of adsorbed species, and heats and entropies of adsorption at any position of the electrocapillary curve (4) can be derived from such measurements. Unfortunately, the direct measurement of interfacial tensions of metals has proven to be practical at very few metal-solution interfaces, most measurements being conducted on mercury or gallium-solution interfaces. In even these instances the measurements are extremely difficult to make. Nevertheless, there has recently been a renewed interest in such adsorption measurements.

Melik-Gaikazyan (18) has reported electrocapillary data for the system mercury-potassium chloride-n-butyl alcohol for several concentrations of the alcohol adsorbate. Blomgren and Bockris (5) investigated the adsorption of a series of aromatic amines in hydrochloric acid solution on mercury and report that the orientation of the adsorbed species was in every instance parallel to the surface. Los and Tompkins (6) investigated the adsorption of methylene blue at positively charged surfaces by a modification of the usual techniques. Interfacial tension depression curves for a number of organic materials were obtained many years ago by Gouy (9) in conjunction with his extensive investigation of

electrocapillary phenomena. However, Butler (10, 11) has given the most comprehensive analysis of this method to date. Despite the enormous experimental difficulties associated with obtaining sensitive interfacial tension measurements, an active interest in this field still persists.

A quantity of comparable thermodynamic significance to the interfacial tension can be obtained by differentiating the slope of the electrocapillary curve once with respect to the polarizing potential at constant composition:

$$\partial \gamma^2 \; / \partial \, E^2 = - \frac{\partial \sigma}{\partial E} = - C_{dl} \quad . \qquad (3)$$

The quantity on the right is called the "differential double layer capacity". The term "double-layer" refers to the electrical double layer which is the array of charges and dipoles which exists at all charged interphases in a solution of inert electrolyte. Many comprehensive reviews of the structure and properties of the electrical double layer are available (3, 12, 13, 41) so a complete discussion of the subject would be superfluous. At the mercury solution interface, however, it is generally conceded that the electrical double layer consists really of three distinct layers of charge, the layer of charges in the surface of the metal, the compact layer of charge of opposite sign designated by the term "Helmholtz plane" adjacent to the metallic phase in the solution, and a diffuse layer of charge extending into the

bulk of the solution of sign opposite to that of the Helmholz plane. A distinction is sometimes made between the inner Helmholtz plane which is the plane of charge formed by the locus of centers of adsorbed dehydrated ions at the electrode interphase and the outer Helmholtz plane which refers to the analogous situation for hydrated non-adsorbed ions (3). The significant observation is made that the thickness of the electrical double layer is of molecular dimensions which means that the term "plane of charge" is fully justified since the radius of curvature of the interphase is usually much greater than the thickness of the double layer and, also, that the specific capacity of a condenser formed by these planes will have an extremely large value of the order of 10-100 microfarads per square centimeter of surface.

Experimentally, the electrical double layer behaves like two parallel plate capacitors in series, one representing the compact double layer and the other the diffuse portion of the double layer. Under certain conditions, namely in the presence of excess inert electrolyte, the capacity of the diffuse region becomes very large compared to that of the compact region. Since the two capacities are in series, the effective capacity is attributable to the compact region of the double layer adjacent to the electrode interface. The great utility of the differential double layer capacity is due to the fact that it is an electrical property subject

to precise measurement. Indeed, electrocapillary curves obtained by double integration of double layer capacity data have proven to be more precise than those obtained by direct measurement of the interfacial tension (3).

Since the differential double layer capacity is related thermodynamically to the interfacial tension, inferences about equilibrium adsorption processes which can be made from interfacial tension depression data can also be inferred from differential capacity data. Some thirty years ago Frumkin (14) published an extensive theoretical treatment of the effects of adsorbable materials which can be investigated by means of differential capacity measurements. Essential features of this treatment are the assumptions of a linear relation between surface coverage and double layer capacity and that the surface coverage can be described by a generalized localized Langmuir adsorption isotherm. Recently, Hansen, Minturn and Hickson (15, 16) and Minturn (17) have extended this treatment to establish the dependence of the differential capacity on polarization and adsorbate activity. Information regarding the orientation of adsorbed species and forces responsible for the adsorption of a series of simple organic adsorbates was obtained. Melik-Gaikazyan (18) has used this procedure to study multimolecular adsorption of n-octyl alcohol on mercury. Recently Laitenen and Mosier (19) have reported an investigation of the adsorption of several organic compounds

also at the mercury-solution interphase. However, these measurements were conducted at the potential of the electrocapillary maximum only. It was reported that in all cases investigated, adsorption data could be interpreted in terms of a simple Langmuir adsorption isotherm. Loveland and Elving (20 through 25) have investigated the effect of a series of simple aliphatic alcohols adsorbed at the mercury solution interphase upon the electrocapillary, surface charge density and differential double layer capacity versus polarization curves by a novel electronic approach. Unfortunately, these authors were unable to represent the results of their investigations by any of the usual adsorption isotherms. Breyer and Hacobian (26) have recently investigated the adsorption of several organic compounds at the mercury-solution interphase by superimposing an a.c. potential of small amplitude upon the d.c. polarization of the electrode and measuring the a.c. current flowing in the circuit. The term "tensammetric wave" was coined by these investigators to refer to the pronounced capacity peaks associated with the adsorption-desorption processes occurring at high field strengths within the double layer at the interphase. These peaks are attributed to a process of dielectric displacement of adsorbate molecules by the more polar solvent molecules which results in an overall decrease in the free energy of the system (26).

The differential double layer capacity possesses an additional advantage for the investigation of adsorption

processes in that it may also be a function of the frequency. This circumstance has been used to investigate the kinetics of adsorption from solution using capacity measurements. Recently Frumkin and Melik-Gaikazyan (27) have proposed a treatment for the inference of the rate controlling mechanism of the adsorption process based upon the observed frequency dispersion of the capacity in the potential regions of the adsorption peaks. Contrary to the observation made by Grahame (28) that the differential double layer capacity exhibits no dispersion with frequency in the presence of inert electrolytes, the differential capacity was observed to display pronounced frequency effects in the neighborhood of the adsorption peaks. Frumkin and Melik-Gaikazyan attributed this dispersion effect to the occurrence of an adsorption process proceeding at a finite rate at the interphase and showed that a supplementary capacitive current arises in the presence of such a process which may be used to characterize the rate controlling mechanism. Two possible mechanisms were proposed: diffusion control and adsorption rate control. Criteria which were diagnostic of the process occurring which was rate controlling were derived. An extensive investigation of the kinetics of adsorption of several aliphatic alcohols on mercury surfaces by Melik-Gaikazyan (18) indicated that diffusion was probably responsible for the rate controlling mechanism in this instance. The treatment of Frumkin was extended by Lorentz

(29) and Lorentz and Mockels (30) to include the case of simultaneous diffusion and adsorption rate control and the case of adsorption followed by a two dimensional association of the adsorbate molecules in the interphase. The results of Melik-Gaikazyan were apparently confirmed for the case of adsorption of simple alcohols. Adsorption followed by two dimensional association of adsorbate molecules was reported to be the rate controlling mechanism for the adsorption of several fatty acids investigated. Delahay and Trachenberg (31, 32) have recently presented a theoretical analysis of adsorption processes occurring at plane, spherical, and expanding surfaces which are diffusion controlled and Delahay and Berzins (33) have also presented an alternate treatment for the case of simultaneous diffusion and rate control. Los and Tompkins (6) have investigated the kinetics of adsorption of methylene blue at the mercury solution interphase by electrocapillary methods. The controlling mechanism was found to be an exchange of methylene blue ions with ions adsorbed on the surface followed by a two dimensional dimerization.

Differential double layer capacity measurements are thus seen to offer a versatile tool for the study of adsorption from solution on adsorbents of small surface area. Virtually all of the information one could desire to know about an adsorption process can be obtained by investigating the

dependence of the differential double layer capacity as a function of the variables composition, polarizing potential, frequency, and temperature. Unfortunately, a complete investigation of all the variables associated with a given adsorption process would be a very arduous task by conventional methods for measuring the differential double layer capacity. Consequently, if the full potentialities of the technique are to be exploited, a fast precise experimental technique capable of measuring the double layer capacities over a wide range of these variables is a necessity.

Electronic Methods for Measuring the Impedance of the Electrical Double Layer

Since in practice the electrical double layer behaves like a condenser of large specific capacity shunted by a large leakage resistance, double layer capacities can be measured by any of the techniques employed in electrical impedance measurements. The procedure most frequently chosen is to insert a cell containing a polarizable electrode into one arm of a conventional a.c. impedance bridge. After impressing a known d.c. potential across the electrode-solution interface from an external potentiometer, the impedance of the cell is balanced against a known impedance in the measuring arm of the bridge. The measurements are then repeated at other values of the d.c. polarizing potential to construct

point by point a differential capacity versus polarizing potential curve. Grahame (34, 35) has devised a very elegant bridge arrangement for measuring the impedance of the electrical double layer which was used in the investigation of the structure and properties of the electrical double layer. Melik-Gaikazyan (18) has also employed an elaborate a.c. bridge capable of measuring capacities at frequencies from 0 to 200,000 cycles which was used in the study of the kinetics of adsorption of alcohols at mercury-solution interfaces. However, a.c. bridge measurements are operationally laborious and time consuming to make but yield the most accurate results.

If an investigation of the effect of other variables such as solution composition, electrode composition, frequency, and temperature upon the properties of the electrical double layer is to be conducted, the bridge technique becomes very burdensome and tedious indeed. Consequently, a method of recording the necessary double layer impedance data which is more rapid and less arduous than the classical bridge procedure is highly desirable even at the sacrifice of some precision.

Several electronic techniques have been reported in the literature for the measurement of differential double layer capacities which do not involve a.c. impedance bridges. In general these techniques fall into one of three categories:

the method of charging curves, oscillographic polarography, and d.c. polarization with superimposed a.c. potential. Several of these methods were considered as possibly adaptable to automatic recording of capacity data.

In the method of charging curves a constant current impulse is impressed across the interface and the rate of change of the potential with time is measured. From the initial slope of the potential-time curve the capacity of the electrical double layer can be obtained from the following expression:

$$C = \frac{i}{(dE/dt)_{t=o}} \quad .$$

From a.c. bridge measurements it is known that the capacity is not constant with changing polarization and, consequently, the initial slope of the charging curve is specified for the calculation of the capacity of the electrode interface.

The capacity at the mercury-aqueous sulfuric acid interface was investigated by Bowden and Grew (36, 37) by this technique and recently at several other metal-solution interfaces by Hackerman and Brodd (38). Hansen and Clampitt (39) have used this technique to infer the equilibrium adsorption of several organic compounds from acid solution by copper and silver electrodes. Difficulties associated with the determination of the initial slope make this procedure a poor choice for possible automatic recording of capacity data.

In oscilloscopic polarography a periodically varying potential sweep of known form is impressed across a cell containing an ideally polarizable electrode immersed in a solution of inert electrolyte. In the absence of any oxidizable or reducible material, the current passed by the cell is due to the alternate charging and discharging of the electrical double layer. This current can be made to generate a potential across a standard resistance which is proportional to the magnitude of the differential double layer capacity. Capacity versus polarizing potential curves can then be displayed directly upon the screen of a cathode-ray oscilloscope. No attempt will be made to review the voluminous literature on this subject as many excellent reviews are available (40 through 44). However, several papers relating directly to the measurement of double layer impedances by means of this technique have appeared in the literature and should be mentioned.

Sevcik (45) utilized a triangular potential sweep to investigate polarographic phenomena and subsequently realized the possibility of suing the oscilloscopic polarograph to investigate electrocapillary phenomena as well. Several simple experiments determining the capacity of mercury interfaces in contact with solutions of inert electrolytes were made. However, these measurements were of an exploratory character and were made primarily to demonstrate the

versatility of the method and were not pursued further.

Recently the square-wave polarograph was applied to the study of the adsorption of organic adsorbates at the mercury-solution interface. The square-wave polarograph was originally designed to permit the resolution of the total polarographic current into its capacitive and Faradaic components. This was accomplished by polarizing a mercury-solution interface with a square-wave signal of sufficiently long period as compared to the time constant of the interfacial impedance. The capacitive component of the total current rapidly decays to zero during the early portion of the polarizing cycle leaving the Faradaic component for measurement at the end of the cycle. However, by measuring the current at the beginning of each polarizing period, Barker and Gardner (46) were able to determine the capacity of the electrical double layer. The effect on the capacity due to the adsorption of n-octyl alcohol at the mercury-solution interface was investigated with particular emphasis on the behavior of the adsorption-desorption peaks with varying adsorbate concentration.

Perhaps the most comprehensive study of the application of the cathode-ray oscilloscope to the investigation of electrocapillary phenomena is that of Loveland and Elving (20 through 25). In a series of papers, these authors describe electronic circuits which permit the direct display

on the screen of a cathode-ray oscilloscope of differential double layer capacity, surface charge density and interfacial tension versus polarization curves. The basic measurement is similar to that made by Sevcik. The cell containing a dropping mercury electrode which serves as the polarizable electrode is swept with an alternating triangular voltage sweep. The output potential developed across a standard resistance in series with the cell is proportional to the differential double layer capacity and can be displayed directly upon the cathode-ray oscilloscope screen to obtain a capacity-polarization trace, integrated electronically once to obtain a surface charge density-polarization trace, or integrated electronically twice to display an electrocapillary trace. This apparatus was used in an extensive investigation of the adsorption of a series of aliphatic alcohols at the mercury interface which would have been extremely difficult and tedious to duplicate by the usual bridge techniques.

Although the actual recording of impedance data is very rapid by this technique, the corresponding loss in accuracy and increase in time due to the translation of photographic traces into numerical data for the purposes of data interpretation may prove detrimental for some applications. In addition it was found that reproducible and undistorted traces could be obtained only at very small frequencies which is an additional limitation to the method.

Breyer and Gutmann (47) have devised an electronic method for measuring the impedance of the electrical double layer which is based on the principle of d.c. polarization of the electrode interface with a superimposed a.c. sinusoidal voltage of small amplitude. The d.c. polarization essentially forms the electrical double layer at the interface while the measurement of its impedance is accomplished by the a.c. component. This measurement closely resembles the procedure used in the a.c. impedance bridge methods but has the additional feature of possible automatic recording of the circuit impedance. The a.c. component of the total current flowing in the circuit which is proportional to the impedance can be separated from any d.c. component by means of a capacitive by-pass. The magnitude of the current can then be measured by monitoring the potential developed across an known standard resistance with a sensitive vacuum tube voltmeter. This signal could, however, be used to drive a recording devise.

Breyer and Hacobian (26) studied the effect of frequency and adsorbate concentration on the adsorption-desorption peaks at the mercury-solution interface of several organic materials and coined the term "tensammetry" to describe the study of electrode processes of this character. Doss and Kalyanasundarum (48) have subsequently employed this technique to infer the adsorption of several organic materials which are commonly used as maximum suppressors in polarography.

Randles (49) has described an apparatus which measures the phase relationship between the current and voltage vectors which can be utilized to construct a vector impedance diagram from which differential double layer capacities can be calculated. However, to the author's knowledge no adsorption experiments have ever been performed by this technique.

Because of the many experimental variables associated with a complete investigation of adsorption processes occurring at electrode interfaces, a fully automatic and rapid technique for measuring the differential double layer capacity as a function of these variables is very desirable. The procedure selected should be sufficiently versatile in this respect and in addition should avoid undue loss in accuracy in the measurement of the impedance of the double layer compared to the usual a.c. bridge methods. The results of the measurements should be immediately and conveniently displayed so that experimental failures can be rapidly detected and corrected and should be in such a form that translation to numerical results for the purposes of data interpretation is easily facilitated. In this respect it is desirable to have the response of the detecting instrument linear in the variable measured to simplify the interpretation of the data. An additional desirable condition not easily accomplished in impedance measurements is the measurement of the impedance vector rather than its magnitude or phase relations. It is

in this respect that a.c. bridge measurements have a considerable advantage.

It was apparent that none of the methods reported in the literature for measuring double layer impedances fulfilled all of these criteria but the oscilloscopic technique of Loveland and Elving and the a.c. procedure of Breyer and Gutmann appeared to offer the most promise as bases for an automatic recording instrument. Subsequently, a novel method for measuring capacities was developed in this work which embodies several of the principles used in these two techniques.

OBJECTIVES

The objectives of the present investigation were fourfold:

1. To devise an experimental technique for the rapid measurement of differential double layer capacities over a sufficiently wide range of experimental operating conditions without undue loss in accuracy.

2. To demonstrate the utility of the method by conducting an investigation of the effect of frequency and temperature on the properties of the compact region of the electrical double layer.

3. To apply this method in an investigation of the equilibrium adsorption of certain organic adsorbates at electrode solution interfaces in the absence of electrochemical reactions.

4. To investigate the kinetics of adsorption of these adsorbates at electrode-solution interfaces in the absence of electrochemical reactions.

EXPERIMENTAL

Automatic Impedance Recording Instrument

Theory of the measurement

In studying and interpreting electrical double layer impedances at ideally polarizable electrode interfaces by a.c. bridge methods, the principle of equivalent circuits first employed by Kruger (50) has proven to be of great value. In the usual bridge methods for measuring interfacial impedances, differential double layer capacities and resistances are obtained in terms of a known impedance vector. Resolution of this impedance vector into its component parts is accomplished by devising an electrical analog circuit which is supposed to represent the electrical properties of the electrode-solution interphase. Usually these analogs are chosen such that the capacities of the working electrode and complimentary electrode interphase are in series when connected to form a cell. Since the interfacial area and, therefore, the interfacial capacitance of the latter is much greater than the former, the capacitive component of the impedance vector is attributable to the interfacial capacitance of the working electrode alone. The electrical analog for this interface is also chosen to be as consistent as possible with some physical model representing the chemical and physical properties of the electrical double layer.

Obviously many models and analog circuits are possible but for primitive solutions of electrolytes the analog which best represents the model proposed by Grahame (3) and other workers in the field is that of a capacitor shunted by a very large resistance (Figure 1.A). This electrical circuit is then placed in parallel with a similar circuit which represents the contribution of any Faradaic current to the overall impedance of the electrode interface (Figure 1.B). The equivalent circuit for the cell is now completed by placing a resistor which represents the solution resistance in series with the impedance of the interface (Figure 1.C). In concentrated solutions of electrolytes, however, the solution resistance is usually considered to be negligible.

In the presence of an electrochemically inert but capillary active material and in the absence of any Faradaic current, the equivalent circuit for the electrode interface can be represented by two parallel resistance-capacitance combinations in turn connected in parallel. One of the former represents the impedance of the adsorbate filled portion of the surface and the other represents the impedance of the vacant surface (Figure 1.D).

In both of the cases considered above, the total interfacial impedance of the working electrode can be represented by a single parallel combination of a resistance which represents the lumped sum of the electrical double layer

Figure 1. Equivalent circuit analogs for the electrical double layer at an ideally polarizable electrode-solution interphase

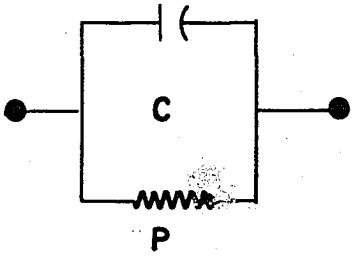

A

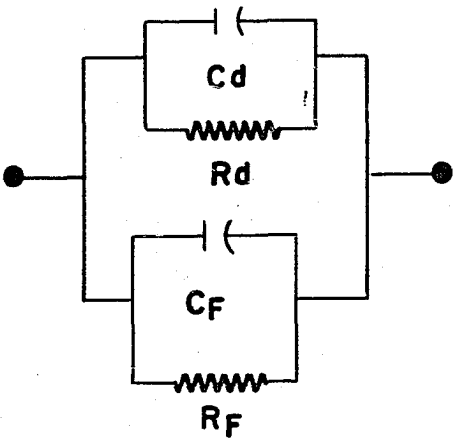

B

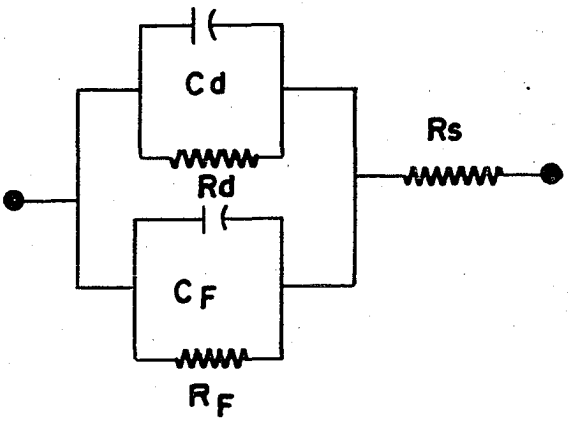

C

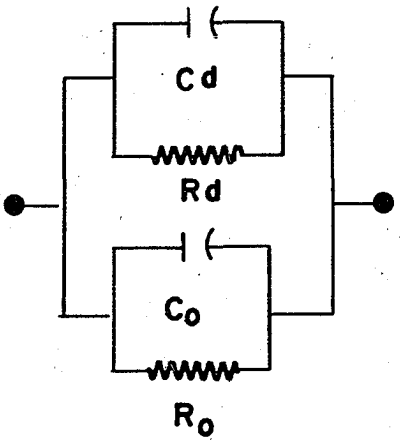

D

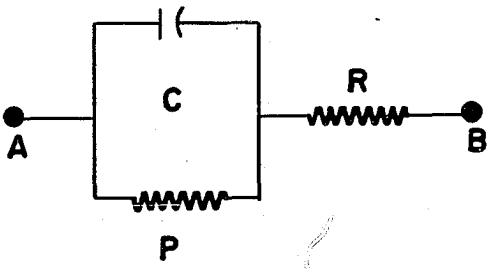

E

resistance and any resistance due to Faradaic processes or adsorption processes occurring at the interface and a capacitance which represents the lumped sum of the analogous capacitances (Figure 1.E).

Assuming that the equivalent circuit of Figure 1.E represented the electrical properties of a cell containing an ideally polarizable electrode immersed in a solution of an inert electrolyte, an electronic apparatus was devised which automatically recorded the impedance of the electrical double layer at a hanging mercury drop electrode as a function of the d.c. polarizing potential. A schematic diagram of the electrical circuit of the automatic recording instrument is presented in Figure 2.

The principle of the measurement is based upon a modification of the procedure used by Breyer and Gutmann (47). A triangular a.c. potential of small amplitude is superimposed upon the d.c. bias potential applied across the interface by means of a motor-driven potentiometer. As the d.c. potential is slowly varied linearly with time, the triangular a.c. potential sweeps the circuit consisting of the cell and a standard resistance. The alternate charging and discharging of the electrical double layer due to the a.c. potential sweep results in a current which flows through the cell and the standard resistance in series with the cell. A square-wave potential develops across this resistance whose amplitude depends upon the circuit impedance. This potential can

Figure 2. A schematic diagram of the automatic impedance recording instrument

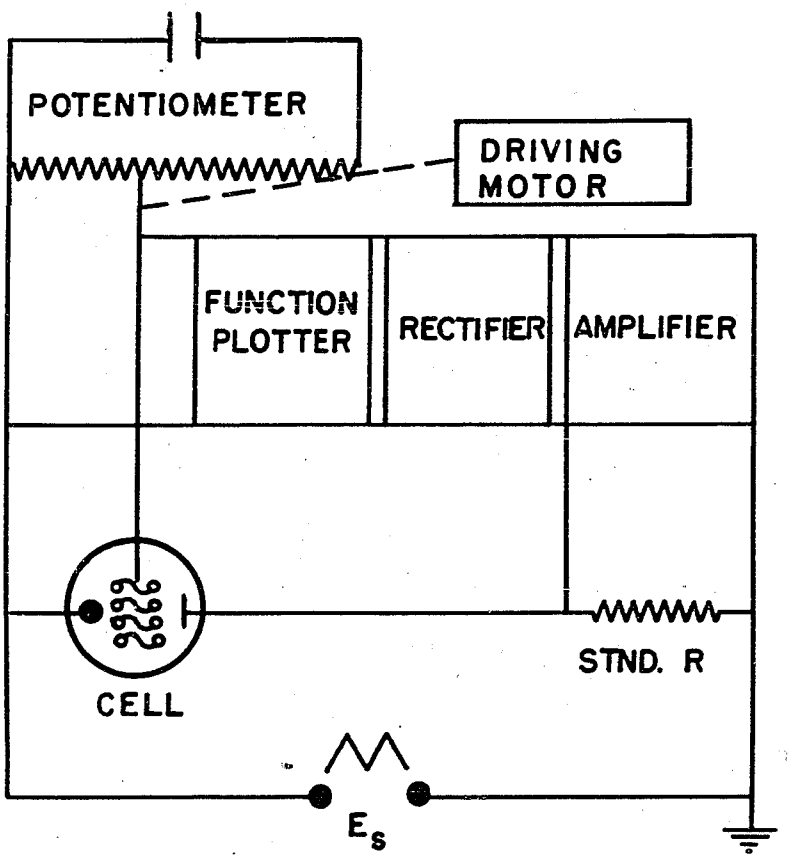
POTENTIOMETER
DRIVING MOTOR
FUNCTION PLOTTER
RECTIFIER
AMPLIFIER
CELL
STND. R
E_s

be amplified, rectified, and used to drive one d.c. circuit of an automatic function plotting devise. The signal which serves to drive the recorder through the second circuit is obtained from the output terminals of the motor-driven potentiometer supplying the d.c. polarization to the cell and, hence, is synchronized with the output signal of the measuring circuit. It was found that impedance data could be rapidly recorded as a function of the d.c. polarizing potential with a precision approaching that of conventional a.c. bridge measurements by this technique.

Considering the a.c. portion of the recording circuit to be represented by the analog circuit of Figure 1.E, Kirchoff's loop rule requires

$$e_s = e_R + e_c \tag{3}$$

and

$$e_c = e_p \tag{4}$$

where e_s is the applied triangular a.c. potential and e_R, e_p, and e_c are the respective potential drops across the series resistance R, shunting resistance p, and capacitance C. If Q_c represents the charge on the plates of the capacitor and dQ_p/dt and dQ_R/dt are the currents flowing through the corresponding resistive circuit components, the following boundary value problem arises

$$d^2Q_p/dt^2 + (p + R)/pRc\ dQ_p/dt = e_s/pRc \tag{5}$$

and

$$(a) \quad dQ_p(0)/dt = 0$$

$$(b) \quad e_s(t) = V^o\omega\, t/\pi \qquad 0 < t < \pi/\omega$$

$$= V^o\omega/\pi\ (2\pi/\omega - t) \qquad \pi/\omega < t < 2\pi/\omega$$

$$e_s(t) = es(t + 2\pi/\omega) \quad .$$

This equation may be solved for the current flowing through the shunting resistance and, hence, by the use of Equation 4 the total current flowing through the standard resistance in series with the cell.

$$i_t = i_c + i_p \quad . \tag{6}$$

This current generates a potential across the resistance which is used to drive the recording devise. The relationship between the instrument response and the capacity of the equivalent circuit is obtained by averaging the instantaneous responses over one-half period of the a.c. potential and multiplying by the gain factor of the amplifiers in the circuit

$$\text{Response} = \frac{G\,\omega}{\pi} \int_{\frac{2n\pi}{\omega}}^{\frac{(2n+1)\pi}{\omega}} R_s \cdot i_t dt \tag{7}$$

The general solution of Equation 5 for the case of any

periodic applied potential is given in Appendix A and the solution for the response of the instrument for the special case of a triangular a.c. potential is also presented. The response of the instrument is found to be

$$\overline{R} = \frac{V^o R_s G}{2(P + R)} \left\{1 + (1/x - 1/x^2 \tanh x)P/R\right\} \qquad (8)$$

where

$$x = \frac{\pi(P + R)}{2\omega PRC} \quad .$$

Consider the practical case in which P is much greater than R and in which conditions are such that $\pi/2\omega RC$ is much greater than unity. Then

$$\overline{R} \approx \frac{G V^o \omega R_s C}{\pi} \qquad (9)$$

or

$$\overline{R} = a C \quad .$$

Consequently, if the resistance shunting the capacity in Figure 1.E is much greater than the total series resistance and $\pi/2\omega RC > 1$, the response of the instrument is proportional to the capacity in the circuit at fixed frequency. This is indeed found to be true for the case in which the cell is replaced by a real capacitor.

The identification of C with the capacity of the electrical double layer capacity when the cell is inserted in the

circuit depends upon the ability of the analog circuit of Figure 1.E to represent the true conditions prevailing at the interface. Until such an identification can be proven experimentally, the C measured by the instrument with the cell in the circuit will be called an apparent capacity. It will subsequently be shown that this identification involves subtleties which are not generally appreciated by many other investigators in the field.

Choice and preparation of solutions

Perchloric acid was selected as the inert electrolyte in preparing solutions in these experiments. This choice was prompted partially by precedent in this laboratory and partially by the fact that the perchlorate ion has little tendency to complex other ions in the solution and is only weakly or not at all specifically adsorbed by mercury (3). A solution about 0.1 molar was prepared by diluting a measured volume of Baker and Adamson reagent grade perchloric acid with conductivity water which was prepared in a Barnsted conductivity still by distillation from alkaline permanganate solution and which had a conductivity of less than 10^{-7} mhos. This molarity was selected because previous investigations (3, 15, 16) revealed that increasing the acid concentration had little effect upon the capacity of the electrical double layer indicating that the diffuse

portion of the double layer had been effectively eliminated.

The chloride concentration of the solution was fixed at 0.001 N by the addition of an appropriate amount of either hydrochloric acid or potassium chloride. This was necessary in order to provide an ion reversible to the silver-silver chloride reference electrode. The hydrochloric acid was prepared by distilling a sample of Du Pont reagent grade hydrochloric acid. The normality of the distillate was determined by titration with standard base and was found to be 6.22 N. The potassium chloride was prepared by treating a solution of Baker and Adamson reagent grade potassium chloride with chlorine gas to remove any traces of bromide or iodide present and subsequently recrystallizing the potassium chloride twice from conductivity water.

The solutions were further purified in the cell just prior to use by preelectrolysis to insure the removal of any ions which might have interferred in the measurement of the double layer capacity.

Mercury

The mercury which was used as an electrode material in this investigation was purified by treating Goldsmith Brothers triple distilled mercury with 50 per cent nitric acid, filtering, distilling once or twice in a stream of air, again filtering, and finally distilling in vacuo. Just prior

to introducing the mercury into the cell, the mercury was filtered through a pin hole filter.

Inert atmosphere

Hydrogen was used in these experiments for the purposes of outgassing the solutions and providing an inert atmosphere within the cell. Tank hydrogen was purified by passage over copper gauze at 600° C. to remove any traces of oxygen, through a dry ice trap, through a bed of activated charcoal maintained at liquid air temperature, and finally through a trap at liquid air temperature to remove any residual stopcock grease from the gas stream. The hydrogen entered the cell through a medium porosity glass disc and was dispersed. The gas left the cell through a water bubbler. Provision was made for bypassing the hydrogen stream above the solution during times when experiments were being conducted. Thus, the cell was continuously flushed and was under a positive pressure of hydrogen at all times.

Adsorbates

The n-amyl alcohol which was used as an adsorbate in some of the experiments was purified by distilling a sample of Baker and Adamson reagent grade normal amyl alcohol through a 30 plate Oldershaw column at a reflux ratio of 10:1. The boiling point of the fraction used in these

experiments was 138.4° C. at S.T.P. The value reported by Lange (51) is 138.1° C. The saturation concentration of n-amyl alcohol in 0.1 N perchloric acid is reported to be 0.222 molal (17).

Electrodes

In order to avoid the necessity of complicated synchronizing circuitry associated with instruments utilizing the dropping mercury electrode, experiments were conducted with stationary hanging-drop electrodes of small surface area. An arrangement for the formation of such electrodes has been described in the literature by Delahay and Berzins (52). A schematic diagram of the arrangement used in these experiments is presented in Figure 3. Suspended in the center of the cell through a small greaseless ball joint was a thin glass tube which had a short length of platinum wire sealed in the tip at one end. This wire was gold plated and amalgamated to insure complete wetting of the wire by the mercury droplets which served as the working electrode. The mercury which formed this electrode was obtained from a dropping mercury capillary which was encased in a glass tube to which a glass spoon was fitted at one end. The mercury drops after detachment from the capillary rolled slowly down the spoon where they were subsequently picked up by the wire support by pivoting the wire tip up to the end of the spoon.

Figure 3. A schematic representation of the cell illustrating the electrode arrangement

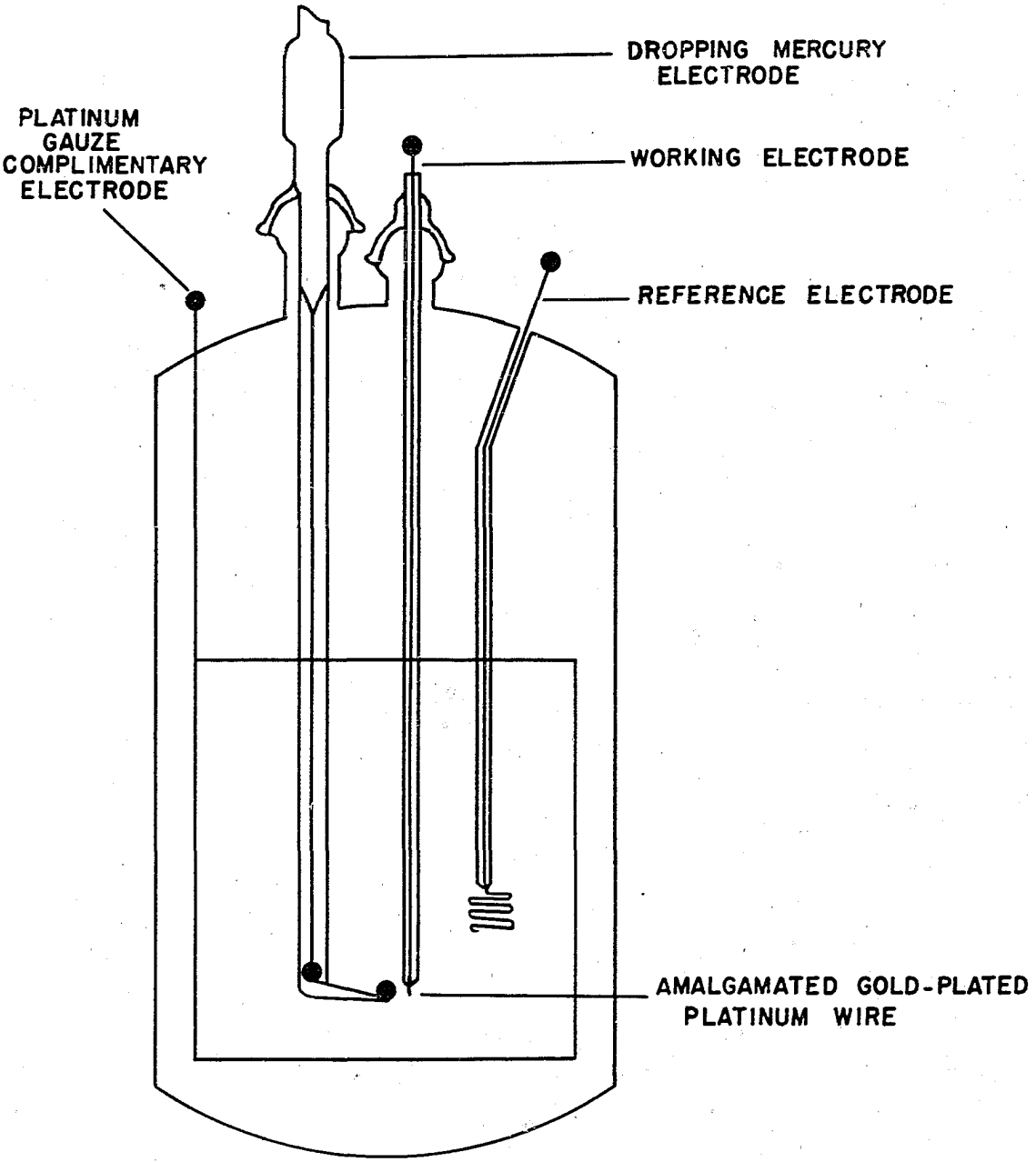
DROPPING MERCURY ELECTRODE
PLATINUM GAUZE COMPLIMENTARY ELECTRODE
WORKING ELECTRODE
REFERENCE ELECTRODE
AMALGAMATED GOLD-PLATED PLATINUM WIRE

After two or three drops of mercury had been collected to form a single droplet of desired size, this droplet was pivoted away from the spoon into the center of the cell. By measuring the rate of flow of the mercury into the cell and knowing the number of drops of mercury picked up to form the working electrode, the surface area of the working electrode could be computed. By this procedure fresh electrodes which were almost identical in surface area with previous electrodes could be obtained as needed. A silver-silver chloride electrode prepared by the thermoelectric procedure of Harned was suspended in the solution just above the working electrode through a standard taper joint and served as the reference electrode in the d.c. polarizing circuit. The whole assembly was surrounded by a platinum wire screen electrode which served as the complimentary electrode in the a.c. portion of the circuit.

The flow rate of the mercury into the cell through the dropping mercury capillary was determined by weighing the mercury which flowed into the cell during a measured interval of time. The dropping time was measured simultaneously by means of a stop watch. The area of the electrode was computed from the following formula which assumes the drop to be spherical in shape, a fairly good approximation for small drops:

$$A = 4\pi \left(3/4\ \pi\ (nmt/Td + V')\right)^{2/3}$$

where

A = the area in square centimeters

n = the number of drops of mercury used to form the working electrode.

m = the weight of mercury which flowed into the cell during the time interval T.

d = the density of mercury at the temperature of the solution.

t = the dropping time.

V' = a small correction equal to the volume of the support wire.

Thermostating

The cell was encased in a jacket through which water at the desired temperature was circulated to insure adequate thermostating. The temperature of the solution was read on a thermometer which was immersed in the solution through a greaseless standard taper joint and was constant to ± 0.5° C. At 0° C. absolute ethanol which had been cooled by passage through copper coils immersed in a mixture of dry ice and ethanol was used in place of the water as the thermostating liquid. Immersion heaters were used to regulate the temperature of the ethanol.

Electronic apparatus

A schematic diagram of the complete circuit used in recording the differential double layer capacity versus polarization curves is presented in Figure 4. The triangular

Figure 4. A complete circuit diagram for the automatic impedance recording apparatus

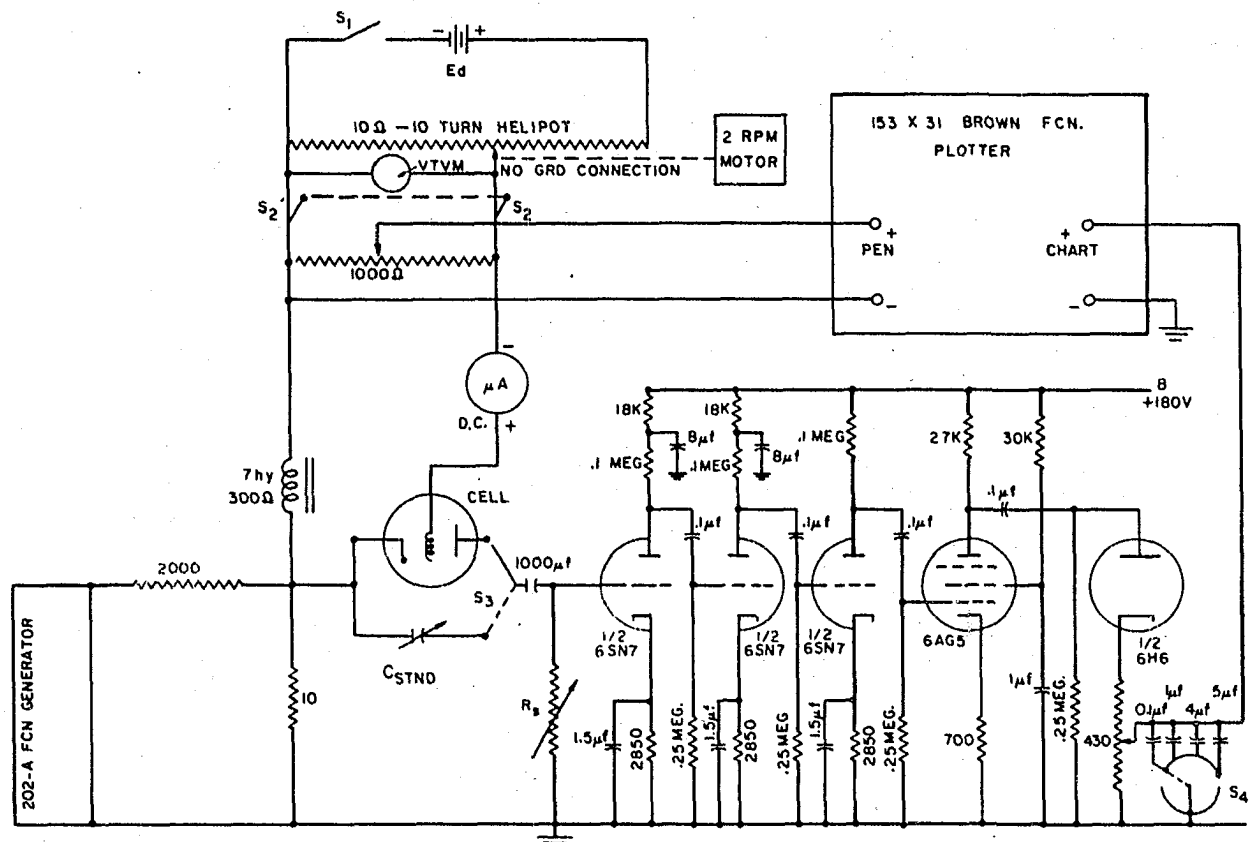
S1
Ed
10Ω -10 TURN HELIPOT
VTVM
NO GRD CONNECTION
2 RPM MOTOR
153 X 31 BROWN FCN. PLOTTER
S2
S2
1000Ω
PEN
CHART
μA
D.C.
7hy 300Ω
CELL
2000
1000μf
S3
CSTND
202-A FCN GENERATOR
10
Rs
18K
18K
8μf
8μf
.1 MEG
.1MEG
.1 MEG
27K
30K
+180V
.1μf
1/2 6SN7
1/2 6SN7
1/2 6SN7
6AG5
1/2 6H6
1.5μf
2850
.25MEG.
700
.25MEG.
430
1μf
.01μf
4μf
5μf
S4

voltage sweep was produced by a Hewlett-Packard 202A low frequency function generator. The standard resistance R_s was a Leeds and Northrup AC-DC decade resistance box variable to 11,000 ohms. The standard capacitance, Cstnd, was a Freed Transformer Co. Model 1350 decade capacitor variable from 0 to 11 μ f. The recorder, manufactured by Minneapolis Honeywell Co., was a Brown Electronic 153x31 Function Plotter. The d.c. polarization was furnished by a ten ohm-ten turn Beckman Helipot precision potentiometer, linear within $\pm$ 0.1 per cent, which was driven after suitable gear reduction by a two RPM reversible electric motor. E_d was six 1.5 volt drycell batteries connected in parallel to insure a stable source. In some experiments a Simpson D.C. Microammeter was inserted in the d.c. portion of the circuit between the potentiometer and the reference electrode in order to measure the current flowing through the cell. A Kay Lab Microvoltmeter and Amplifier Model 202B was placed across the terminals of the motor-driven potentiometer in order to measure the d.c. potential across the cell. This instrument has an accuracy of 3 per cent of full scale on all ranges according to the manufacturer and was used to calibrate the potential scan of the function plotter. A potentiometer which formed a portion of the 1000 ohm resistance in parallel with the polarizing potentiometer was used to scale the d.c. signal to the recorder. The 1000 μ f capacitor in series

with the cell was included to eliminate a parallel path for the d.c. current while permitting the a.c. current to pass through the measuring circuit.

The signal developed across the standard resistance was amplified by a four stage amplifier of conventional design. Rectification of the output signal was accomplished with the aid of the 6H6 diode. The amplitude of the output signal was varied by means of a 50 ohm potentiometer which formed part of the load resistance of the cathode follower circuit. A Hewlett-Packard Power Supply Model 710A was used to furnish the necessary d.c. potential bias for the amplifier portion of the circuit. Two eight microfarad capacitors were included in the first two stages of amplification to eliminate a parasitical ground loop through the power supply.

Method of procedure

After cleaning the cell thoroughly, the bottom portion was filled with conductivity water. The platinum gauze electrode was then heated to a red glow in the flame of a Meker burner after withdrawing the dropping mercury capillary up into the cap. The cell (Figure 5) was then assembled immersing the gauze electrode in the conductivity water. Plugs were then inserted into the standard taper joints and hydrogen was flushed through the cell. The conductivity water was drained through a teflon stopcock in the bottom of

Figure 5. The cell

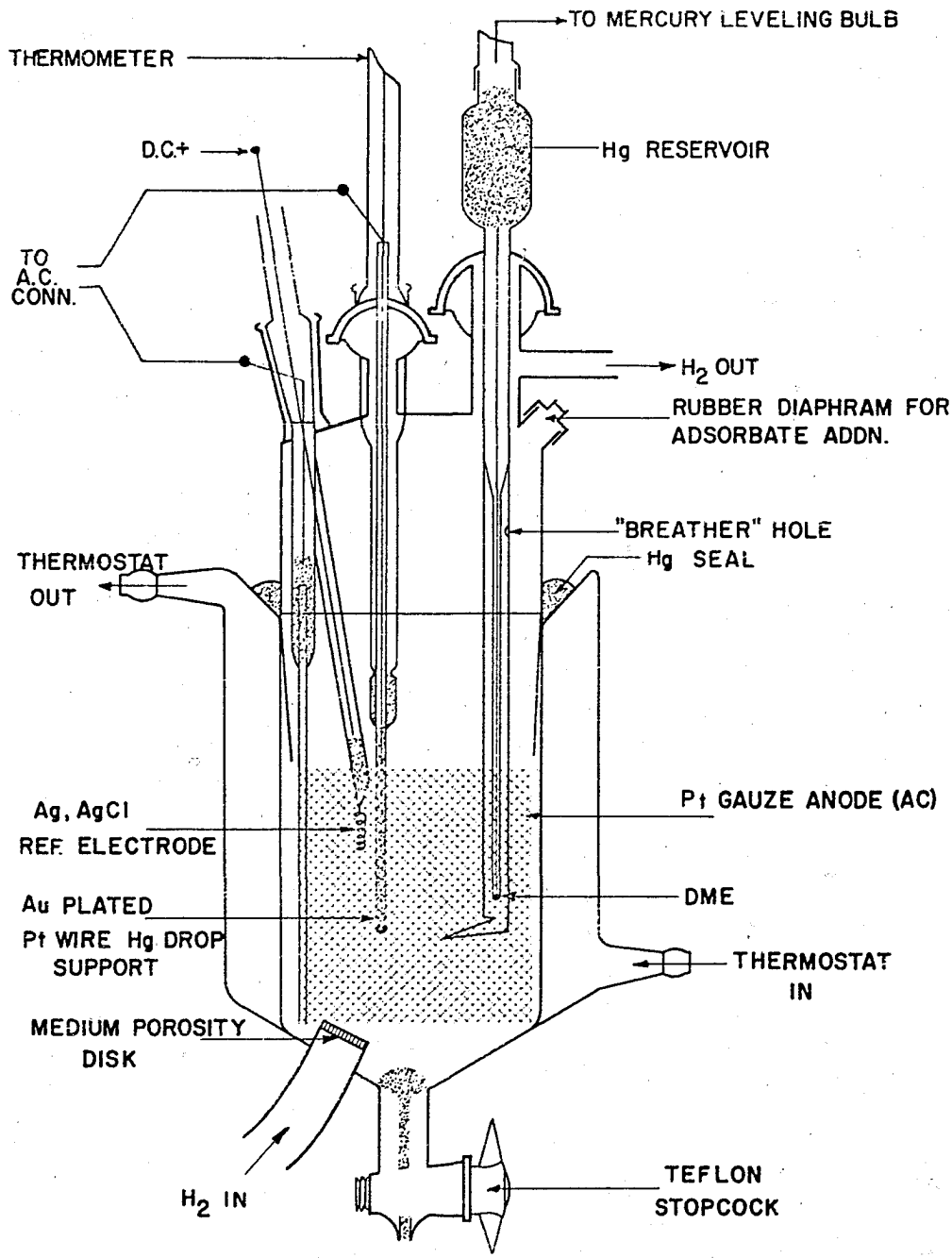
TO MERCURY LEVELING BULB
THERMOMETER
D.C.+
Hg RESERVOIR
TO
A.C.
CONN.
H_2 OUT
RUBBER DIAPHRAM FOR
ADSORBATE ADDN.
"BREATHER" HOLE
Hg SEAL
THERMOSTAT
OUT
Ag, AgCl
REF. ELECTRODE
Pt GAUZE ANODE (AC)
Au PLATED
Pt WIRE Hg DROP
SUPPORT
DME
THERMOSTAT
IN
MEDIUM POROSITY
DISK
H_2 IN
TEFLON
STOPCOCK

the cell. A half-cell consisting of a medium porosity glass disc and a platinum flag electrode was inserted through one of the taper joints. A second platinum flag electrode was inserted through the other taper joint. About one milliliter of purified mercury was forced back through the teflon stopcock by means of a hypodermic syringe to form a continuous mercury ribbon. About five milliliters of purified mercury were also placed in the reservoir of the dropping mercury capillary and connection with a leveling bulb was made. After starting the capillary dropping within the cell by raising the leveling bulb, about 250 milliliters of the perchloric acid-chloride primitive solution were added to the cell. Some of the solution was sucked up into the half-cell and electrical connections from the two electrodes were made to a d.c. power supply. Preelectrolysis of the solution was conducted at 5×10^{-2} amps at 240 volts for at least two hours and in many cases over night. A silver-silver chloride electrode and a thermometer were then substituted for the half-cell and platinum flag electrode and the support rod was inserted into the cell. Degassing of the solution with hydrogen was continued for at least one hour. The apparatus was then activated by turning on the recorder, power supply, microvoltmeter and generator. The appropriate frequency was then selected and the output of the generator adjusted to give the desired input. After a sufficient warmup time,

switch S_1 was closed, S_2 opened, and S_3 set at "standard capacitor". A new cycle on the motor driven potentiometer was started by allowing the motor to run until the reversing switch in the gear train clicked over at the most anodic potential of the potentiometer as read on the microvoltmeter. With the motor and S_1 off, the microvoltmeter was zeroed on the 300 millivolt scale. With S_1 on, the motor was then turned on and the potentiometer was driven until the microvoltmeter read exactly 240 millivolts. The motor was then stopped. Switch S_2 was closed and the pen of the recorder was set to read 10 millivolts on the chart paper by use of the "pen" scaling potentiometer. The standard capacitance was set at five microfarads and the "chart" scaling potentiometer was adjusted to read the maximum vertical displacement on the chart paper as determined by the stops on the recorder. The range of the microvoltmeter was then changed to three volts and the motor driven potentiometer turned on. At every cardinal division of the chart paper the capacitance of the standard capacitor was reduced one microfarad until two microfarads remained. Thereafter, the capacitor was reduced by two-tenths of a microfarad at each cardinal division until one microfarad remained. As the pen reached the end of the chart paper the motor was turned off. The capacitor was then reduced to zero and switch S_2 was opened. The potential read on the microvoltmeter was noted and the motor again

turned on to complete the half cycle and return to a potential just above the shut off potential read previously. This completed one cycle of the calibration procedure.

The bypass valve was then opened deflecting the gas stream above the solution. The mercury in the bottom of the cell was then drained out of the cell until the meniscus was approximately half way up the capillary tube which led to the teflon stopcock. The hairline of a telemicroscope was trained on a point above the meniscus. As the mercury filled the capillary tube and as the meniscus passed the hairline, a "Timeit" electric timer was started. As the mercury continued to flow, the dropping time of three or four drops was measured with a stopwatch to a tenth of a second. After recording several drop times, the mercury in the capillary tube was drained to below the hairline into a five millliliter sample bottle. As the meniscus passed the hairline the second time the timer was stopped. The total flow time, weight of mercury collected, dropping time, potential scan calibration data and other pertinent information were recorded on special data sheets (Figure 6). After recording the pertinent information, the wire tip of the support rod was pivoted up to the spoon and several drops of mercury were allowed to congeal to form a working electrode. This electrode was then pivoted into the center of the cell away from the spoon. The electrical connections to the cell were made,

Figure 6. The format of the data sheets

Data Work Sheet

Date:

Time:

Experimental System:

Run No.:

Temperature: frequency:

Density of Hg:

Bottle No:

wt. A:

wt. B:

wt. T:

Total Time:_____ m:

Dropping Time: No. of drops taken (n)=____

1_____ 6_____

2_____ 7_____

3_____ 8_____

4_____ 9_____

5_____ 10_____ t ave_____

n m t ave =

Bo =

$\sum_{i=1} liCi$ =

Φ = _____

k = 89.400

Comments:

S_2 was closed, S_3 switched to "cell", and the motor driven potentiometer was turned on. A polarization curve was measured over a complete cycle. As the pen once more reached the end of the chart the motor was stopped, S_3 was switched to "StndCap", and S_2 opened. The motor was then started and the whole cycle completed and returned to the terminating potential. S_2 was then closed and the motor was turned on. One microfarad was set on the standard capacitor. As the next cardinal division was passed, the capacitor was increased by one microfarad to two microfarads. Thereafter, the capacitor was increased by two-tenths of a microfarad per cardinal division. At three microfarads and thereafter the capacitance was increased by one microfarad per cardinal division until the instrument returned to zero where it was shut off. This rather complicated calibration procedure was followed to facilitate the treatment of the data.

A.C. Impedance Bridge Measurements

In one series of experiments the impedance of the electrical double layer at the mercury-0.1 N perchloric acid-0.001 N potassium chloride solution interphase was investigated for frequency dispersion effects by means of a conventional a.c. impedance bridge. In these experiments the solution purification and electrode preparation were conducted in the same cell and manner described in the section

on the automatic recording instrument. The cell with a freshly formed mercury-drop electrode was inserted into the unknown impedance arm of the bridge circuit which is schematically represented in Figure 7. This bridge circuit was designed to measure the impedance of the cell in terms of a series combination of a standard resistance, R_b, and standard capacitance, C_b. R_b, R_1 and R_2 were Leeds and Northrup AC-DC Decade Resistance Boxes variable from 0 to 11,000 ohms in five decades. C_b was a Freed Transformer Co. Model 1350 decade capacitance box variable in decades from 0 to 11 microfarads. The input signal to the bridge was a sinusoidal a.c. potential generated by a Hewlett-Packard Model 200 CD Wide Range Oscillator and was applied across the bridge circuit through a General Radio Co. 578-A shielded bridge transformer. The amplitude of the input signal was adjusted at the oscillator to produce a four millivolt a.c. signal across the cell terminals as measured on a Heathkit Model AC-2 vacuum tube voltmeter. The detector unit in the bridge consisted of a high-gain "twin-tee" amplifier with provision for wide range frequency selection by means of plug-in tee units[1] which was connected to the vertical deflection plates of a Du Mont 304H cathode ray oscilloscope. Bridge balance

---

[1]This instrument was designed and built by the Electronic Instrumentation Group, U.S. Atomic Energy Commission, Ames Laboratory, (Iowa State College) Ames, Iowa.

Figure 7. A schematic diagram of the a.c. impedance bridge apparatus

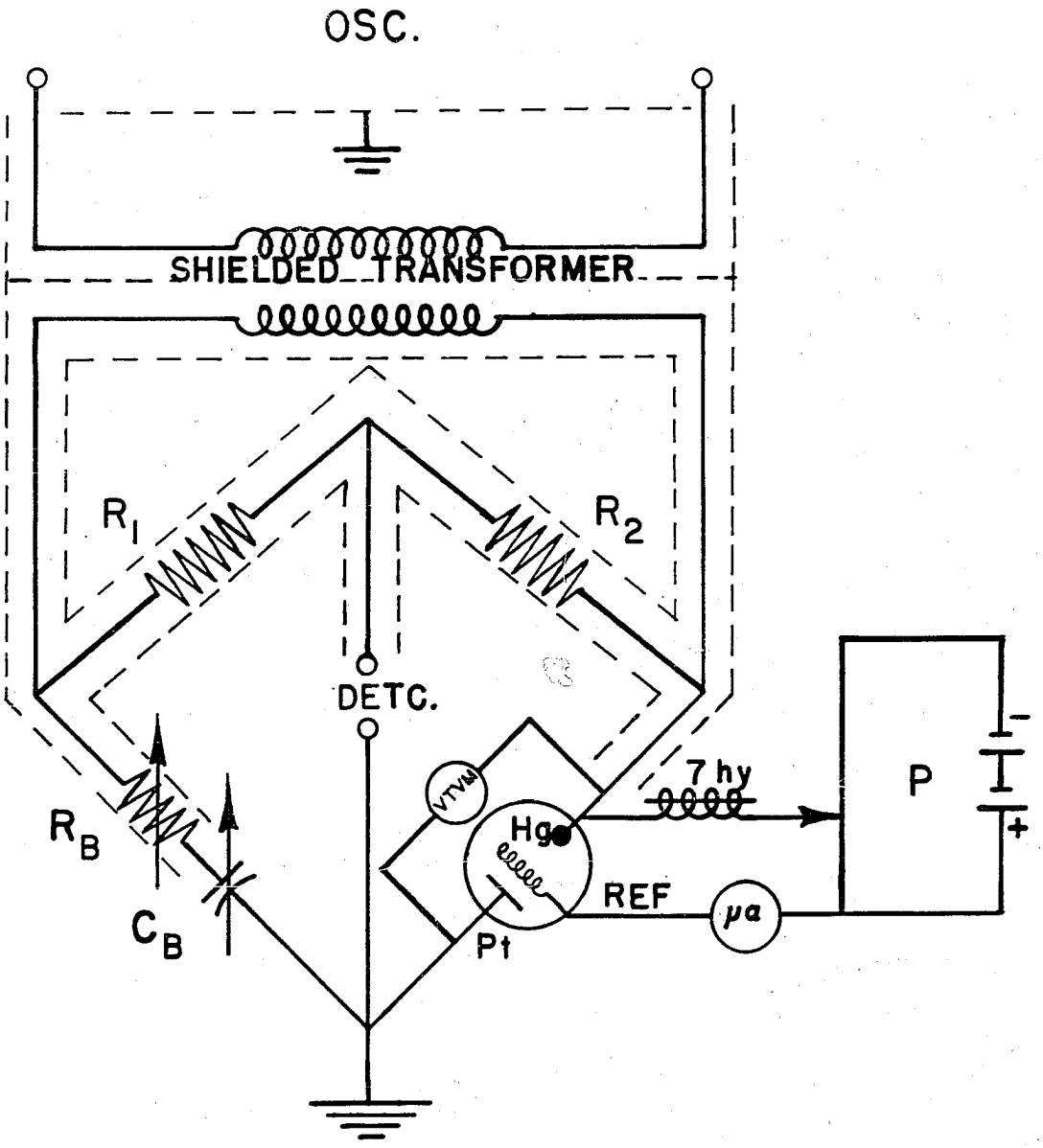
OSC.
SHIELDED TRANSFORMER
R1
R2
DETC.
RB
CB
VTVM
Hg
Pt
REF
μa
7 hy
P
-
+

was detected by a null signal in the vertical trace on the screen of the cathode ray oscilloscope. The mercury electrode was polarized at a known d.c. potential by means of the external potentiometer, P. A seven henry-300 ohm choke coil was inserted in the d.c. circuit to remove any a.c. signal which might have entered the potentiometer portion of the circuit. A d.c. microammeter was inserted in the d.c. circuit to measure the residual current flowing through the cell. Impedance measurements were ceased when this current exceeded ten microamperes. Extensive precautions were taken to shield the bridge from stray capacitances and induced currents. Shielded cable was used throughout in construction and the general precautions for good bridge operation outlined by Hague (53) were observed.

After forming the working mercury-drop electrode in the cell in the manner described in the section on the automatic recording instrument and making the proper connections to the cell from the bridge, the mercury electrode was polarized at a known d.c. potential relative to a silver-silver chloride reference electrode immersed in the same solution by means of the potentiometer, P. An initial balance was made. The amplitude of the a.c. signal across the cell was then adjusted to four millivolts and the final bridge balance attained by varying the impedance in the measuring arm until a null signal was observed on the cathode ray oscilloscope.

The procedure was then repeated at different d.c. potentials to construct an impedance versus polarizing potential curve point by point at any given frequency and temperature. At each frequency investigated two curves were recorded, one for increasing cathodic polarization of the mercury electrode and one for decreasing polarization. Fresh mercury electrodes were used for each curve recorded. The observed resistances and capacitances were converted into specific quantities by multiplying the observed series resistance by the surface area of the mercury-drop electrode and dividing the observed capacity by the surface area of the mercury drop. The final specific impedance used in the calculation was obtained by averaging the two specific impedances obtained at any given polarization at the frequency and temperature at which the measurements were made.

RESULTS

Automatic Recording Instrument

The results of the investigations with the automatic recording instrument were presented in the form of response curves and needed to be translated into numerical form for the purposes of computation and interpretation. For each curve obtained at a given frequency, temperature, and solution composition, two calibration curves representing the response of the instrument with a real capacity in the circuit in place of the cell were obtained. As was indicated in the discussion of the theory of the measurement, the response of the instrument to varying apparent capacity should be linear and the calibration lines should pass through the origin. This fact facilitates the treatment of the experimental results if a certain procedural form is followed.

The response of the instrument to a given capacity, C, is observed as a vertical deflection, l, from the zero base line on the recorder. According to the theory of the instrument response,

$$l = K'C \quad .$$

Now K' is determined by measuring the slope of the calibration line which is obtained by measuring the deflection l_i for a set of standard capacitors, C_i. The best least-squares

representation for the slope of the line passing through the origin is given by

$$K' = \sum_i l_i C_i / \sum_i C_i^2 \quad .$$

But by standardizing the calibration procedure, $\sum C_i^2$ can be made a constant, K. Therefore, if L_m is the deflection from the base line to the experimental curve, the apparent capacity of the electrode interface is given by

$$C_m = \sum_i \frac{K}{l_i C_i} \cdot L_m = \Phi L_m \quad .$$

To convert this apparent capacity to the apparent specific capacity the latter expression was divided by the surface area of the mercury drop.

$$C_s = \Phi/A \; L_m = B_o L_m \quad .$$

In the calibration procedure described above, K is 89.40. Since one full recording cycle on the recorder results in two experimental curves, one for the cathodic potential to anodic potential scan and one for the reverse scan, an average of the two values of the apparent specific capacity calculated at any particular polarization potential was made.

In Figure 8 the response of the instrument with a standard capacitor inserted in the circuit in place of the cell is presented. This is a typical calibration curve which

Figure 8. A typical calibration curve obtained with real capacitors inserted in the circuit

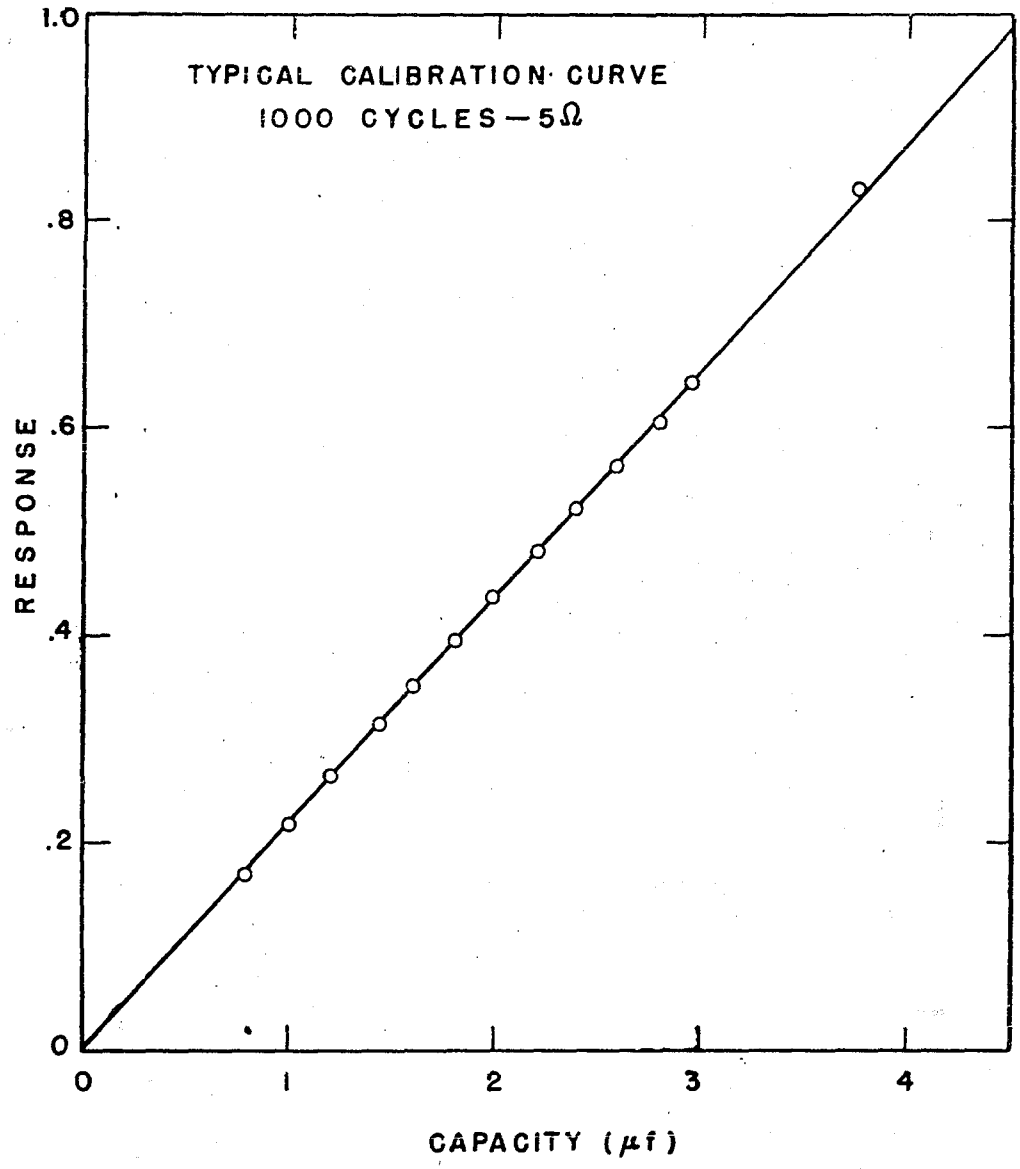
TYPICAL CALIBRATION CURVE
1000 CYCLES — 5Ω
RESPONSE
1.0
.8
.6
.4
.2
0
0
1
2
3
4
CAPACITY (μf)

illustrates the linearity of the response of the instrument to varying capacity in the circuit.

The results of the experiments performed on the primitive 0.1 N perchloric acid-0.001 N hydrochloric acid solutions in order to investigate the effect of varying temperature and frequency upon the properties of the compact region of the electrical double layer are presented in Tables 1 to 4. Complete apparent capacity versus polarization curves were obtained at frequencies of 230, 500, 750 and 1000 cycles/sec. at any specified temperature. Each of the latter experiments were then repeated at temperatures of 0°, 25°, 50° and 75° C. to furnish information over a sufficiently wide range of temperatures and frequencies. The apparent capacity calculated on the assumption of a linear dependence of the instrument response on the capacity in the circuit is plotted as a function of the polarizing potential at various frequencies for temperatures of 0°, 25°, 50° and 75° C. (Figures 9 to 12). All polarization potentials are reported relative to the silver-silver chloride-0.001 N chloride ion reference electrode at 25° C. The data for the variation with temperature of the standard potential of the silver-silver chloride electrode tabulated by Kortüm and Bockris (54) was used to calculate the correction factor for converting the standard electrode potential at other temperatures to 25° C.

In Figure 13 the apparent capacity-polarization curves obtained at a frequency of 1000 cycles/sec. are plotted as a

Table 1. Dependence of apparent differential capacity at the mercury-aqueous 0.1 N perchloric acid solution interface on polarizing potential, temperature and frequency. Capacity in μ f/cm^2. Potential in minus volts relative to Ag-AgCl in 0.001 N chloride solution at 25° C

Temperature 0° C.

Polarization	Frequency 230	500	750	1000
0.011		49.0	42.3	34.6
0.012	61.9			
0.061		39.6	35.3	30.3
0.064	50.8			
0.111		35.0	31.3	27.3
0.116	45.8			
0.186		31.3	27.6	24.6
0.194	42.4			
0.236		30.2	26.9	23.8
0.246	41.4			
0.311		29.9	26.8	23.7
0.324	41.0			
0.361		30.3	27.5	24.2
0.376	42.0			
0.436		32.0	28.8	25.5
0.454	43.4			
0.486		32.6	29.4	26.1
0.506	44.0			
0.561		32.7	28.8	25.9
0.584	42.4			
0.611		31.0	27.4	24.6
0.636	40.8			
0.686		28.1	24.2	22.1
0.714	38.0			
0.736		26.2	22.3	20.4
0.766	36.8			
0.811		24.1	20.6	18.3
0.814	36.0			
0.861		23.3	19.8	17.5
0.896	35.3			
0.936		22.5	19.0	16.7
0.974	34.8			
0.986		22.0	18.6	16.3
1.026	34.4			
1.061		21.6	18.3	15.8
1.104	34.1			
1.111		21.5	18.0	15.7

Table 1 (continued)

Polarization	Frequency 230	500	750	1000
1.156	34.1			
1.186		21.5	18.0	16.4
1.234	34.0			
1.236		21.5	18.0	15.6
1.286				

Table 2. Dependence of apparent differential capacity at the mercury-aqueous 0.1 N perchloric acid solution interface on polarizing potential, temperature and frequency. Capacity in $\mu f/cm^2$. Potential in minus volts relative to Ag-AgCl in 0.001 N chloride solution at 25° C.

Temperature 25° C.

Polarization	Frequency 230	500	750	1000
.026	64.2	58.8	50.4	40.6
.078	51.1	46.1	41.0	34.9
.130	44.6	39.9	35.5	31.0
.208	40.2	34.8	30.9	27.3
.260	38.7	33.3	29.5	26.0
.338	38.0	32.8	28.9	25.6
.390	38.4	33.2	29.4	25.8
.468	38.8	33.7	29.8	26.3
.520	38.7	33.4	29.6	26.3
.598	36.2	31.6	27.8	24.6
.650	34.5	29.5	25.8	22.8
.728	33.2	26.8	23.0	20.4
.780	32.2	25.5	21.8	19.2
.858	30.9	24.0	20.5	17.8
.910	30.5	23.3	19.8	17.3
.988	29.9	22.7	19.1	16.6
1.040	29.8	22.3	18.7	16.3
1.118	29.7	22.0	18.6	16.1
1.170	29.7	22.0	18.4	16.1
1.248	29.9	22.0	18.5	16.1
1.300	30.1	22.2	18.5	16.3

Table 3. Dependence of apparent differential capacity at the mercury-aqueous 0.1N perchloric acid solution interface on polarizing potential, temperature and frequency. Capacity in $\mu f/cm^2$. Potential in minus volts relative to Ag-AgCl in 0.001N chloride solution at 25° C.

Temperature 50° C.

Polarization	Frequency			
	230	500	750	1000
.044			51.0	50.0
.093	57.5	48.5		
.096			46.0	42.0
.143	50.3	41.7		
.148			39.3	36.6
.218	44.5	35.7		
.226			31.6	31.4
.268	42.5	33.6		
.278			31.0	29.4
.343	41.1	32.1		
.356			29.5	28.1
.393	40.8	31.7		
.408			29.1	27.7
.468	40.2	31.1		
.486			28.5	27.1
.518	39.3	30.5		
.538			27.5	26.4
.593	37.4	28.4		
.616			25.4	24.3
.643	35.9	26.7		
.668			23.9	22.7
.718	34.4	24.6		
.746			21.9	20.5
.768	33.7	23.5		
.798			20.9	19.5
.843	33.0	22.3		
.876			20.0	18.6
.893	32.7	21.8		
.928			19.5	18.1
.968	32.3	21.3		
1.006			19.0	17.6
1.018	32.2	21.1		
1.058			18.9	17.3
1.093	32.15	20.8		
1.163			18.7	17.0
1.143	32.15	20.6		
1.188			18.6	17.0
1.218	32.2	20.6		

Table 3 (continued)

Polarization	Frequency 230	500	750	1000
1.266			18.5	17.0
1.268	32.3	20.6		
1.318			18.6	17.0

Table 4. Dependence of apparent differential capacity at the mercury-aqueous 0.1N perchloric acid solution interface on polarizing potential, temperature and frequency. Capacity in $\mu f/cm^2$. Potential in minus volts relative to Ag-AgCl in 0.001N chloride solution at 25° C.

Temperature 75° C.

Polarization	Frequency 230	500	750	1000
.063			54.6	47.8
.113	52.8	52.5	44.5	40.6
.163	45.6	44.0	37.9	35.4
.238	39.6	36.9	31.7	30.0
.288	37.3	34.2	29.2	27.6
.363	35.3	31.5	27.0	25.2
.413	34.2	30.4	26.0	24.3
.488	33.6	29.0	24.8	22.9
.538	32.0	27.9	23.7	22.0
.613	30.3	25.5	21.5	20.1
.663	29.3	24.0	20.4	18.9
.738	27.9	22.6	18.7	17.2
.788	27.3	21.7	18.1	16.5
.863	26.9	20.7	17.3	15.8
.913	26.6	20.6	17.0	15.6
.988	26.6	20.4	16.8	15.4
1.038	26.5	20.3	16.6	15.3
1.113	26.5	20.3	16.6	15.3
1.163	26.6	20.3	16.7	15.3
1.238	26.9	20.4	16.9	15.3
1.288	27.1	20.6	17.0	15.4

Figure 9. Apparent specific capacity of the electrical double layer on mercury in 0.1N perchloric acid versus polarizing potential at several operating frequencies at 0° C.

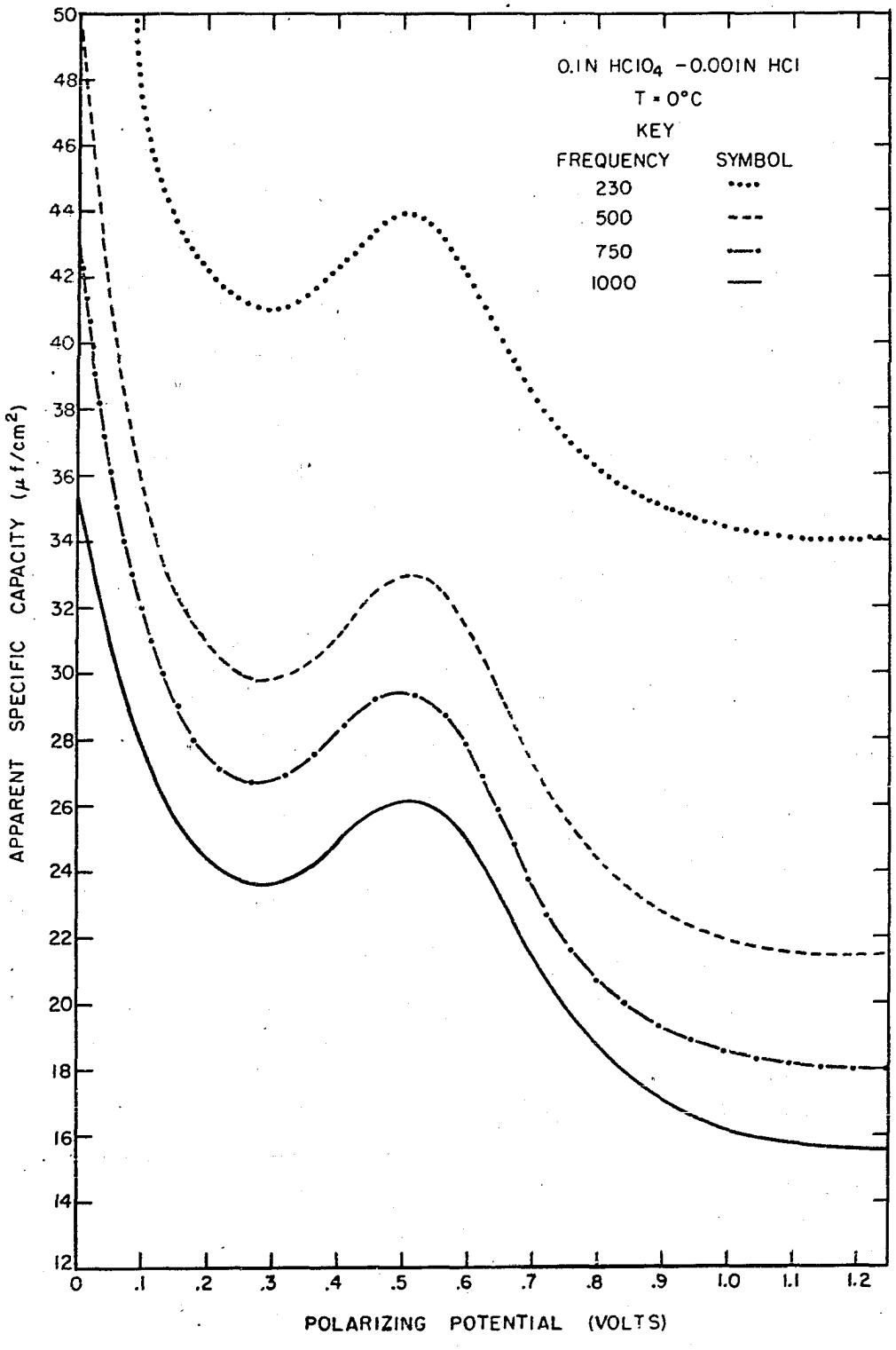
0.1N HClO4 -0.001N HCl
T = 0°C
KEY
FREQUENCY SYMBOL
230
500
750
1000
APPARENT SPECIFIC CAPACITY (μf/cm²)
POLARIZING POTENTIAL (VOLTS)
50
48
46
44
42
40
38
36
34
32
30
28
26
24
22
20
18
16
14
12
0
.1
.2
.3
.4
.5
.6
.7
.8
.9
1.0
1.1
1.2

Figure 10. Apparent specific capacity of the electrical double layer on mercury in 0.1N perchloric acid versus polarizing potential for several operating frequencies at 25° C.

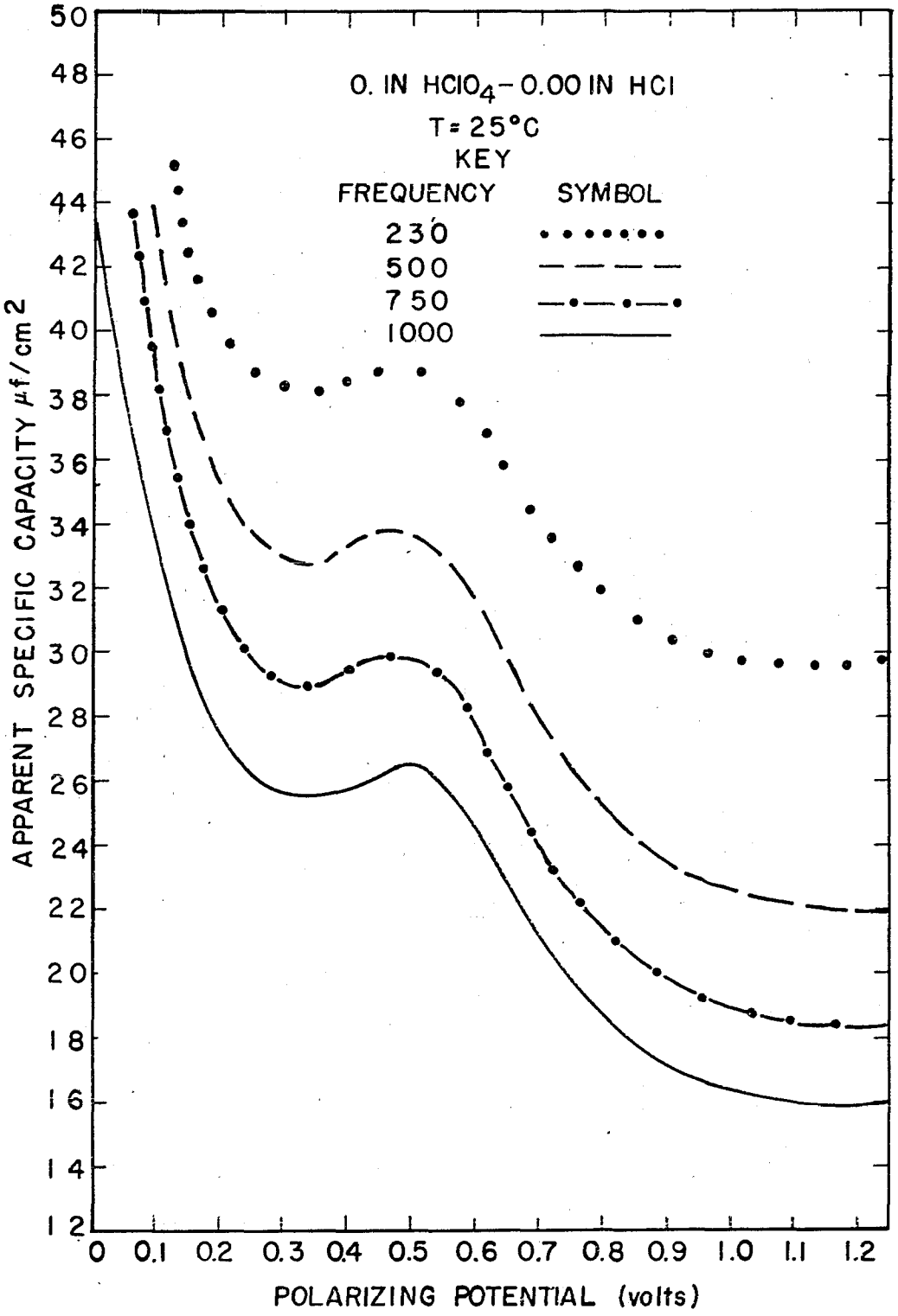
0. IN HClO4 – 0.00 IN HCl
T = 25°C
KEY
FREQUENCY SYMBOL
230
500
750
1000
APPARENT SPECIFIC CAPACITY μf/cm2
POLARIZING POTENTIAL (volts)
50
48
46
44
42
40
38
36
34
32
30
28
26
24
22
20
18
16
14
12
0 0.1 0.2 0.3 0.4 0.5 0.6 0.7 0.8 0.9 1.0 1.1 1.2

Figure 11. Apparent specific capacity of the electrical double layer on mercury in 0.1N perchloric acid versus polarizing potential for several operating frequencies at 50° C.

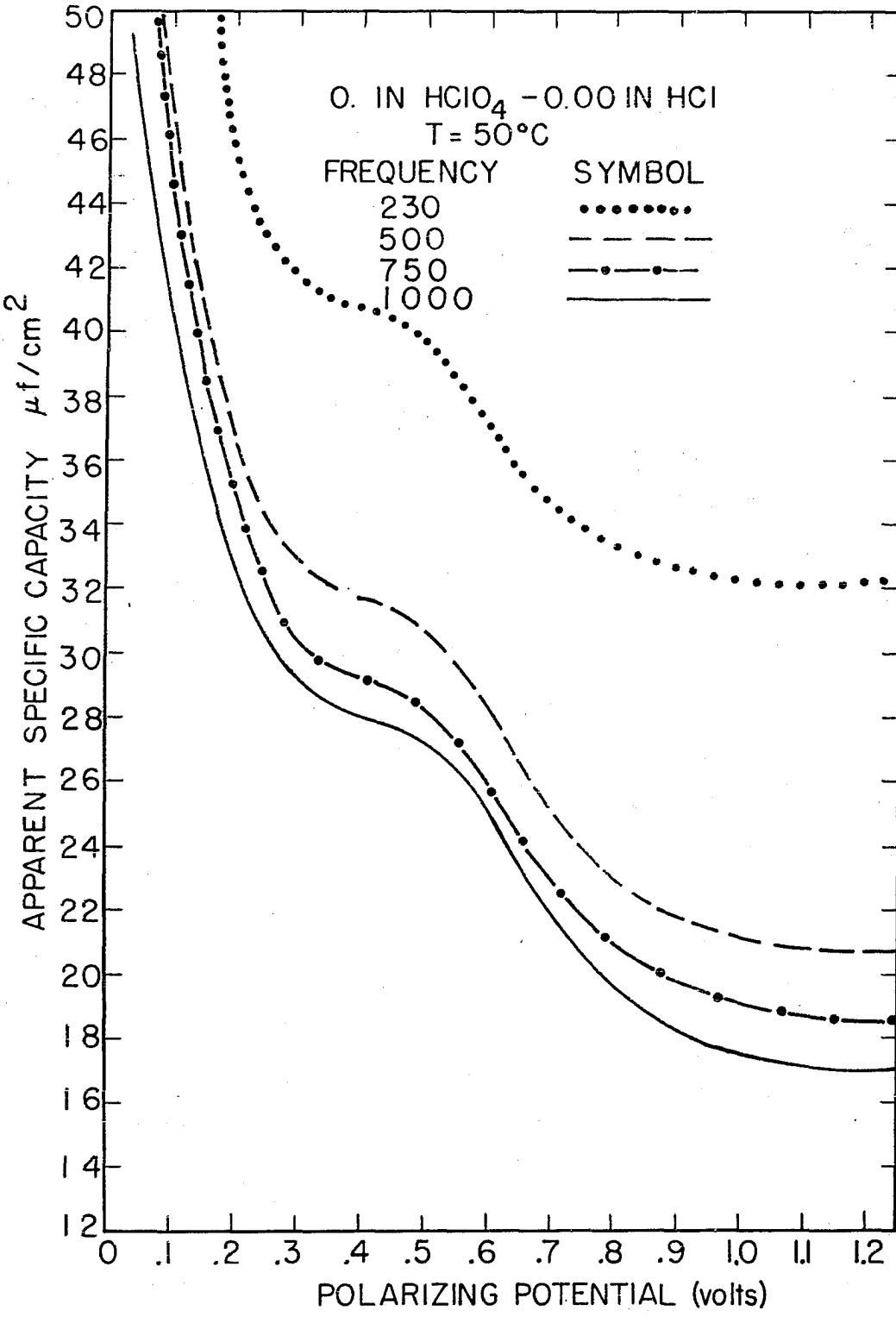
0. IN HClO4 - 0.00 IN HCl
T = 50°C
FREQUENCY SYMBOL
230
500
750
1000
APPARENT SPECIFIC CAPACITY μf/cm2
POLARIZING POTENTIAL (volts)
50
48
46
44
42
40
38
36
34
32
30
28
26
24
22
20
18
16
14
12
0
.1
.2
.3
.4
.5
.6
.7
.8
.9
1.0
1.1
1.2

Figure 12. Apparent specific capacity of the electrical double layer on mercury in 0.1N perchloric acid versus polarizing potential for several operating frequencies at 75° C.

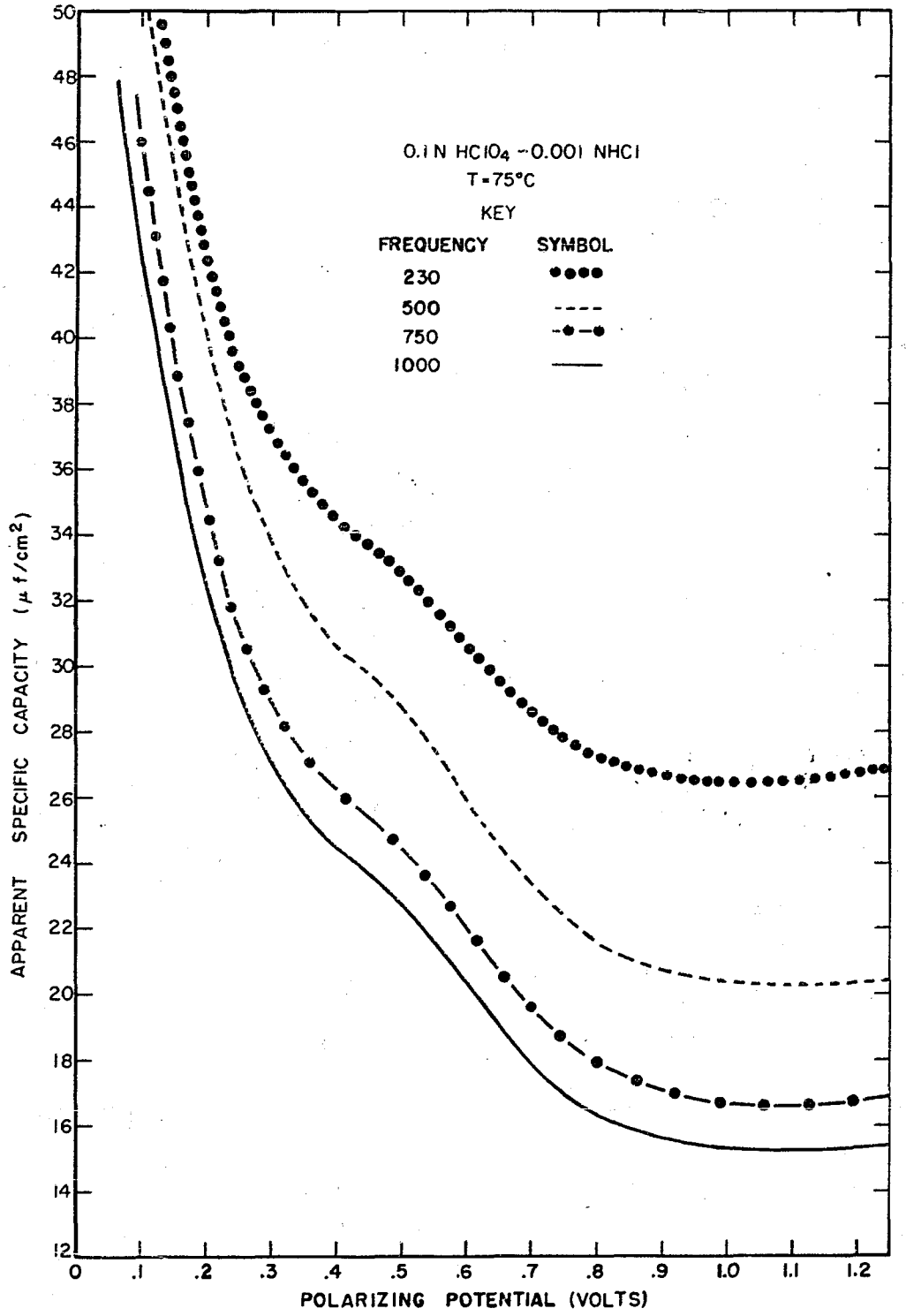
0.1 N HClO4 - 0.001 NHCl
T = 75°C
KEY
FREQUENCY
SYMBOL
230
500
750
1000
APPARENT SPECIFIC CAPACITY (μf/cm²)
POLARIZING POTENTIAL (VOLTS)
50
48
46
44
42
40
38
36
34
32
30
28
26
24
22
20
18
16
14
12
0
.1
.2
.3
.4
.5
.6
.7
.8
.9
1.0
1.1
1.2

Figure 13. Apparent capacity of the electrical double layer on mercury in 0.1N perchloric acid versus polarizing potential for several operating temperatures at a frequency of 1000 cycles

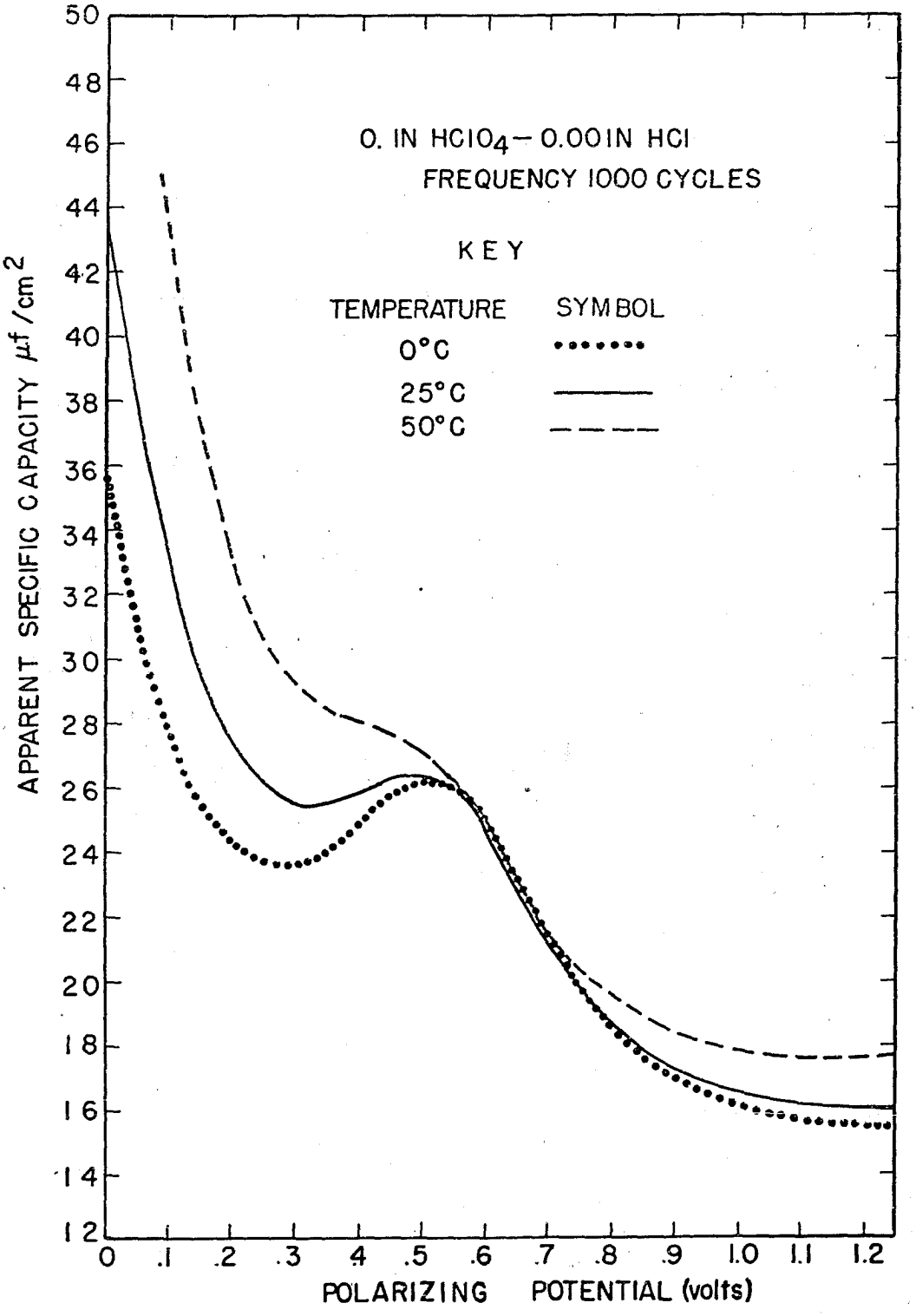
0. IN HClO4 – 0.001N HCl
FREQUENCY 1000 CYCLES
KEY
TEMPERATURE SYMBOL
0°C
25°C
50°C
APPARENT SPECIFIC CAPACITY μf/cm²
POLARIZING POTENTIAL (volts)
50
48
46
44
42
40
38
36
34
32
30
28
26
24
22
20
18
16
14
12
0
.1
.2
.3
.4
.5
.6
.7
.8
.9
1.0
1.1
1.2

function of the temperature. The polarizing potential is referred to the potential of the silver-silver chloride reference electrode at 25° C. as explained above.

The effect of the adsorbate pentanol-1 on the apparent capacitance at mercury-0.1N perchloric acid-0.001N hydrochloric acid solution interfaces was investigated as a function of adsorbate activity and frequency at 25° C. The activity was taken to be the reduced concentration (ratio of concentration to saturation concentration). The apparent differential double layer capacity was investigated as a function of the polarizing potential at frequencies of 230, 500, 750 and 1000 cycles for each of six different adsorbate concentrations covering the complete solubility range for this adsorbate. The results obtained at the various adsorbate concentrations are presented in Tables 5 to 8 as a function of the frequency and polarization and are plotted in Figures 14 to 17 as a function of the polarizing potential at each of the frequencies investigated at 25° C.

A.C. Impedance Bridge Measurements

The impedance of the electrical double layer at a mercury-0.1N perchloric acid-0.001N potassium chloride solution interphase was investigated at temperatures of 0°, 25°, 50° and 75° C. at frequencies of 250, 500, 750, 1000, 5000 and 9200 cycles, respectively, by means of an a.c. impedance

Table 5. Dependence of apparent differential capacity at the mercury-solution interface at 25° C. on polarizing potential, frequency and concentration of pentanol-1 in 0.1N $HClO_4$. Capacity in μ f/cm^2. Potential in minus volts relative to Ag-AgCl in 0.001N chloride solution

Frequency 230 cycles/sec.

	Reduced concentration				
Polarization	0.0	0.075	0.15	0.30	0.60
.026	64.2	64.1	--	68.1	
.028					87.4
.078	51.1	53.4	57.7	59.8	
.084					84.0
.130	44.6	48.1	53.4	59.7	
.140					54.7
.208	40.2	44.7	51.5	64.1	
.224					32.8
.260	38.7	45.1	54.7	50.8	
.280					28.0
.338	38.0	50.6	40.1	31.8	
.364					25.9
.390	38.4	46.3	32.7	28.7	
.420					25.2
.468	38.8	31.9	29.3	27.2	
.504					24.6
.520	38.7	29.0	28.5	26.8	
.560					24.5
.598	36.2	27.8	27.9	26.6	
.644					24.2
.650	34.5	27.6	27.8	26.6	
.700					24.5
.728	33.2	27.7	27.8	26.5	
.780	32.2	27.9	27.8	26.6	
.784					24.5
.840					24.5
.858	30.9	29.0	28.0	26.8	
.924					24.6
.910	30.5	30.2	28.4	27.1	
.980					24.9
.988	29.9	33.2	29.5	27.6	
1.040	29.8	35.2	30.7	28.4	
1.064					25.2
1.118	29.7	35.4	34.1	31.2	
1.120					25.4
1.170	29.7	34.5	36.7	36.1	
1.204					26.6
1.248	29.9	33.6	38.0	44.6	
1.260					28.7
1.300	30.1	32.9	37.4	45.0	
1.344					34.8
1.400					37.1

Table 6. Dependence of apparent differential capacity at the mercury-solution interface at 25° C. on polarizing potential, frequency and concentration of pentanol-1 in 0.1N $HClO_4$. Capacity in μ f/cm^2. Potential in minus volts relative to Ag-AgCl in 0.001N chloride solution

Frequency 500 cycles/sec.

	Reduced concentration				
Polarization	0.0	0.075	0.15	0.30	0.60
.026	58.8	56.5	57.3	57.3	
.028					67.2
.078	46.1	45.2	47.9	49.8	
.084					76.1
.130	39.9	40.0	43.1	49.8	
.140					56.8
.208	34.8	36.1	45.5	61.0	
.224					25.1
.260	33.3	37.1	50.7	40.0	
.280					17.8
.338	32.8	41.4	28.6	21.1	
.364					13.3
.390	33.2	34.5	19.9	16.6	
.420					12.4
.468	33.7	20.6	15.4	13.9	
.504					11.8
.520	33.4	16.9	14.3	13.1	
.560					11.5
.598	31.6	15.0	13.7	12.7	
.644					11.4
.650	29.5	14.7	13.6	12.6	
.700					11.5
.728	26.8	15.0	13.7	12.7	
.780	25.5	15.6	14.0	12.8	
.784					11.6
.840					12.0
.858	24.0	17.7	14.8	13.1	
.910	23.3	19.9	15.8	13.5	
.924					12.7
.980					13.2
.988	22.7	24.3	18.9	14.7	
1.040	22.3	25.9	22.0	15.8	
1.064					14.9
1.118	22.0	25.4	28.5	19.7	
1.120					17.1
1.170	22.0	24.7	30.9	24.4	

Table 7. Dependence of apparent differential capacity at the mercury-solution interface at 25° C. on polarizing potential, frequency and concentration of pentanol-1 in 0.1N $HClO_4$. Capacity in μ f/cm^2. Potential in minus volts relative to Ag-AgCl in 0.001N chloride solution

Frequency 750 cycles/sec.

Polarization	Reduced concentration				
	0.0	0.075	0.15	0.30	0.60
.026	50.4	48.6	49.3	56.9	
.028					59.9
.078	41.0	40.4	41.8	51.3	
.084					64.5
.130	35.5	36.0	38.5	51.3	
.140					53.6
.208	30.9	32.6	40.4	57.8	
.224					24.4
.260	29.5	33.3	44.6	39.3	
.280					16.3
.338	28.9	36.5	26.1	19.8	
.364					11.4
.390	29.4	30.3	17.3	14.9	
.420					10.1
.468	29.8	17.5	12.4	11.7	
.504					9.2
.520	29.6	13.1	11.1	11.0	
.560					9.0
.598	27.8	11.8	10.4	10.6	
.644					8.7
.650	25.8	11.4	10.3	10.6	
.700					8.9
.728	23.0	11.7	10.4	10.6	
.780	21.8	12.4	10.6	10.9	
.784					9.0
.840					9.4
.858	20.5	14.5	11.8	11.7	
.910	19.8	16.7	12.7	12.4	
.924					10.1
.980					10.9
.988	19.1	20.8	15.9	14.1	
1.040	18.7	22.4	19.5	16.6	
1.064					12.4
1.118	18.6	22.1	26.0	23.1	
1.120					14.7
1.170	18.4	21.3	27.2	30.6	

Table 8. Dependence of apparent differential capacity at the mercury-solution interface at 25° C. on polarizing potential, frequency and concentration of pentanol-1 in 0.1N $HClO_4$. Capacity in μ f/cm^2. Potential in minus volts relative to Ag-AgCl in 0.001N chloride solution

Frequency 1000 cycles/sec.

	Reduced concentration				
Polarization	0.0	0.075	0.15	0.30	0.60
.026	40.6	44.4	42.8	44.3	48.1
.078	34.9	38.0	43.3	40.8	51.1
.130	31.0	34.3	34.9	40.3	50.6
.208	27.3	31.6	36.2	43.9	27.6
.260	26.0	31.5	37.9	32.8	15.0
.338	25.6	34.2	23.4	16.7	11.1
.390	25.8	31.0	15.5	12.1	9.3
.468	26.3	18.0	10.8	9.6	8.0
.520	26.3	13.7	9.8	8.8	7.6
.598	24.6	11.0	9.0	8.4	7.4
.650	22.8	10.4	8.9	8.4	7.4
.728	20.4	10.4	9.0	8.4	7.5
.780	19.2	10.9	9.3	8.6	7.6
.858	17.8	12.6	10.1	9.1	7.9
.910	17.3	14.4	11.0	9.6	8.3
.988	16.6	18.3	13.4	10.9	9.0
1.040	16.3	20.5	16.0	12.5	9.8
1.118	16.1	21.6	21.5	16.6	11.8
1.170	16.1	21.0	24.0	21.0	14.3
1.248	16.1	19.9	24.3	28.6	21.7
1.300	16.3	19.5	22.9	30.3	30.8

Figure 14. Apparent specific capacity of the electrical double layer for pentanol-1 on mercury in 0.1N perchloric acid solution versus polarizing potential at 25° C. for a frequency of 230 cycles

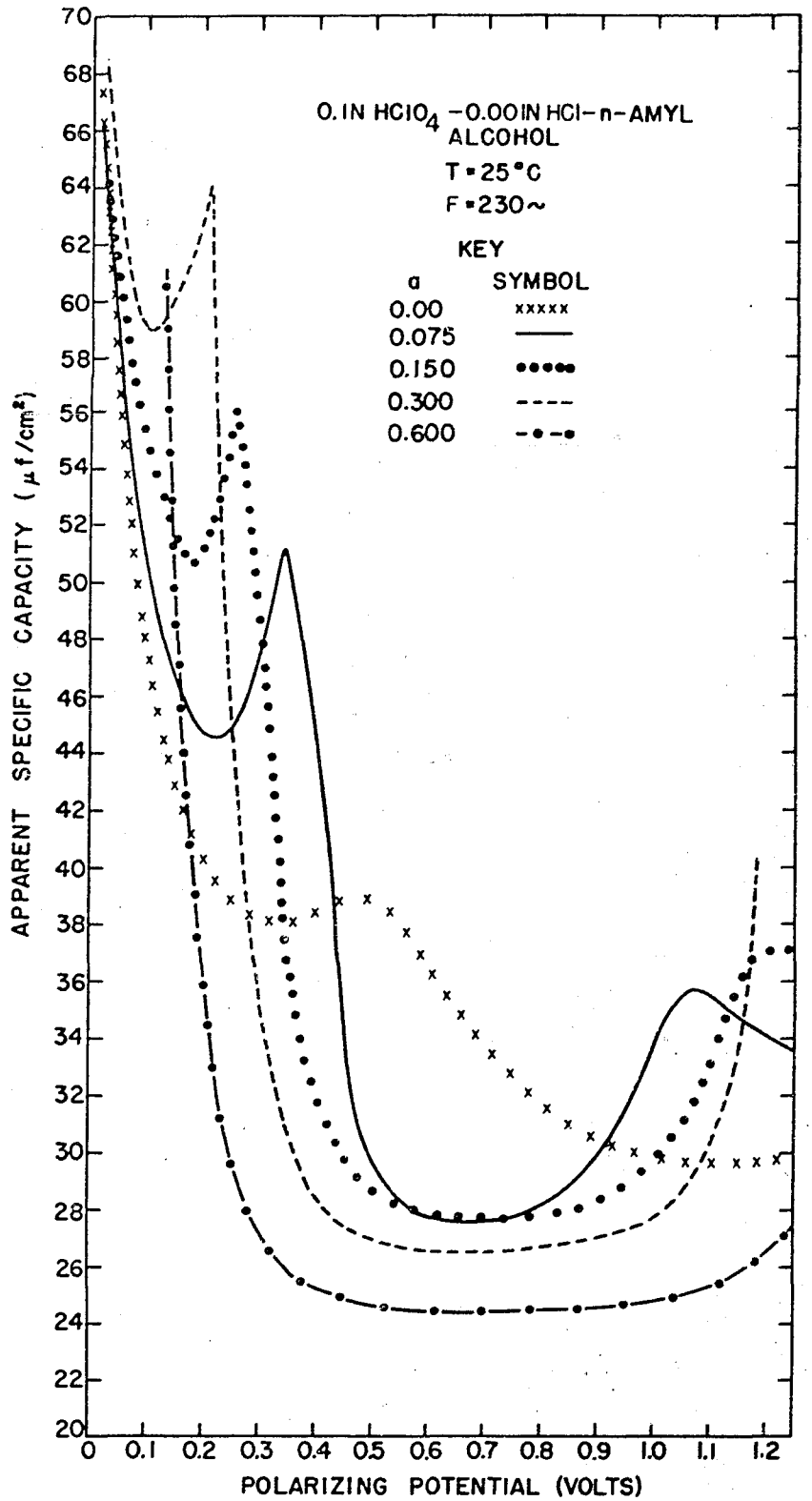
0.1N HClO4 -0.00IN HCl-n-AMYL ALCOHOL
T=25°C
F=230~
KEY
a SYMBOL
0.00 xxxxx
0.075 ——
0.150 ●●●●●
0.300 - - - -
0.600 -●-●
APPARENT SPECIFIC CAPACITY (μf/cm²)
POLARIZING POTENTIAL (VOLTS)
70
68
66
64
62
60
58
56
54
52
50
48
46
44
42
40
38
36
34
32
30
28
26
24
22
20
0
0.1
0.2
0.3
0.4
0.5
0.6
0.7
0.8
0.9
1.0
1.1
1.2

Figure 15. Apparent specific capacity of the electrical double layer for pentanol-1 on mercury in 0.1N perchloric acid solution versus polarizing potential at 25° C. for a frequency of 500 cycles

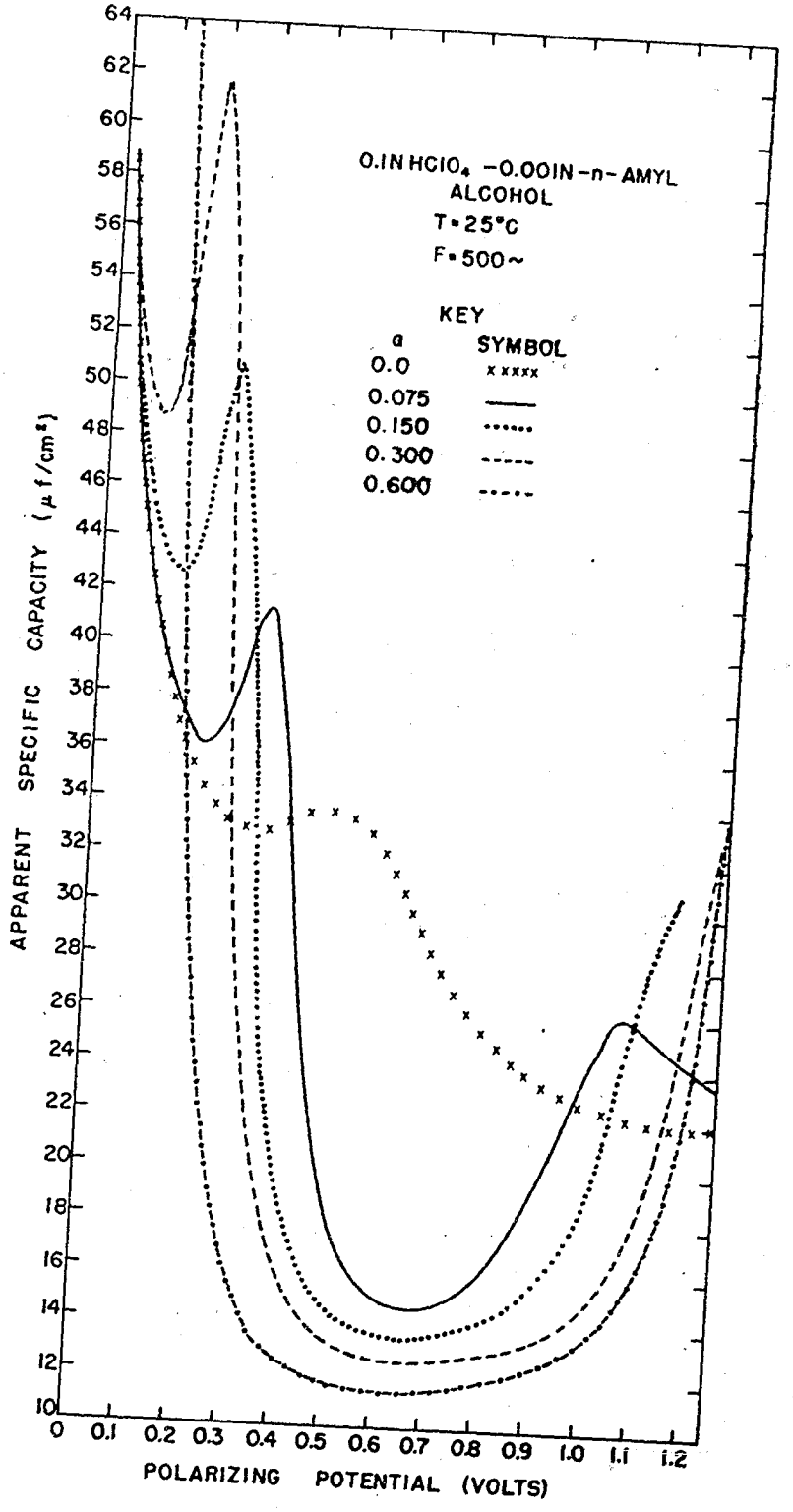
0.1N HClO4 -0.00IN-n-AMYL ALCOHOL
T=25°C
F=500~
KEY
a SYMBOL
0.0 xxxxx
0.075 ——
0.150 .....
0.300 - - - -
0.600 - . - .
APPARENT SPECIFIC CAPACITY (μf/cm²)
POLARIZING POTENTIAL (VOLTS)
64
62
60
58
56
54
52
50
48
46
44
42
40
38
36
34
32
30
28
26
24
22
20
18
16
14
12
10
0 0.1 0.2 0.3 0.4 0.5 0.6 0.7 0.8 0.9 1.0 1.1 1.2

Figure 16. Apparent specific capacity of the electrical double layer for pentanol-1 on mercury in 0.1N perchloric acid solution versus polarizing potential at 25° C. for a frequency of 750 cycles

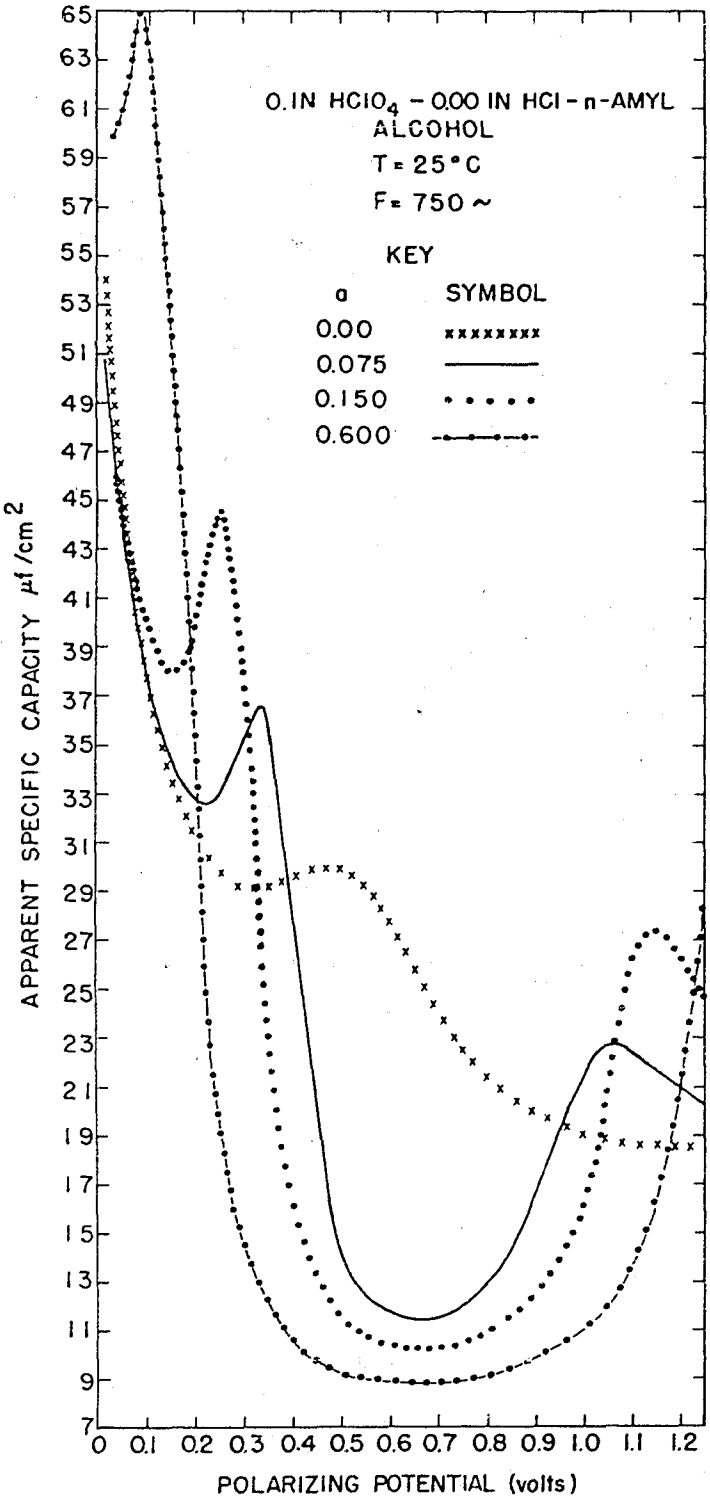
0.1N HClO4 – 0.00 IN HCl – n-AMYL ALCOHOL
T = 25°C
F = 750 ~
KEY
a SYMBOL
0.00
0.075
0.150
0.600
APPARENT SPECIFIC CAPACITY μf/cm²
POLARIZING POTENTIAL (volts)
65 63 61 59 57 55 53 51 49 47 45 43 41 39 37 35 33 31 29 27 25 23 21 19 17 15 13 11 9 7
0 0.1 0.2 0.3 0.4 0.5 0.6 0.7 0.8 0.9 1.0 1.1 1.2

Figure 17. Apparent specific capacity of the electrical double layer for pentanol-1 on mercury in 0.1N perchloric acid solution versus polarizing potential at 25° C. for a frequency of 1000 cycles

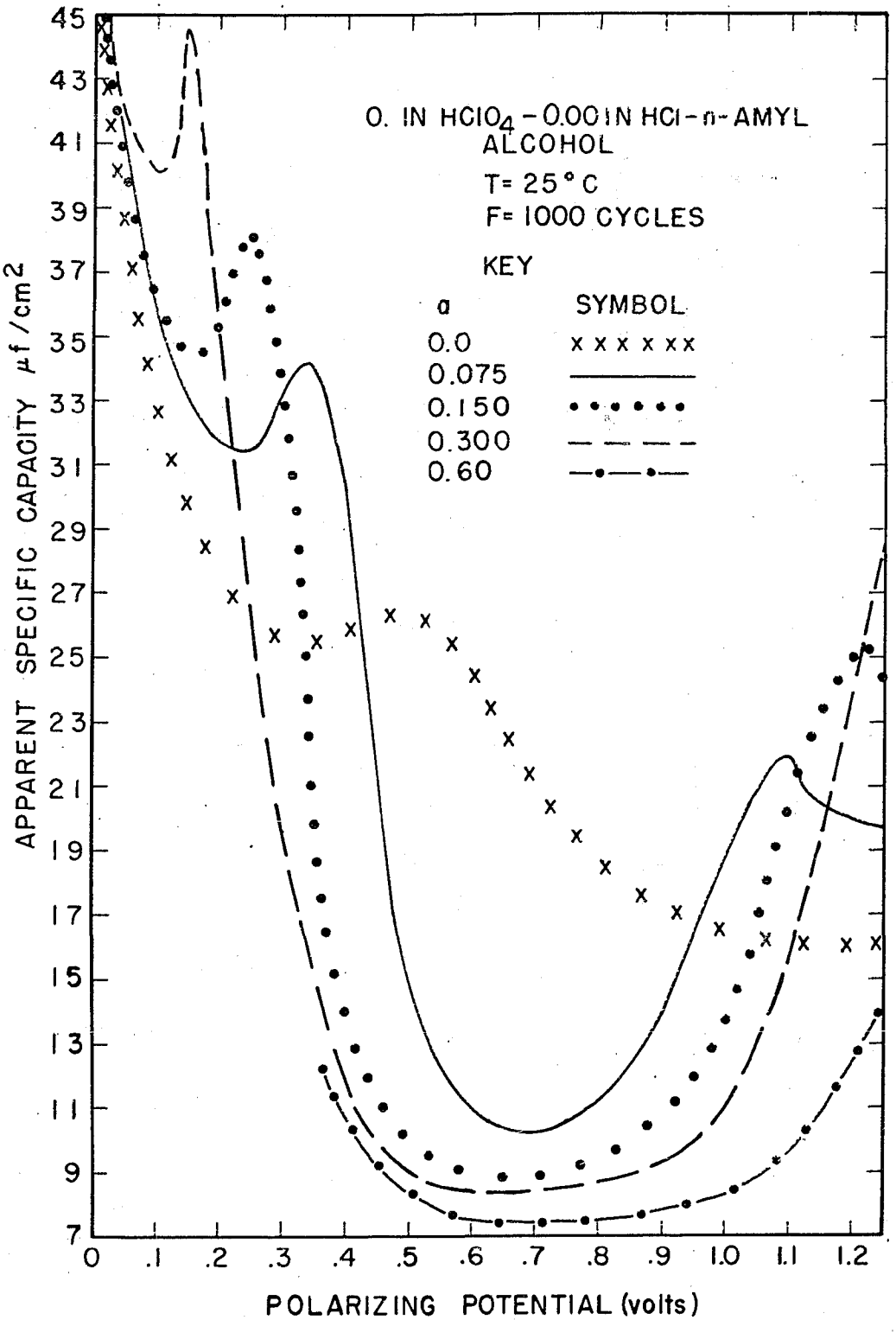
0. IN $HClO_4$ – 0.001N HCl – n-AMYL ALCOHOL
T= 25° C
F= 1000 CYCLES
KEY
a SYMBOL
0.0
0.075
0.150
0.300
0.60
APPARENT SPECIFIC CAPACITY μf/cm²
POLARIZING POTENTIAL (volts)
45
43
41
39
37
35
33
31
29
27
25
23
21
19
17
15
13
11
9
7
0
.1
.2
.3
.4
.5
.6
.7
.8
.9
1.0
1.1
1.2

bridge. One set of frequency data was recorded at each temperature. The impedance of the cell was measured in terms of an equivalent impedance consisting of a series combination of a resistance and capacitance. The solution resistance was obtained by extrapolating to infinite frequency a plot of the observed series specific resistance, R_m, at fixed polarization versus the reciprocal of the angular frequency at every temperature investigated. The equivalent series impedance of the electrical double layer was obtained by subtracting the solution resistance from the total impedance measured. The series impedances were then converted into the equivalent parallel impedances by the transformation equations

$$Rp = \left[(1 + \theta^2)/\theta^2\right] Rs$$

$$Cp = \left[\theta/(1 + \theta^2)\right] 1/\omega Rs$$

$$\theta = \omega RsCs$$

to conform to the analog circuit of Figure 1A. Since Rs and Cs were reported as specific quantities, Rp and Cp were also specific quantities. All calculations were conducted on an IBM 650 digital computer. The values for the solution resistances found at the temperatures investigated for 0.1-1 N perchloric acid-0.001N potassium chloride solutions are presented in Table 9 and the equivalent parallel specific capacity and specific resistance corresponding to the equivalent circuit of Figure 1A are presented in Tables 10 to 13.

Table 9. The solution resistance of a 0.1N perchloric acid solution as a function of the temperature

Temperature °C.	R^* ohms - cm^2
0	36.4
25	22.9
50	16.5
75	13.4

All polarizing potentials are relative to the silver-silver chloride-0.001N chloride reference electrode at the temperature reported.

In the experiments performed on the a.c. impedance bridge, θ was of the order of magnitude of 0.1. The estimated precision measure of the observed series capacity, Cb, was at most one per cent. The precision measure of the actually observed values of Rb, the series resistance in the measuring arm of the bridge was somewhat greater but was never more than three per cent. Using these estimates for the precision measures, it is seen from the form of the transformation equations that the precision value for Cp will be about that of Cs or one per cent at most. However, since Ro was obtained by subtracting the solution resistance, R^*, from Rb, the precision measure of Rs will be about six per cent.

Table 10A. The dependence of the specific capacity of the electrical double layer at the mercury-0.1N perchloric acid solution interphase versus polarizing potential for several frequencies at a temperature of 0° C. Capacity in $\mu f/cm^2$. Polarizing potential in minus volts relative to the Ag-AgCl electrode at the same operating temperature

Polarizing potential	Frequency				
	250	500	750	1000	9200
.05	33.8	32.7	32.4	31.9	28.5
.10	28.5	28.0	27.9	27.8	26.3
.15	25.8	25.5	25.4	25.5	24.2
.20	24.2	24.1	24.0	24.2	23.3
.25	23.5	23.4	23.4	23.4	23.0
.30	23.5	23.5	23.4	23.5	23.2
.35	24.1	24.2	24.1	24.2	24.0
.40	25.5	25.5	25.4	25.5	25.3
.45	27.3	27.3	27.2	27.3	27.1
.50	29.3	29.3	29.1	29.3	28.9
.55	30.9	30.8	30.7	30.8	30.4
.60	31.3	31.3	31.2	31.3	30.7
.65	30.2	30.0	30.0	30.0	29.7
.70	27.6	27.5	27.4	27.4	27.2
.75	24.6	24.6	24.5	24.5	24.4
.80	22.0	22.0	21.9	21.8	21.8
.85	20.1	20.1	20.0	20.0	19.9
.90	18.7	18.7	18.6	18.7	18.6
.95	17.6	17.6	17.6	17.6	17.6
1.00	16.8	16.8	16.8	16.9	16.8
1.05	16.2	16.3	16.2	16.3	16.2
1.10	15.8	15.8	15.7	15.8	15.8
1.15	15.3	15.4	15.4	15.6	15.4

Table 10B. The dependence of the specific resistance of the electrical double layer at the mercury-0.1N perchloric acid solution interphase versus polarizing potential for several frequencies at a temperature of 0° C. Resistance in ohm-cm^2. Polarizing potential in minus volts relative to a Ag-AgCl electrode at the same operating temperature

Polarizing potential	Frequency				
	250	500	750	1000	9200
.05	272	137	60.5	57.8	7.0
.10	499	263	115	103	8.9
.15	644	379	165	133	11.6
.20	899	559	241	185	14.0
.25	1126	750	320	254	18.5
.30	1200	804	341	288	18.1
.35	1202	821	347	287	17.0
.40	1253	789	332	275	15.3
.45	1236	721	303	256	13.4
.50	1175	644	270	223	11.7
.55	1130	609	255	201	9.3
.60	1122	592	247	202	9.0
.65	1167	640	268	227	11.1
.70	1267	728	305	272	13.2
.75	1369	871	366	354	16.4
.80	1400	940	399	400	20.7
.85	1638	1124	476	460	24.6
.90	1710	1252	531	514	28.2
.95	1719	1304	555	594	36.8
1.00	1741	1333	569	629	40.4
1.05	1621	1323	567	655	43.6
1.10	1641	1302	559	692	46.1
1.15	1637	1347	579	751	57.9

Table 11A. The dependence of the specific capacity of the electrical double layer at the mercury-0.1N perchloric acid solution interphase versus polarizing potential for several frequencies at a temperature of 25° C. Capacity in μ f/cm^2. Polarizing potential in minus volts relative to the Ag-AgCl electrode at the same operating temperature

Polarizing potential	Frequency					
	250	500	750	1000	5000	9200
.05	36.0	35.8	35.0	35.0	31.9	30.3
.10	29.8	30.2	29.7	29.8	28.2	27.4
.15	26.6	27.1	26.8	26.8	26.2	25.6
.20	24.8	25.4	25.2	25.2	24.9	24.7
.25	24.0	24.6	24.4	24.5	24.4	24.2
.30	23.9	24.6	24.4	24.5	24.4	24.2
.35	24.4	25.1	25.0	25.0	25.0	24.9
.40	25.2	26.0	25.9	25.8	26.0	25.7
.45	26.1	26.8	26.9	26.6	27.1	26.6
.50	26.4	27.2	27.7	26.8	27.9	27.1
.55	26.4	27.2	28.0	26.0	28.1	27.3
.60	25.3	26.5	27.4	24.8	27.7	26.9
.65	23.5	25.1	25.9	23.3	26.1	25.5
.70	20.4	23.1	23.8	21.6	23.7	23.5
.75	18.7	21.4	21.8	20.3	21.3	21.5
.80	18.0	19.9	20.2	19.0	19.7	20.0
.85	17.3	18.7	19.0	18.0	18.6	18.8
.90	16.7	17.8	18.1	17.4	17.8	18.0
.95	16.3	17.1	17.4	16.9	17.4	16.9
1.00	15.8	16.7	16.8	16.5	16.6	16.5
1.05	15.5	16.3	16.4	16.1	16.1	16.1
1.10	15.3	15.0	16.0	15.9	15.8	15.8
1.15	15.1	15.7	15.7	15.7	15.4	15.4

Table 11B. The dependence of the specific resistance of the electrical double layer at the mercury-0.1N perchloric acid solution interphase versus polarizing potential for several frequencies at a temperature of 25° C. Resistance in ohm-cm^2. Polarizing potential in minus volts relative to a Ag-AgCl electrode at the same operating temperature

Polarizing potential	Frequency					
	230	500	750	1000	5000	9200
.05	260	96.9	80.0	56.4	11.7	2.6
.10	477	238	152	114	20.4	3.4
.15	650	369	215	190	30.1	4.1
.20	878	567	306	290	45.3	4.8
.25	1131	775	447	412	74.6	5.3
.30	1242	926	564	497	74.3	5.6
.35	1313	933	623	531	87.6	5.2
.40	1316	1026	714	559	81.1	4.9
.45	1356	1102	728	606	74.7	4.6
.50	1374	1067	814	556	70.5	4.2
.55	1376	1101	851	465	69.1	3.9
.60	1403	1159	950	457	71.5	4.5
.65	1626	1213	993	550	105.3	5.0
.70	1873	1433	985	799	127.8	5.9
.75	2278	1661	1012	1122	120.6	6.7
.80	2151	1800	1179	1390	184.5	7.8
.85	2164	2263	1469	1421	158.0	8.8
.90	2144	2131	1458	1229	172.0	9.7
.95	2125	2302	1386	1159	180.4	11.0
1.00	2044	1922	1319	1040	160.8	11.0
1.05	1812	1885	1303	946	170.4	11.6
1.10	1692	1801	1315	869	219.7	12.0
1.15	1425	1551	1175	725	106.1	12.6

Table 12A. The dependence of the specific capacity of the electrical double layer at the mercury-0.1N perchloric acid solution interphase versus polarizing potential for several frequencies at a temperature of 50° C. Capacity in $\mu f/cm^2$. Polarizing potential in minus volts relative to the Ag-AgCl electrode at the same operating temperature

Polarizing potential	Frequency					
	250	500	750	1000	5000	9200
.05	39.3	40.4	37.0	36.7	34.0	27.9
.10	31.7	33.2	30.8	30.7	28.9	26.7
.15	28.3	29.7	27.5	27.6	26.6	25.1
.20	26.0	27.5	25.6	25.8	25.3	24.0
.25	24.5	26.3	24.6	24.4	24.4	23.4
.30	24.1	26.0	24.3	24.6	24.2	23.3
.35	24.0	26.0	24.4	24.7	24.4	24.0
.40	24.2	26.4	24.7	25.2	24.8	23.9
.45	24.5	26.8	25.1	25.6	24.7	24.3
.50	24.4	27.0	25.2	25.8	25.5	24.4
.55	23.8	26.6	24.8	25.4	25.1	24.2
.60	22.6	25.5	23.8	24.4	23.9	23.2
.65	20.9	23.8	22.1	22.7	22.4	21.7
.70	19.2	22.0	20.3	20.9	20.6	19.9
.75	17.7	20.5	18.8	19.4	19.2	18.5
.80	16.4	19.3	17.7	18.2	18.1	17.4
.85	15.7	18.3	17.0	17.2	17.2	16.8
.90	15.4	17.7	16.4	16.6	16.3	16.2
.95	15.1	17.2	16.0	16.0	16.1	15.7
1.00	15.1	16.8	15.7	15.6	15.7	15.4
1.05	14.9	16.5	15.5	15.3	15.3	15.1
1.10	14.8	16.3	15.3	15.1	15.1	14.9
1.15	14.8	16.0	15.1	15.0	15.0	14.8

Table 12B. The dependence of the specific resistance of the electrical double layer at the mercury-0.1N perchloric acid solution interphase versus polarizing potential for several frequencies at a temperature of 50° C. Resistance in ohm-cm^2. Polarizing potential in minus volts relative to a Ag-AgCl electrode at the same operating temperature

Polarizing potential	Frequency					
	230	500	750	1000	5000	9200
.05	226	118	68.8	48.9	5.1	1.7
.10	380	252	141	99.7	9.2	2.9
.15	396	330	207	142	11.7	3.7
.20	684	707	331	234	15.3	4.3
.25	1027	1185	457	277	17.2	4.6
.30	1219	1461	540	328	21.4	4.8
.35	1274	1920	663	446	21.0	4.5
.40	1300	2100	645	452	20.3	4.6
.45	1403	2704	710	485	20.5	4.4
.50	1465	3533	773	506	20.4	4.4
.55	1478	4092	882	553	21.0	4.7
.60	1604	5143	1015	602	20.8	4.9
.65	1707	3773	1050	654	23.6	5.6
.70	1979	2282	1187	658	26.5	6.4
.75	2427	3010	1456	848	30.7	7.7
.80	2530	6145	1567	1021	34.7	8.7
.85	2478	6199	1631	1070	38.1	9.4
.90	2322	6135	1590	1097	42.5	10.1
.95	2238	5224	1545	1061	43.7	10.7
1.00	2144	3978	1381	901	45.0	11.2
1.05	1886	3126	1217	762	48.0	11.6
1.10	1655	2327	1011	662	49.5	12.4
1.15	1380	1502	871	656	50.4	12.1

Table 13A. The dependence of the specific capacity of the electrical double layer at the mercury-0.1N perchloric acid solution interphase versus polarizing potential for several frequencies at a temperature of 75° C. Capacity in $\mu f/cm^2$. Polarizing potential in minus volts relative to the Ag-AgCl electrode at the same operating temperature

Polarizing potential	Frequency				
	250	500	750	1000	9200
.05	43.0	42.7	39.9	40.9	33.7
.10	34.1	34.2	32.6	33.4	29.9
.15	30.2	29.5	28.8	29.2	27.5
.20	27.4	26.6	26.5	26.6	25.9
.25	25.5	24.7	25.2	25.0	25.5
.30	24.6	23.7	24.6	24.1	24.5
.35	24.1	22.9	24.3	23.5	24.5
.40	23.7	22.2	24.1	23.0	24.4
.45	23.4	21.6	23.9	22.5	24.1
.50	22.8	21.0	23.4	21.8	23.6
.55	21.9	20.2	22.6	21.0	22.7
.60	20.5	19.1	21.2	19.9	21.2
.65	19.0	18.0	19.7	18.6	19.8
.70	17.6	16.8	18.2	17.3	18.5
.75	16.1	15.8	17.0	16.2	17.4
.80	15.4	14.9	16.1	15.3	16.6
.85	14.9	14.3	15.5	14.7	16.0
.90	14.5	14.6	15.2	14.4	15.5
.95	14.3	13.9	14.9	14.3	15.3
1.00	14.2	13.9	14.7	14.2	15.0
1.05	14.2	14.0	14.6	14.1	14.9
1.10	14.2	14.0	14.6	14.1	14.8
1.15	14.6	14.3	14.6	14.1	14.8

Table 13B. The dependence of the specific resistance of the electrical double layer at the mercury-0.1N perchloric acid solution interphase versus polarizing potential for several frequencies at a temperature of 75° C. Resistance in ohm-cm^2. Polarizing potential in minus volts relative to a Ag-AgCl electrode at the same operating temperature

Polarizing potential	Frequency				
	250	500	750	1000	9200
.05	176	92.3	55.3	45.1	2.8
.10	269	208	111	105	4.5
.15	308	373	166	203	6.1
.20	605	718	284	400	8.0
.25	880	1059	412	686	9.8
.30	1023	1259	496	802	11.9
.35	1201	1479	541	1004	10.7
.40	1360	1528	603	1044	11.9
.45	1458	1664	614	1348	11.1
.50	1534	1659	662	1161	11.5
.55	1387	1166	606	794	12.5
.60	1670	1683	757	1176	13.0
.65	1883	2075	876	1601	15.0
.70	1911	2128	987	1684	17.2
.75	2373	2248	1359	1931	19.5
.80	2661	4036	1575	3295	23.4
.85	2599	4377	1561	3542	25.2
.90	2444	3634	1848	3710	26.6
.95	2304	3785	1643	3794	27.7
1.00	2001	3670	1469	3044	28.5
1.05	1634	3149	1293	2536	29.0
1.10	1173	2151	921	1506	29.3
1.15	951	1079	617	845	26.8

By simple differentiation of the transformation equation for Rp, the precision estimate, K, for Rp is found to be

$$K = 100 \times \Delta Rp/Rp = \left[2\Delta Cp/Cs + \Delta Ro/Rs \right] \times 100 \text{ per cent}$$

which amounts to about eight per cent maximum error when the previous precision estimates are introduced. Thus, for θ^2 small compared to unity, little uncertainty is observed in the values for the differential double layer capacity. However, the propagation of errors in the computation of Rp can result in a maximum error as great as eight per cent.

DISCUSSION

Interpretation of Results Obtained in the Absence of Adsorbable Materials

A most striking and unexpected result is illustrated in Figure 10 in which the apparent capacity versus polarization curves for the primitive solutions at 25° C. are plotted over a fourfold frequency range. The observed decrease in apparent capacity with increasing frequency appears to present an anomaly when compared to the results obtained from the a.c. impedance bridge experiments. This is quite apparent from Figure 18 in which no appreciable dispersion of the differential double layer capacity obtained from a.c. impedance bridge experiments on the same primitive solutions at 25° C. is observed over a twenty-fold variation of the frequency. Indeed, these curves are very nearly identical within the experimental error in agreement with the results reported by other investigators (28). This anomaly was resolved by the application of classical dielectric theory to the capacity of the compact region of the electrical double layer.

It was assumed initially that the dielectric material contained between the planes of charge consisting of the surface charge on the metal side of the compact region of the electrical double layer and the counterions on the solution side of the double layer consists of two different

Figure 18. Differential double layer capacity on mercury in 0.1N perchloric acid solution versus polarizing potential at 25° C. for several operating frequencies obtained with the a.c. impedance bridge

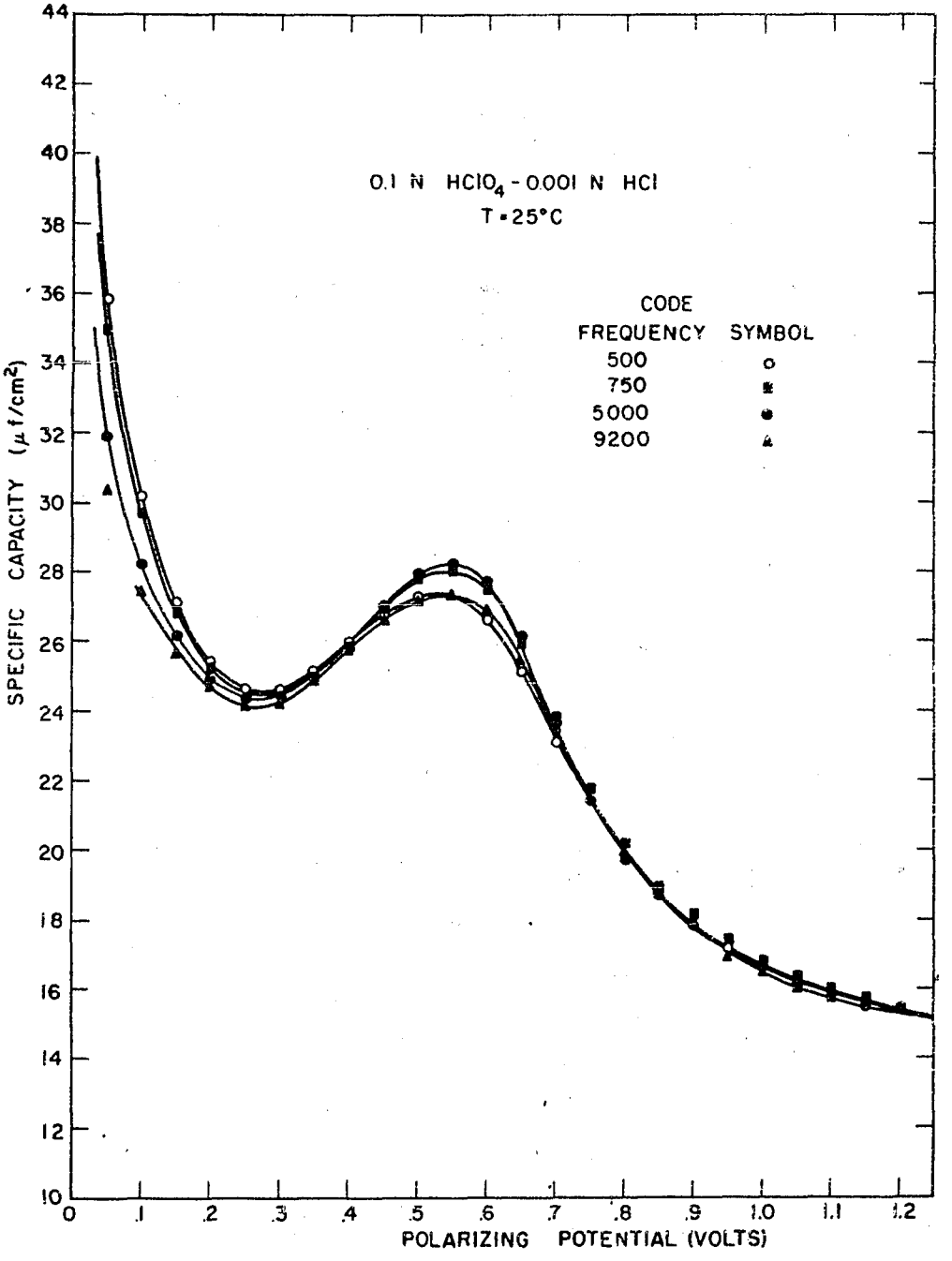
0.1 N $HClO_4$ - 0.001 N HCl
T = 25°C
CODE
FREQUENCY SYMBOL
500
750
5000
9200
SPECIFIC CAPACITY (μf/cm^2)
POLARIZING POTENTIAL (VOLTS)
44
42
40
38
36
34
32
30
28
26
24
22
20
18
16
14
12
10
0
.1
.2
.3
.4
.5
.6
.7
.8
.9
1.0
1.1
1.2

species of solvent molecules. One species was considered "bound" in the sense that the dipoles lose a degree of orientational freedom because the molecule is physically restricted by the field and forces due to adsorption at the interface. The other species possesses the orientational freedom of the bulk molecules and in this sense was considered "free". Each of these species of molecules is associated with a particular relaxation time τ which is an index of the ease with which the dipole of the molecule is able to rotate in the presence of an alternating field. Using this assumption, it is possible to represent the observed frequency dispersion of the apparent capacity quantitatively.

From the classical macroscopic theory of the behavior of homogeneous dielectrics in a time-dependent electric field, the time dependence of the electric displacement which can be derived from the principle of superposition of relaxation times as shown by Fröhlich (55) is given by:

$$D(t) = \epsilon_\infty E(t) + \int_0^t E(u)\alpha(t - u)du \qquad (8)$$

where $\alpha(u)$ is the decay function describing the gradual decrease of D upon the removal of an applied external field, ϵ_∞ is the optical dielectric constant, and E is the field. By applying Maxwell's equation for the dielectric displacement current,

$$i = \frac{A}{4\pi} dD/dt \qquad (9)$$

one obtains the basic equation for the behavior of the displacement current in the presence of a time dependent field:

$$i = \frac{A}{4\pi}\left[\epsilon_\infty \, dE(t)/dt + \int_0^t \frac{\partial E(u)}{\partial u} \alpha(t - u)du\right] \quad (10)$$

If the decay function is assumed to be of exponential form as originally proposed by Debye (56) in the classical theory of dielectric relaxation phenomena, then

$$\alpha(t) = \frac{\Delta\epsilon}{\tau} \exp(- t/\tau) \quad (11)$$

where $\Delta\epsilon = \epsilon_o - \epsilon_\infty$ and τ is the relaxation time or the time required for the field inside the dielectric to decay to 1/e of the value at the instance of cessation of the external electric field. The solution of Equation 10 for the displacement current in the presence of a periodic triangular field given by

$$\begin{aligned} E(t) &= \frac{E^o \omega}{\pi} \cdot t \qquad && o < t < \pi/\omega \\ &= E^o \omega/\pi(2\pi/\omega - t) \qquad && \pi/\omega < t < 2\pi/\omega \\ E(t) &= E(2\pi/\omega + t) \end{aligned} \quad (12)$$

can be obtained. Performing the integration indicated in Equation 10 for the case in which the measurement ends on the first half cycle of the triangular field and ignoring transients, the steady-state current is obtained:

$$i_{ss} = \frac{A}{4\pi}\left[\epsilon_{\infty} dE(t)/dt + \frac{\Delta\epsilon\,\omega\,E^{o}}{\pi}\left\{1 - \sum_{n=1}^{2m}(-1)^{n} \cdot 2 \cdot e^{n\pi/\omega\tau} - t/\tau\right\}\right] . \quad (13)$$

Since this is the current flowing through the capacitor, it is also the current flowing through the standard resistance in series with the capacitor in the measuring circuit of Figure 2. The response of the instrument to this current is obtained by taking a time average of all instantaneous responses over a half period of the triangular field:

$$\bar{R} = \frac{G\,\omega}{\pi}\int_{2n\pi/\omega}^{(2n+1)\pi/\omega} i_{ss} \cdot R_{s}\, dt$$

$$= \frac{GAE^{o}\omega\,R_{s}}{4\pi^{2}}\left[(\epsilon_{\infty} + \Delta\epsilon) - \frac{2\Delta\epsilon\,\omega\tau}{\pi}\tanh(\pi/2\omega\tau)\right] \quad (14)$$

For the case in which the measurement ends on the last half cycle of the triangular field, the steady-state current reverses sign indicating the reversal on the direction of polarization. The absolute value of the response remains the same, however.

Considering the $\lim_{\omega\tau\to 0}\bar{R} = K(\epsilon_{\infty} + \Delta\epsilon) = \bar{R}_{o}$ and $\lim_{\omega\tau\to\infty}\bar{R} = K(\epsilon_{\infty} + \Delta\epsilon - \Delta\epsilon) = \bar{R}_{\infty}$ where $K = GE\,\omega R_{s}/4\pi^{2}$, the relationship between the instrument response and frequency in the case of a homogeneous dielectric material is obtained which may be written in the following form:

$$(\bar{R}_o - \bar{R})/(\bar{R}_o - \bar{R}_\infty) = 1/x \tanh x \qquad (15)$$

where

$$x = \pi/2\omega\tau \quad .$$

To illustrate the relationship between Equation 14 for the response of the instrument to changing frequency and Equation 9 derived for the response of the instrument based upon the equivalent circuit of Figure 1E, it is noted that Equation 14 can be written in a form which includes as a frequency dependent dielectric coefficient the functions

$$\epsilon(\omega) = \epsilon_\infty + \Delta\epsilon - \frac{2\Delta\epsilon\,\omega\tau}{\pi} \cdot \tanh(\pi/2\omega\tau) \quad . \qquad (16)$$

One can now write

$$\bar{R} = GAE^o\omega\, R_s\, \epsilon(\omega)/4\pi^2 \quad . \qquad (17)$$

Assuming the field decreases linearly across the compact portion of the electrical double layer, this equation becomes

$$\bar{R} = GAV^o\omega\, R_s\, \epsilon(\omega)/4\pi^2 l \qquad (18)$$

where l is the thickness of the compact region. However, from classical dielectric theory, the capacity of a parallel plate capacitor of plate area A separated by a distance l, and filled with a dielectric material of dielectric constant $\epsilon(\omega)$ is given by

$$C = \frac{\epsilon(\omega)}{4\pi}\,\frac{A}{l} \quad . \qquad (19)$$

Substitution of the last equation into Equation 17 results in the following expression for the response

$$\overline{R} = \frac{GV^{o}\omega R_{s}C}{\pi} = a\ C \qquad (20)$$

which is precisely Equation 9 for the response of the instrument based upon the equivalent circuit of Figure 1E. The significance of the apparent capacity measured by the instrument is now clear for:

$$C_{app} = \epsilon(\omega)\ C_{dl} \qquad (21)$$

where C_{dl} is the capacity of the electrical double layer which would be measured in vacuo.

It is now assumed that the total capacity of the compact region of the electrical double layer consists of a parallel combination of capacitances associated with each species of molecule exhibiting a different relaxation time within the electrical double layer as shown by Hansen, Minturn and Hickson (15). A linear combination of responses of the form of Equation 15 must represent the total response of the instrument. Suppose the dielectric constants for the two species of molecules can be added linearly to give the observed dielectric constant, i.e., $\Delta\epsilon_1 + \Delta\epsilon_2 = \Delta\epsilon$, then the response function becomes

$$\overline{R}_o - \overline{R}/\overline{R}_o - \overline{R}_\infty = \frac{\Delta\epsilon_1}{\Delta\epsilon_1+\Delta\epsilon_2} \cdot \frac{2\omega\tau_1}{\pi} \tanh \frac{\pi}{2\omega\tau_1} + \frac{\Delta\epsilon_2}{\Delta\epsilon_1+\Delta\epsilon_2} \cdot \frac{2\omega\tau_2}{\pi} \tanh \frac{\pi}{2\omega\tau_2} \qquad (22)$$

or

$$1/4f(\bar{R}_o - \bar{R}/\bar{R}_o - \bar{R}_\infty) = \Phi_1 \tau_1 \tanh \frac{1}{4f\tau_1}$$

$$+ \Phi_2 \tau_2 \tanh 1/4f\tau_2 \qquad (23)$$

where f is the linear frequency. The latter equation indicates that the response of the instrument should exhibit a dispersion with frequency and can be used to establish the relaxation times of each species of water molecule within the compact layer if the response of the instrument to varying frequency is known.

Evaluation of the relaxation times can be accomplished experimentally through the use of Equation 23 by means of a treatment of the experimental data to be presented. Let

$$F(x) = 1/x \tanh x \qquad (24)$$

where

$$x = 1/4f\tau \quad .$$

Then, Equation 23 can be written in the following manner:

$$\bar{R}_o - \bar{R}/\bar{R}_o - \bar{R}_\infty = \Phi_1 F(x_1) + \Phi_2 F(x_2) \quad . \qquad (25)$$

For large values of the argument of F(x), <u>i.e.</u>, small values of f, F(x) is approximately equal to 1/x. Using this fact and recalling that $\Phi_1 + \Phi_2 = 1$, the previous equation becomes:

$$\bar{R}_o - \bar{R}/R_o - R_\infty = 1/x_1 + \Phi_2 \left[(x_1 - x_2)/x_1 x_2\right] \quad . \qquad (26)$$

Solving for $\bar{R}$, the observed response, and introducing the definition of x_1 and x_2 results in the linear relationship:

$$\bar{R}/4f = \bar{R}_o/4f - \tau_1 \left[1 - \Phi_2(1 - \tau_2/\tau_1)\right] (\bar{R}_o - \bar{R}_\infty) . \qquad (27)$$

Consequently, a plot of $\bar{R}/4f$ versus $1/4f$ for small values of f is a straight line of slope $\bar{R}_o$ and intercept b where:

$$b = -\tau_1 \left[1 - \Phi_2(1 - \tau_2/\tau_1)\right] (\bar{R}_o - \bar{R}_\infty) \quad . \qquad (28)$$

The response of the instrument at infinite frequency can be obtained by expanding F(x) in a power series. For small values of the argument terms of third order or greater may be neglected. Hence,

$$F(x) \approx 1 - x^2/3 \quad . \qquad (29)$$

Substituting the expansion of F(x) into Equation 25 and solving for $\bar{R}$, one obtains:

$$\bar{R} = \bar{R}_\infty + a(\bar{R}_o - \bar{R}_\infty)/48f^2 \quad . \qquad (30)$$

By plotting the response versus $1/f^2$ and extrapolating to infinite frequency, $\bar{R}_\infty$ is easily found.

From the values of the intercept b, $\bar{R}_o$ and $\bar{R}_\infty$, Φ_2 can be inferred if τ_1 and τ_2 are known. Thus,

$$\Phi_2 = \left[(b/\bar{R}_o - \bar{R}_\infty)\tau_1 + 1)\right] \tau_1/(\tau_1 - \tau_2) \quad . \qquad (31)$$

By arbitrarily selecting values of τ_1 and τ_2 which at any given frequency establishes $F(x_1)$ and $F(x_2)$ through Equation 24 and Φ_2 through Equation 31 the response function of Equation 23 can be computed. However, only one particular pair of values for τ_1 and τ_2 will represent the response function at two experimental frequencies and these are the true relaxation times. A check on the correctness of the values ultimately chosen to represent the data at any fixed polarization and temperature can be made by computing the responses at other frequencies and comparing these results with the observed values. It was not expected that the values of τ_1 and τ_2 would remain constant with polarization because the field across the double layer varies and hence, the degree of electrostriction of the molecules changes. Similarly, varying the temperature will also change the relaxation time by changing the thermal energy of the molecules. Consequently, it was necessary to repeat this curve fitting procedure at various polarizations and at several temperatures. The results of these calculations are presented in Table 14 where the relaxation times of each species and the quantity Φ_2 are tabulated at several polarizations and temperatures.

The assumption of two different species of water molecules within the compact region of the electrical double layer is not without precedence in the interpretation of

Table 14. Experimental evaluation of relaxation times

	Polarization	$\tau_1 x10^3$	$\tau_2 x10^4$	Φ_2
T = 0° C.	0.35	1.00	1.44	.309
	0.51	0.80	1.34	.354
	0.60	0.96	1.45	.346
T = 25° C.	0.20	1.00	0.94	.935
	0.35	1.03	1.21	.843
	0.51	1.30	1.26	.859
	0.60	1.06	1.27	.799
	0.67	0.48	1.13	.721
	0.80	0.48	1.06	.556
	1.00	1.67	1.61	.804
T = 50° C.	0.80	0.71	0.9	.160
T = 75° C.	0.35	7.50	1.72	.988
	0.51	2.20	1.73	.938
	0.60	1.10	1.82	.821

electrocapillary phenomena. In Figure 13 the dependence of the apparent capacity on temperature at constant frequency is illustrated. The significant observation to be made is the gradual disappearance of the "hump" in the capacity curves in the region of the electrocapillary maximum. This phenomenon was first investigated by Grahame (57, 58) who conducted a series of experiments on the effect of temperature and concentration on the capacity of the electrical double layer between mercury and aqueous sodium fluoride solutions. The occurrence of the "hump" was attributed to the formation of a pseudo-crystalline semi-rigid layer of solvent molecules at the mercury interface through which

anions pass with difficulty but which can be melted in a manner reminiscent of an amorphous material. The solvent molecules in this layer were supposed to have lost some of the rotational freedom available in the bulk liquid. This circumstance was offered as a partial explanation for the observed decrease of the dielectric coefficient of the substance comprising the compact portion of the double layer. An experimental observation of the slow melting of the pseudo-crystalline layer was made in 0.1N potassium nitrate solutions. The possibility of such phenomena was predicted from calculations based upon experimental values for the capacity of the compact region of the electrical double layer on mercury in sodium fluoride solutions coupled with the values of the diffuse double layer capacity computed from the theory of the electrical double layer. In all cases reported by Grahame the observed behavior closely resembled that of Figure 13 for the same effect observed in 0.1N perchloric acid solutions.

In a recent paper by Bockris and Conway (59) dealing with the determination of the Faradaic impedance at copper and mercury electrodes in aqueous potassium iodide solutions, the observed variation of the impedance of the electrical double layer at these interfaces was interpreted on the basis of dielectric loss. The observed frequency dispersion was quantitatively interpreted by assuming a relaxation time

for the solvent molecules of 10^{-8} seconds on mercury and 10^{-7} seconds on copper. These values which are considerably smaller than those reported in Table 14 were obtained, however, by including an additional adjustable parameter in deriving the loss relationships by the procedure of Cole and Cole (60) and assuming only one type of solvent species to be present in the compact double layer. However, the inclusion of such an adjustable parameter can be avoided in the calculations and the impedances represented quantitatively just as well by the classical Debye approach if one assumes the presence of two species of solvent molecules within the compact region of the electrical double layer as was done in this investigation. Values found by Hansen and Hickson (7) for the respective relaxation times of the two species of water molecules computed from Equations 8 and 9 of reference (59) or by the application of the method used by Debye (56) for computing the various components of the impedance vector were 3.58×10^{-4} sec. and 9.8×10^{-3} sec. which are in excellent agreement with the values reported in Table 14 of this investigation.

An attempt was made to represent the impedance data for the mercury-0.1N perchloric acid-0.001N potassium chloride solution interface which were obtained from the a.c. impedance bridge experiments reported herein by use of the same treatment which was applied by Hansen and Hickson (7) to the data

for impedances recorded at mercury-aqueous potassium iodide solution interphases by Bockris and Conway. Since the double layer capacitance exhibits no dispersion with frequency, representation of the data must be accomplished through the frequency dispersion observed in the resistance of the electrical double layer. Unfortunately, the solution resistance in 0.1N perchloric acid constitutes a large part of the total measured resistance so that the equivalent series resistance was obtained as the difference between two large numbers. This results in considerable uncertainty in the series resistance which is commuted in the calculation of the equivalent parallel resistances which were reported. In addition, it was found that in order to obtain a sufficiently accurate representation of the data, additional experimental information at frequencies at least an order of magnitude both higher and lower than the range investigated (250-10,000 cycles) was needed. Consequently, it was not possible to obtain the relaxation times of the two molecular solvent species in these primitive solutions using the resistance data available. However, the success attained in the evaluation of the relaxation times from the data on aqueous potassium iodide solutions reported by Bockris and Conway leaves little doubt that these data would be in close agreement with the values reported in Table 14.

In any event, the assumption regarding the presence of two species of solvent molecules within the compact region

of the electrical double layer each exhibiting a characteristic relaxation time is consistent with the interpretation of the temperature dependence of the "hump" phenomenon proposed by Grahame and can be used to devise a reasonable interpretation of the apparently anomalous dispersion of the apparent capacity with frequency which is also compatible with results obtained from a.c. impedance bridge experiments involving a polarizable electrode.

Interpretation of Results Obtained in the Presence of an Adsorbable Polar Organic Material in the Region of the Electrocapillary Maximum

The dependence of the differential double layer capacity on adsorbate activity and polarizing potential at a fixed temperature and frequency has already been commented upon. A quantitative representation of the results obtained in this investigation for the dispersion of the apparent capacity with frequency in the presence of adsorbable polar organic substances remains to be considered.

It was found possible to represent the results obtained for the adsorption of pentanol-1 on mercury in the region of the electrocapillary maximum by means of an extension of the dielectric relaxation theory which was used to interpret the results in the primitive solutions. The response function in the latter instance was assumed to consist of a linear

combination of contributions derived from each species of molecules present in the interface. If an adsorbable polar material is added to a solution of inert electrolyte, it will concentrate at all of the interphases which will mean the addition of a third molecular species to those already present in the compact layer at the mercury-solution interface. Since this molecule is polar in the case of pentanol-1, the dipole of the adsorbate will also tend to rotate in the presence of an alternating field and will also be associated with a characteristic relaxation time within the electrical double layer under the equilibrium conditions existing at the interface. This is the situation prevailing near the region of the electrocapillary maximum where displacement of the adsorbed molecules due to field effects is absent. The response function is now assumed to be of the form:

$$\frac{\bar{R}_o - \bar{R}}{R_o - R_\infty} = r_a^f = \Phi_1 'F(\tau_1) + \Phi_2 'F(\tau_2) + \Phi_3 'F(\tau_3) \qquad (32)$$

where r_a^f represents the response function at frequency f and adsorbate activity a and τ_3 is the relaxation time associated with the dipolar orientation of the organic adsorbate in the presence of an alternating field. The assumption is now made that the parallel capacity model for the total capacity of the electrical double layer is valid and that the capacities

arising from the presence of other (solvent) molecular species within the double layer are not effected by the addition of a third species. That is, it is assumed that $\Phi_1/\Phi_1' = a$ and $\Phi_2/\Phi_2' = a$ where Φ_1', Φ_2' and Φ_3' are the ratios of the contributions of the dielectric coefficients of each species to the total observed dielectric constant within the compact region of the electrical double layer. In this event the response function becomes

$$r_a^f = \Phi_1'/a\, F(\tau_1) + \Phi_2/a\, F(\tau_2) + \Phi_3'\, F(\tau_3) \quad . \tag{33}$$

Recalling that $\Phi_1' + \Phi_2' + \Phi_3' = 1$, the latter expression reduces to $1 - \Phi_3' = 1/a$ and,

$$r_a^f - r_o^f = \Phi_3'(F(\tau_3) - r_o^f) \quad . \tag{34}$$

At constant adsorbate activity,

$$\Phi_3' = (r_a^f - r_o^f)/(F(\tau_3) - r_o^f) = \text{constant}. \tag{35}$$

Since the actual response is known in both the presence and absence of adsorbate, a choice of τ_3 establishes $F(\tau_3)$ through Equation 24 and if τ_3 is correctly chosen to be the true relaxation time, Φ_3' will remain constant if different values of r_a^f and r_o^f are used in its computation.

A check on the self-consistency of the results can be made by observing the behavior at constant frequency

established through the use of Equation 35 thus,

$$r_a^f = \Phi_3'(F(\tau_3) - r_o^f) + r_o^f = ax + b \quad . \tag{36}$$

Therefore, a plot of r_a^f versus Φ_3' will be a straight line.

The relaxation time of pentanol-1 was determined by this procedure at a potential of 0.67 volts relative to the potential of the silver-silver chloride electrode at 25° C. The results for the best representation of τ_3 are presented in Table 15. In carrying out these computations R_∞ was evaluated by the method previously described. $\bar{R}_o$ was evaluated by noting that $F(x) \approx 1/x$ for large values of the argument (small values of the frequency) as seen from Equation 24. Consequently, substitution of this limiting form for $F(x)$ in Equation 32 gives the following expression for the response function:

$$r_a^f = \Phi_1'/x_1 + \Phi_2'/x_2 + \Phi_3'/x_3 \quad . \tag{37}$$

Introducing the definition of x_i (Equation 24) and simplifying, the following linear relationship results from which $\bar{R}_o$ can be easily established

$$\bar{R} = \bar{R}_o - bf \tag{38}$$

where b is a constant and f is the linear frequency.

The value of $_3$ is but slightly less than the relaxation times for either of the species of water molecules

Table 15. Estimation of the relaxation time of pentanol-1 $\tau_3 = 6.78 \times 10^{-4}$ sec. Quantity actually tabulated, $1/\Phi_3'$

	Frequency					
Activity	230	500	750	1000	Ave.	Φ_3'
0.075	1.420	1.013	.968	.984	1.096	.96
0.600	1.202	.984	.998	.985	1.042	.91

recorded in Table 14. This might have been anticipated since it is the hydroxyl group of the alcohol which determines the polar character of the molecule. The organic chain on the alcohol molecule might be expected to decrease the hydrogen bonding with adjacent molecules in bulk and permit a somewhat higher degree of rotational freedom for the dipole. The value for Φ_3' is consistent with the known surface coverages calculated by Minturn (17).

There exists a considerable amount of uncertainty in the value for τ_3 which is a reflection of the uncertainty involved in the evaluation of $\bar{R}_0$ and $\bar{R}_\infty$. It is now apparent that more data at both higher and lower frequencies should have been collected to permit a more accurate evaluation of the limiting responses $\bar{R}_0$ and $\bar{R}_\infty$. However, under the circumstances, a fair degree of success was obtained in representing the data which were available on the adsorption of pentanol-1 by this extension of the relaxation theory

of the compact region of the electrical double layer.

Interpretation of the Frequency Dispersion of the Apparent Capacity at the Adsorption-desorption Peaks

The effect of a strong field imposed upon the dielectric material of the compact region of the electrical double layer in the presence of an adsorbable substance depends upon the nature of the adsorbate. In the presence of a polar material such as pentanol-1 the application of a strong d.c. field results in a firm orientation of the dipoles of the adsorbate molecules in the direction of the applied field as well as a compression of the adsorbed layer due to electrostrictive forces. Ultimately a condition of dielectric saturation will be reached in which a further increase in the field will promote stress which cannot be alleviated by further polarization or compression of the organic molecules. At such a point the system may find it energetically advantageous to displace the electrically saturated dielectric material which is adsorbed at the interface with a more polarizable material. Since the dielectric constant of the (water) solvent molecules exceeds that of the alcohol, the adsorbate molecules are rejected from the compact region of the double layer and replaced by solvent molecules. The event is observed as pronounced peaks in the capacity-polarization

curves. As previously mentioned, these peaks exhibit pronounced frequency dispersion which fact has been utilized to characterize the mechanism of the adsorption-desorption process which is occurring at these electrodes.

Using a modification of the treatment proposed by Frumkin and Melik-Gaikazyan (27), diagnostic criteria which can be utilized to infer the rate controlling process in the adsorption of organic materials at the polarizable electrode in terms of the response function for the automatic recording apparatus were obtained.

Assuming that the displacement current at the potentials of the peaks is a function only of the polarizing potential, V, and the surface excess, Γ, Maxwell's equation for the displacement current may now be written in the following manner:

$$i_t = A/4\pi \, dD/dt = A/4\pi \left[\left(\partial D/\partial V \right)_\Gamma \, dV/dt + \left(\partial D/\partial \Gamma \right)_V \, d\Gamma/dt \right] = i_n + i' \quad . \tag{39}$$

In this equation i_n is the current which is normally passed by the alternate charging and discharging of the electrical double layer. The second quantity represents a supplementary current due to the adsorption process occurring at the interface. At zero frequency the surface excess is a function of the polarizing potential and adsorbate activity in the bulk solution as indicated in Equation 2. At constant

composition the supplementary current becomes

$$i' = A/4\pi(\partial D/\partial \Gamma)_v \, (\partial \Gamma/\partial V)_c \, dV/dt$$

$$= A/4\pi \, C_{\omega=0} \, dV/dt \qquad (40)$$

where $C_{\omega=0}$ represents a supplementary capacity associated with the adsorption process occurring at the interface. However, if the frequency is not zero, the surface excess depends upon the kinetics of the electrode process and, consequently, so does the supplementary current.

If diffusion is assumed to be the rate controlling mechanism of the adsorption process, the concentration of the adsorbate at the electrode interface in the presence of an alternating triangular applied potential will be obtained by solving Fick's diffusion equation

$$dC(x,t)/dt = kd^2C(x,t)/dx^2 \qquad (41)$$

subject to the boundary conditions

a. $\partial \Gamma/\partial t = kdC(0,t)/dt$

b. $C(\infty, t) = C(x,0) = C_o$

where k is the diffusion coefficient of the organic adsorbate in the solution of electrolyte selected.

The solution of Equation 41 subject to the specified boundary conditions may be obtained by the application of the

Laplace transformation. The transform of the concentration as a function of the distance from the electrode interface and variable of the transform is

$$c(x,s) = A_2 \exp(-\sqrt{s/k}\cdot x) + C_o/s \quad . \tag{42}$$

The constant of integration, A_2, can be evaluated from the boundary condition Equation 41a. Remembering that the surface excess depends only upon the potential and bulk concentration of the adsorbate at the electrode interface, Γ can be expanded to give

$$\partial\Gamma/\partial t = (\partial\Gamma/\partial V)_c \, dV/dt + (\partial\Gamma/\partial C)_V \frac{dC(0,t)}{dt} = K \frac{dC(0,t)}{dx} \quad . \tag{43}$$

Let $\alpha_o = (\partial\Gamma/\partial V)_c/(\partial\Gamma/\partial C)_V$ and introducing the Laplacian of the triangular a.c. potential given by

$$V = V_o \, \omega/\pi \, H(\pi/\omega, t) \tag{44}$$

so that

$$dV/dt = V_o \, \omega/\pi \, M(\pi/\omega, t)$$

where $M(\pi/\omega, t)$ is the well known meander function (61) results in the transform of the solution of Equation 41. Upon inversion an expression for the dependence of the adsorbate concentration on time and distance from the interface is obtained.

$$C(x,t) = -\alpha_o V_o \omega/\pi \; M(\pi/\omega, t) * \exp(ax/\sqrt{k})$$

$$\exp(a^2 t)\operatorname{erfc}(a\sqrt{t} - x/2\sqrt{kt}) + C_o \qquad (45)$$

where

$$a = \sqrt{k}/(\partial\Gamma/\partial C)_V \quad .$$

Evaluating this expression at $x = 0$ and differentiating with respect to time, one obtains

$$dC(0,t)/dt = -\alpha_o V_o \omega/\pi \exp(a^2 t)\operatorname{erfc}(a\sqrt{t}) \quad . \qquad (46)$$

Now at constant potential

$$\partial\Gamma/\partial t = (\partial\Gamma/\partial C)_V \; \partial C(0,t)/\partial t \qquad (47)$$

and

$$(\partial D/\partial\Gamma)_V = C_{\omega=o}/(\partial\Gamma/\partial V)_c \qquad (48)$$

which when substituted into Equation 40 for the supplementary current results in

$$i' = -AC_{\omega=o} V_o \omega/\pi \exp(a^2 t)\operatorname{erfc}(a\sqrt{t}) \quad . \qquad (49)$$

The additional response of the instrument which is due to the appearance of the supplementary current is obtained as before by integration of the instantaneous responses over a half period of the triangular a.c. potential.

$$\bar{R}' = \omega/\pi \int_0^{\pi/\omega} i' R_s dt \quad . \qquad (50)$$

Introducing the supplementary current into this equation results in

$$\bar{R}' = - AR_s C_{\omega=0} V_o \omega^2/\pi^2 \int_0^{\pi/\omega} \exp(a^2 t) \operatorname{erfc}(a\sqrt{t})dt. \quad (51)$$

Let $x = \sqrt{a^2 t}$, then $dt = 2xdx/a^2$ and Equation 51 for the supplementary response, $\bar{R}'$, becomes

$$\bar{R}' = - 4AR_s C_{\omega=0} V_o f/x^2 \int_0^x t \exp(t^2)\operatorname{erfc}(t)dt \quad (52)$$

where

$$x = \sqrt{a^2\pi/\omega} = \sqrt{a^2/2f} \quad .$$

The latter expression may be written in the form

$$\bar{R}'/f = - AR_s C_{\omega=0} V_o 4F_1(x)/x^2 \quad (53)$$

where

$$F_1(x) = \int_0^x t \exp(t^2)\operatorname{erfc}(t)dt \quad .$$

Hence, if the rate of the overall adsorption process is diffusion controlled, $\bar{R}'/f$ will vary with frequency in the manner prescribed by Equation 53. The variation with frequency of experimentally determined values of $\bar{R}'/f$ can then be compared to the expected values calculated on the basis of this equation to infer the kinetics of the adsorption process and are in this sense diagnostic. For convenience the following quantity is introduced:

$$\bar{r}_f = \bar{R}'/f = - AR_s C\,\omega=0\; V^{\circ}\; 4F_1(x)/x^2 \qquad (54)$$

where

$$x = \sqrt{a^2/2f} \quad .$$

If the rate of the adsorption process does not depend upon diffusion but rather upon the rate of the actual adsorption step, the response function which is attributable to this process may be obtained in a similar manner. Suppose a function ϕ is defined which represents the velocity of the actual adsorption reaction, then

$$\phi = \phi(a, \Gamma, V) = 0 \qquad (55)$$

at equilibrium. By expanding ϕ in a Taylor' series in the variables V and Γ at constant composition and noting $\phi = \partial\Gamma/\partial t$ for small departures from equilibrium

$$\partial\Gamma/\partial t = \phi = \Delta\Gamma(\partial\phi/\partial\Gamma)_{V,a} + \Delta V(\partial\phi/\partial V)_{\Gamma,a} \quad . \qquad (56)$$

Now

$$\Gamma = \Gamma_o + \Delta\Gamma \quad . \qquad (57)$$

Therefore

$$\partial\,\Delta\Gamma/\partial t = (\partial\phi/\partial\Gamma)_{V,a}\left[\Delta\Gamma - (\partial\Gamma/\partial V)_{\phi,a}\Delta V\right] . \qquad (58)$$

If $\Delta V = V_o\,\omega/\pi\; H(\pi/\omega\;, t)$ where $H(\pi/\omega\;, t)$ is the notation for the triangular function of unit amplitude and period

$2\pi/\omega$ (61) is introduced into the latter equation, the resulting differential equation can be solved by the application of the Laplace transformation to obtain an expression for the variation of the surface excess with time.

$$\Delta\Gamma = -\left(\partial\phi/\partial\Gamma\right)_V \left(\partial\Gamma/\partial V\right)_{\phi,c} V^\circ\omega/\pi\left[H(\pi/\omega,t) * \exp\left(\partial\phi/\partial t\right)_V t\right]$$

$$= -A_2 V^\circ\omega/\pi\left[H(\pi/\omega,t) * E(t)\right] \quad . \tag{59}$$

From the latter solution there readily follows

$$\partial\Gamma/\partial t = -A_2 V^\circ\omega/\pi \frac{\partial}{\partial t}\left[H(\pi/\omega,t) * E(t)\right] \quad . \tag{60}$$

Inserting this expression into Equation 39 for the supplementary current and using Equation 40, the following result is obtained for the supplementary current due to an adsorption-rate controlled mechanism.

$$i' = AC_{\omega=0}\alpha V_o \omega/\pi \; \partial/\partial t \left[H(t) * E(t)\right] \tag{61}$$

where

$$\alpha = \left(\partial\phi/\partial\Gamma\right)_V \quad .$$

The supplementary response of the instrument can also be derived in the manner previously described.

$$\bar{R}' = \frac{A\, R_s\, C_{\omega=0}\, V^o\, \omega}{\pi} \cdot \frac{\alpha\omega}{\pi} \int_0^{\pi/\omega} \frac{\partial}{\partial t} \left[H(t) * E(t) \right] dt$$

$$= 2\, f\, A\, R_s\, C_{\omega=0}\, V^o \left[1 + 2\omega/\pi\alpha \tanh \pi\alpha/2\omega \right]$$

$$= 2\, f\, A\, R_s\, C_{\omega=0}\, V^o \left[1 + 1/x \tanh x \right] \qquad (62)$$

where $x = \alpha/2f$. This expression may be rearranged to give the response function $\bar{r}_f = \bar{R}'/f$ which was introduced in Equation 54.

$$\bar{r}_f = 4AR_sC_{\omega=0}V_o\, F_2(x)/2 \quad , \qquad (63)$$

where

$$F_2(x) = 1 + 1/x \tanh x \quad . \qquad (64)$$

Hence, if the kinetics of the overall adsorption process is determined entirely by the rate of the adsorption step, the response function $\bar{r}_f$ will vary with the frequency in the manner prescribed by Equation 63. Thus,

$$\bar{r}_f = 4AR_sC_{\omega=0}\, V^o\, F_2(x)/2 \qquad (65)$$

where $x = \alpha/2f$.

Equations 54 and 65 describe two possible ways in which $\bar{r}_f$ can vary with changing frequency. It is therefore possible to distinguish between diffusion and adsorption-rate controlled mechanisms by comparing experimentally observed values of $\bar{r}_f$ with expected values of $\bar{r}_f$ computed on the basis

of these equations since in principle the parameters $C_{\omega=0}$, a,k, and α can be evaluated experimentally.

However, it is possible to construct a set of diagnostic curves based on Equations 54 and 65 for the different mechanisms which can be plotted on a reduced basis so that experimental data can be referred to them directly to ascertain the mechanism without evaluating all of the parameters indicated. It is to be noted that the argument x in Equation 54 for the case of diffusion controlled mechanisms is given by

$$x = \sqrt{a^2/2f}$$

and in Equation 65 for the case of adsorption-rate controlled processes by

$$x = \alpha/2f \quad .$$

Taking the logarithms of these arguments, one obtains

$$\log x = 1/2 \log a^2/2 + 1/2 \log 1/f$$

in the former case and

$$\log x = \log \alpha/2 + \log 1/f$$

in the latter case. If now a plot of $4F_1(x)/x^2$ as a function of the log x and $F_2(x)/2$ as function of 1/2 log x is made, both plots will be on the same reduced basis, i.e., F(x) versus 1/2 log 1/f. The effect of the parameters α and a on

this basis is merely a displacement of the curves parallel to the abscissa and may be neglected. Consequently, experimental curves of $\bar{r}_f$ as a function of 1/2 log 1/f can be referred to these theoretical curves to decide which of the proposed rate controlling mechanisms is operative.

The function $F_1(x) = \int_0^x t \exp(t^2) \operatorname{erfc}(t)dt$ was evaluated by graphical integration of a plot of $x \exp(x^2) \operatorname{erfc} x$ as a function of its argument using the tables in Crank (62) to obtain values for $\exp(x^2) \operatorname{erfc} x$ as a function of its argument. The quantity $4F_1(x)/x^2$ was then plotted as a function of log x. Similarly, $F_2(x) = (1 + 1/x \tanh x)$ was evaluated and the quantity $F_2(x)/2$ was plotted as a function of 1/2 log x. These curves which are each characteristic of a particular mechanism are presented in Figure 19.

Since the evaluation of all the parameters necessary for an exact representation of the experimental curves is very tedious, the following procedure was devised for reducing the experimental data for $\bar{r}_f$ to a single criterion which permitted a decision to be made as to which mechanism determined the kinetics of the adsorption process.

From Figure 19 the function F(x) for the adsorption rate controlled mechanism is observed to approach 0.5 asymptotically. Therefore, at no region of the curve will the ratio of F(x) at low frequencies to F(x) at high frequencies be less than 0.5. However, this ratio can become

Figure 19. Diagnostic curves for the inference of kinetic mechanisms

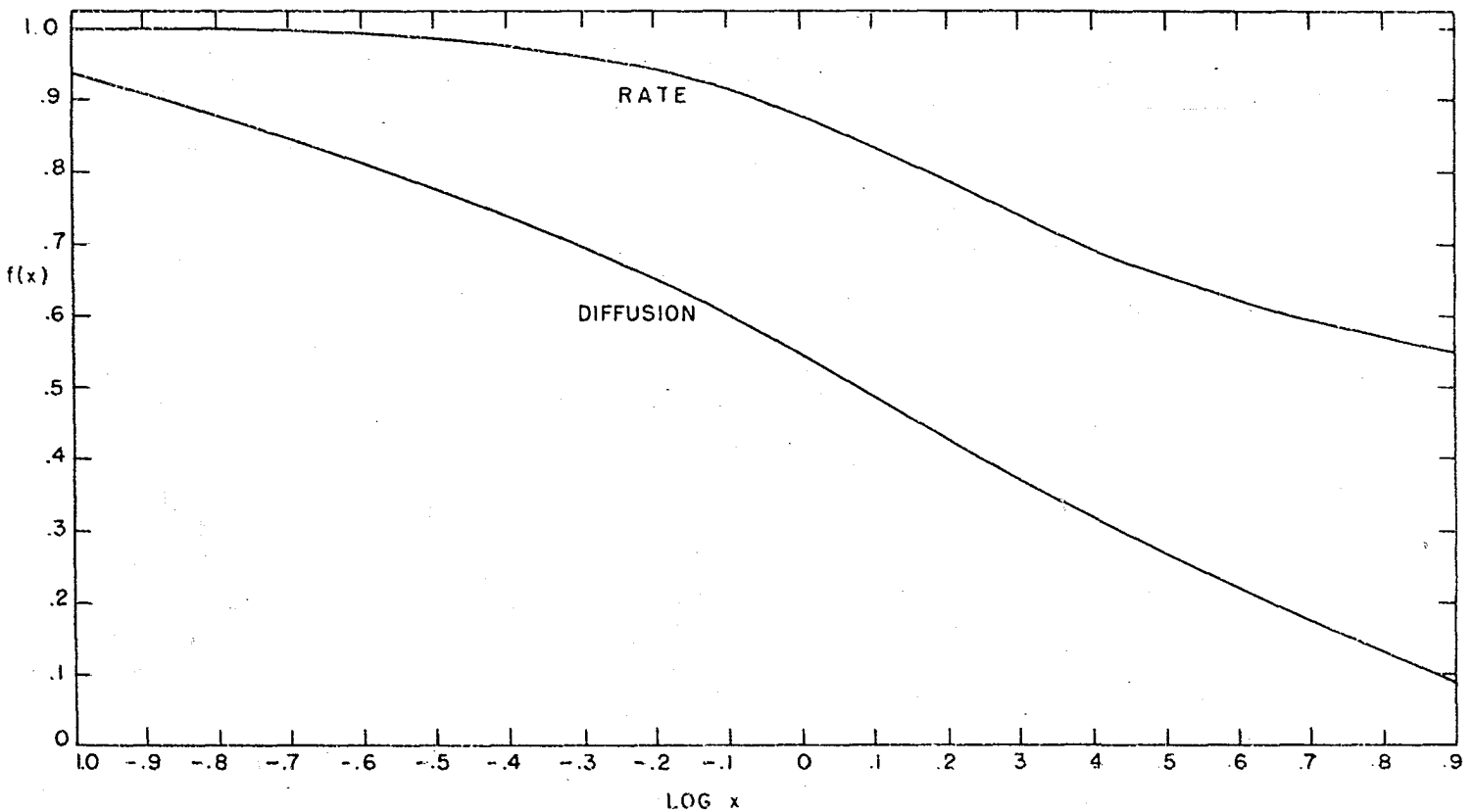
1.0
.9
.8
.7
f(x)
.6
.5
.4
.3
.2
.1
0
RATE
DIFFUSION
1.0 -.9 -.8 -.7 -.6 -.5 -.4 -.3 -.2 -.1 0 .1 .2 3 4 5 .6 .7 .8 .9
LOG x

less than 0.5 in the case of diffusion controlled mechanisms. Therefore, an observation of the quantity

$$M = \overline{r}_f/\overline{r}_{1000} = \overline{R}'/f \; /\overline{R}'_{1000}/1000 \quad f < 1000 \text{ cycles} \qquad (66)$$

should suffice to establish the rate controlling step of the overall adsorption process if it is found that M is less than 0.5 anywhere on the experimental curves.

The procedure which was used to decide which, if any, of the two proposed kinetic mechanisms was operative in determining the rate of the overall adsorption process was (1) to determine experimentally the response of the instrument which was due to the appearance of the supplementary current at a number of different frequencies, (2) compute $\overline{R}'/f$ at each of these frequencies and (3) apply the "M" test described above to determine the rate controlling mechanism.

The supplementary response, $\overline{R}'$, was obtained from the experimentally observed responses, $\overline{R}$, at the potentials of the adsorption-desorption peaks in the following fashion.

It has been shown that the adsorption isotherms describing the dependence of the surface coverage upon adsorbate concentration over the complete range of polarizing potentials are of a generalized localized Langmuir type which can be expressed in the form

$$\theta/(1 - \theta) = Ba \exp(\alpha \theta) \qquad (67)$$

where θ is the surface coverage, a the adsorbate activity, and B and α are constants. A plot of $\log \theta/1 - \theta - \alpha\theta = \log Ba$ versus θ can be used to establish θ if Ba is known. Consequently, the surface coverage as a function of the adsorbate activity can be found.

The observed response at the potentials of the adsorption peaks consists of the sum of contributions due to the normal response plus a supplementary response. That is

$$\overline{R} = \overline{R}_n + \overline{R}' \quad . \tag{68}$$

The normal response is that which would be observed at equilibrium at the peak potential in the absence of the supplementary response due to variation of the surface excess with changing potential. The normal response is given by the following expression

$$\overline{R}_n = \overline{R}_w - \theta(\overline{R}_w - \overline{R}_{mono.}) \tag{69}$$

where $\overline{R}_{mono.}$ is the normal response which is observed at monolayer coverages of the mercury interface. A plot of $\overline{R}$ as a function of θ at the electrocapillary maximum can be extrapolated to $\theta = 1$ to obtain $R_{mono.}$.

Since θ as a function of a is known and the response of the instrument in the absence of adsorbate is also known ($\overline{R}_w$), $\overline{R}_n$ can be obtained through Equation 69 and hence the supplementary response, $\overline{R}'$, as a function of the frequency

can be calculated from

$$\overline{R}' = \overline{R} - \overline{R}_n \quad . \tag{70}$$

Thus, the response function $\overline{r}_f$, can be established as a function of the frequency since

$$\overline{r}_f = \overline{R}'/f \quad . \tag{71}$$

This quantity is used to compute $M = \overline{r}_f/\overline{r}_{1000}$ which is utilized to infer the kinetics of the adsorption process by applying the test described in the previous section.

The function $f(\theta) = \log \theta/(1 - \theta) - \alpha\theta = \log Ba$ is plotted as a function of the surface coverage θ in Figure 20. This curve which is a modified adsorption isotherm for pentanol-1 was computed by using arbitrary values for the surface coverages and the necessary adsorption parameters for pentanol-1 tabulated by Hansen, Minturn and Hickson (15). The response of the instrument at monolayer coverage of the mercury interphase was obtained from a plot of the observed response at the potential of the electrocapillary maximum as a function of the surface coverage extrapolated to monolayer coverage, $\theta = 1$ (Figure 21). Values for θ at the potential of the electrocapillary maximum were obtained by using the reported value (16) for Bo for pentanol-1 to compute $f(\theta)$ for each activity which in turn establishes θ through Figure 20. The apparent surface coverages at the

Figure 20. A modified adsorption isotherm for pentanol-1

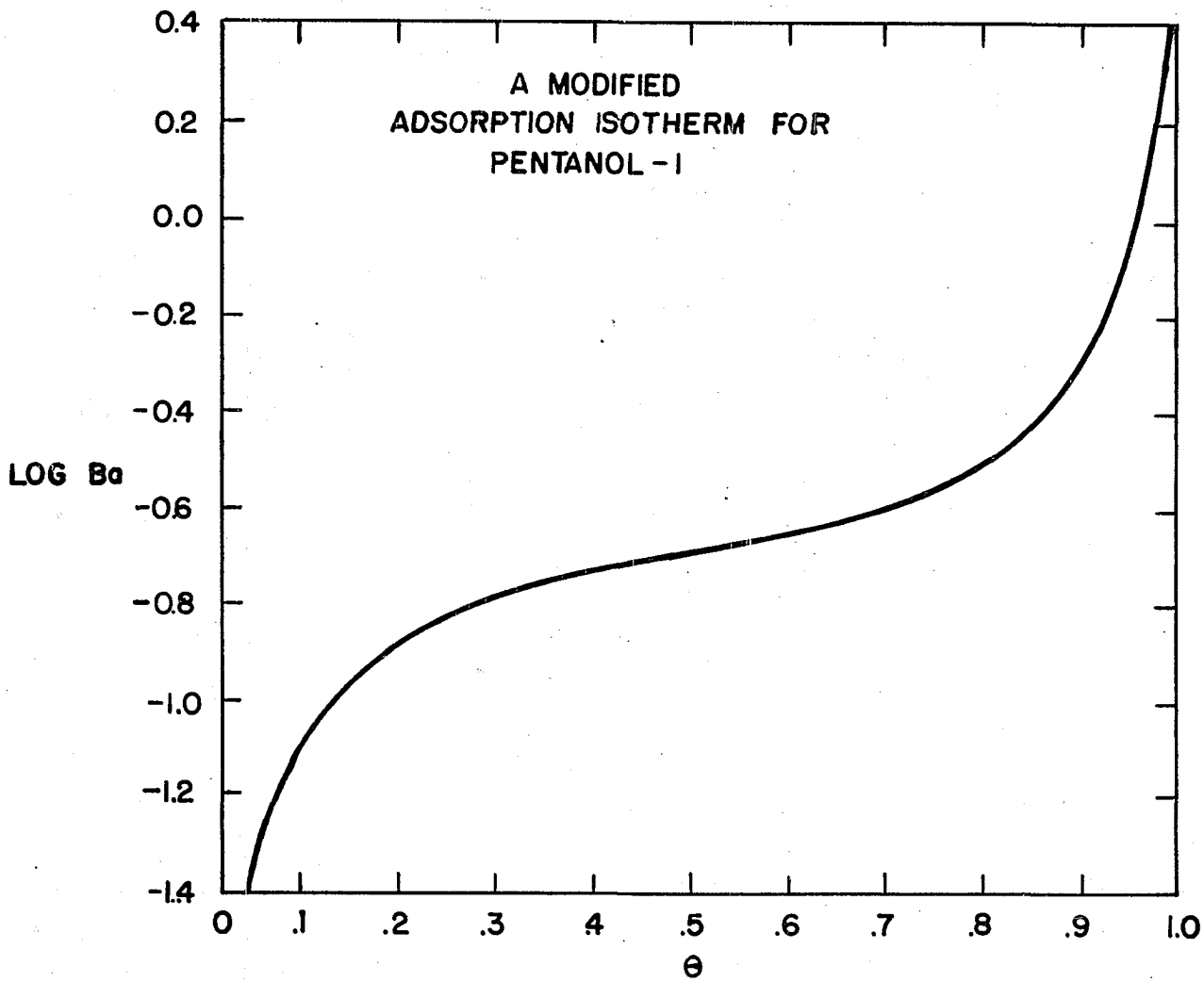
A MODIFIED
ADSORPTION ISOTHERM FOR
PENTANOL - I
LOG Ba
0.4
0.2
0.0
-0.2
-0.4
-0.6
-0.8
-1.0
-1.2
-1.4
0
.1
.2
.3
.4
.5
.6
.7
.8
.9
1.0
θ

Figure 21. The evaluation of R_{mono}.

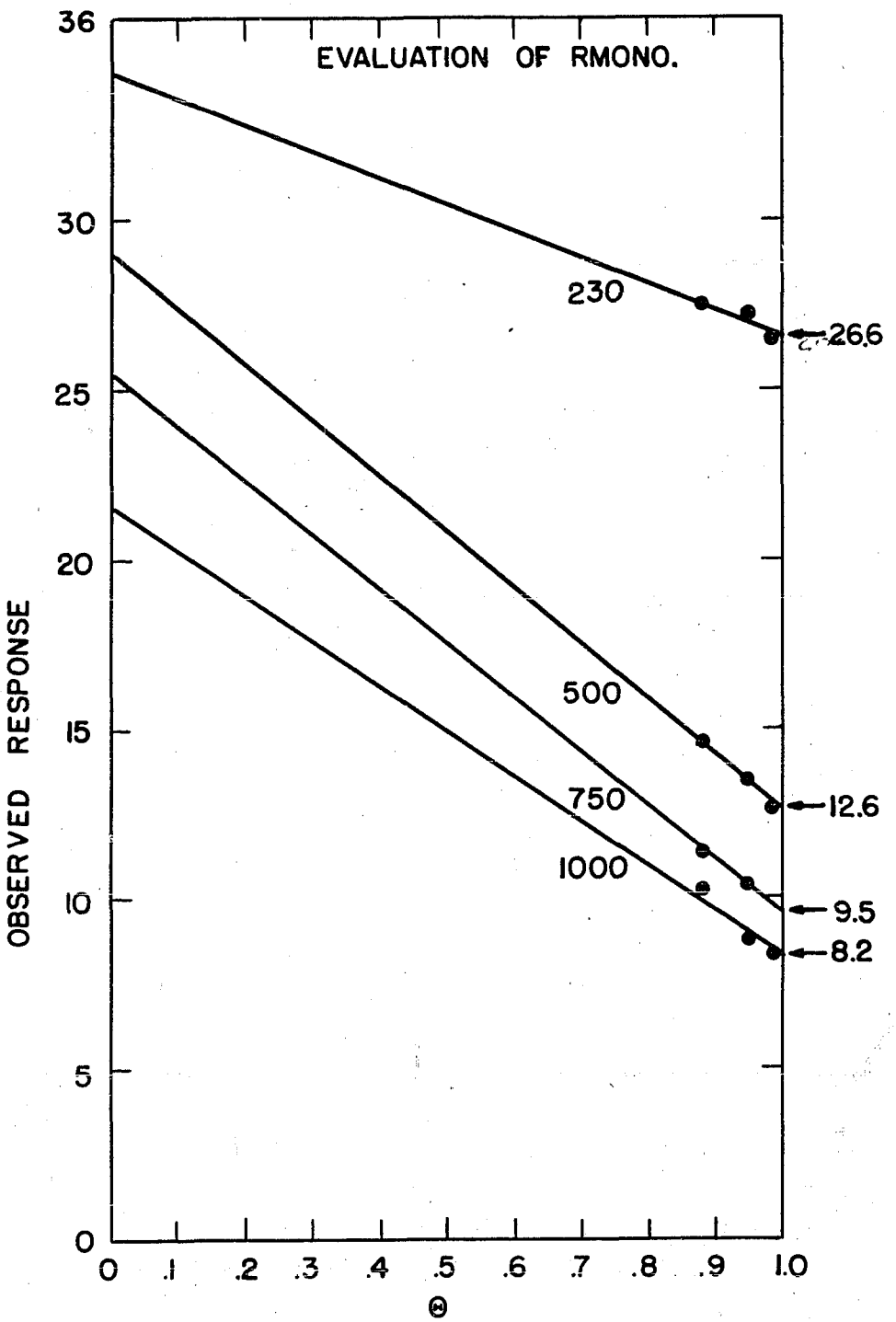
EVALUATION OF RMONO.
OBSERVED RESPONSE
Θ
230
500
750
1000
26.6
12.6
9.5
8.2
0
5
10
15
20
25
30
36
0
.1
.2
.3
.4
.5
.6
.7
.8
.9
1.0

peak potentials for each activity were obtained from the tabulated values of Ba as a function of potential reported by Minturn (17) and application of the modified adsorption isotherm, Figure 20. It was then possible to compute the test ratio, M, through the use of Equations 67, 70, 71 and 66 for pentanol-1. The results of the test are presented in Table 16 where M is tabulated as a function of the frequency and adsorbate activity for four peak potentials. Directly below the activity headings are the potentials relative to the electrocapillary maximum at which the peaks appear and the calculated surface coverages at that potential for the activity listed directly above.

Table 16. Results of the diagnostic M test for pentanol-1

	Activity			
	0.075	0.150	0.300	0.075
f	E = -0.29	E = -0.38V	E = -0.44V	E = -0.43V
	θ = 0.145	θ = 0.133	θ = 0.135	θ = 0.100
230	5.82	5.93	6.22	4.27
500	2.09	2.86	3.28	1.76
750	1.27	1.64	2.28	1.00

The observation is made that M never is less than 0.5 which by the nature of the test indicates an ambiguous result concerning the mechanism of the reaction. Attempts to fit the experimental response curves directly through the use of Equations 54 and 65 were also unsuccessful due mainly to insufficient experimental information. However, it has been demonstrated that in principle adsorption kinetics can be inferred by the method described herein and that diagnostic criteria can be derived in terms of instrument responses which are directly observable.

On the General Applicability of the Equivalent Circuit Concept

It has been demonstrated that it is possible to devise electrical analog circuits which are comprised of ideal capacitors and resistors which will actually represent the electrical properties of a real dielectric material which is polarized by a sinusoidal periodic field. In this instance it is possible to resolve the displacement current into components which can be identified with the currents flowing through the various elements of the analog circuit. However, when this concept was utilized to represent the behavior of the dielectric material within the compact region of the electrical double layer polarized by a triangular periodic field, the identification of equivalent circuit elements with

the capacity and resistance of the electrical double layer led to an apparently anomalous behavior for the differential double layer capacity with changing frequency. Only after a complete analysis of the displacement current flowing through the cell by means of classical dielectric theory was the anomaly resolved and were conditions defined under which the usual identifications were valid. In view of these results, the application of the equivalent circuit concept to the representation of the electrical properties of a dielectric material polarized by a general periodic field seems to be somewhat tenuous in character. The question is posed that if a real dielectric material is subjected to a general periodic field, will the expressions for the equivalent circuit elements depend only on the frequency or will they depend on the form of the applied periodic field?

Let the analog circuit for a capacitor filled with a real dielectric material be represented by Figure 1A and suppose the field within the dielectric material decays exponentially with time in the manner described by Equation 11. The expression for the displacement current flowing through the capacitor polarized by a general periodic field, $E(t) = E(t + 2\pi/\omega)$, can be written in the following form using Maxwell's relation Equation 9.

$$i = A/4\pi \left\{ \epsilon_\infty \, dE(t)/dt + \Delta\epsilon/\tau \exp(-t/\tau) \left[\frac{\int_0^{2\pi/\omega} dE/dx \exp(x/\tau)\,dx}{\exp\left(\frac{2\pi}{\omega\tau}\right) - 1} + \int_0^t \frac{dE}{dx} \exp(x/\tau)\,dx \right] \right\} \tag{72}$$

where

$$0 < t < 2\pi/\omega \quad .$$

Now the total current flowing through the circuit is

$$i = i_c + i_p \tag{73}$$

or

$$i = C dV(t)/dt + V/p \tag{74}$$

where V is the applied potential. Assuming the field decreases linearly with distance across the dielectric, i.e., V = El, where l is the thickness of the dielectric material, Equation 72 becomes

$$i = A/4\pi l \left\{ \epsilon_\infty \, dV(t)/dt + \frac{\Delta\epsilon}{\tau} \exp(-t/\tau) \left[\frac{\int_0^{2\pi/\omega} dV/dx \exp(x/\tau)\,dx}{\exp(2\pi/\omega\tau) - 1} + \int_0^t \frac{dV}{dt} \exp(x/\tau)\,dx \right] \right\} \tag{75}$$

where

$$o < t < 2\pi/\omega$$

and

$$i(t + 2n\pi/\omega) = i(t)$$

n = an integer.

If now the applied potential can be represented by a generalized Fourier exponential series of the form

$$V = \sum_{n=-\infty}^{\infty} B_n \exp(jn\omega t) \qquad j = \sqrt{-1}$$

then

$$dV(t)/dt = \sum_{n=-\infty}^{\infty} B_n \, jn\omega \exp(jn\omega t) \quad . \tag{76}$$

Using this relationship to evaluate the integrals in Equation 75 one finds:

$$\int_o^{2\pi/\omega} dV/dx \exp(x/\tau)dx$$

$$= \sum_{n=-\infty}^{\infty} nj\omega B_n \int_o^{2\pi/\omega} \exp(1/\tau + jn\omega)x \, dx$$

$$= \sum_{n=-\infty}^{\infty} nj\omega B_n \frac{1}{1/\tau + jn\omega} \left[\exp(1/\tau + jn\omega)x\right]_{x=o}^{x=2\pi/\omega}$$

and since $\exp(2\pi jn) = 1$,

$$\int_0^{2\pi/\omega} dV/dx \exp(x/\tau)\,dx$$

$$= \sum_{n=-\infty}^{\infty} B_n \frac{nj\omega\tau}{1 + nj\omega\tau} \left[\exp(2\pi/\omega\tau - 1)\right] \qquad (77)$$

Similarly

$$\int_0^{t} dV/dx \exp(x/\tau)\,dx$$

$$= \sum_{n=-\infty}^{\infty} B_n \frac{nj\omega\tau}{1 + nj\omega\tau} \left[\exp(1/\tau + jn\omega)t - 1\right] . \qquad (78)$$

Equation 75 for the displacement current now becomes

$$i = A/4\pi l \left\{ \epsilon_\infty\, dV/dt + \Delta\epsilon/\tau \sum_{n=-\infty}^{\infty} B_n \frac{nj\omega\tau + n^2\omega^2\tau^2}{1 + n^2\omega^2\tau^2} \exp(jn\omega t) \right\} . \qquad (79)$$

In the special case for a pure harmonic applied potential V, $B_1 = B$ and $B_n = 0$ for n unequal to one. Noting also that $Bj\omega \exp(j\omega t) = dV(t)/dt$, one obtains the following expression for the displacement current

$$i = A/4\pi l \left\{ \left(\epsilon_\infty + \frac{\Delta\epsilon}{1 + \omega^2\tau^2}\right) dV/dt + (\Delta\epsilon/\tau \quad \omega^2\tau^2/1 + \omega^2\tau^2)\, V \right\} . \qquad (80)$$

Identifying the coefficients of V and dV/dt in the last equation with the coefficients of the same terms in Equation 74

for the total current, one finds

$$C = A/4\pi l \ (\epsilon_\infty + \Delta\epsilon/1 + \omega^2\tau^2) \ ) \qquad (81)$$

and

$$p = 4\pi l/A\Delta\epsilon(1 + 1/\omega^2\tau^2) \quad . \qquad (82)$$

The latter equations are similar to those found by Debye (56).

Now the significant observation is made that it is generally impossible to make such an identification of the coefficients of V and dV/dt in Equations 74 and 79. The current is not proportional to the potential except for a phase shift but differs in form. Consequently, the conclusion is reached that unless the applied field is a pure harmonic in form, an equivalent circuit does not exist which will represent the electrical properties of a real dielectric material.

Recently several investigations of the capacity of the electrical double layer at various polarizable metal electrodes have been reported which utilize a multisweep voltammetric measuring technique (44). The tendency to use the equivalent circuit concept to represent the electrical properties of the electrical double layer is very prevalent. However, one must conclude from the foregoing arguments that the equivalent circuit concept is rigidly applicable only if the form of the applied periodic field is a pure harmonic.

Otherwise, the only way in which information about the electrical double layer can be obtained is to conduct a complete analysis of the displacement current using Maxwell's relation for the displacement current and classical dielectric theory. This point has not been fully appreciated in the past by many investigators in this field.

SUMMARY

An investigation of the dependence of the impedance of the electrical double layer at a mercury-electrolytic solution interface upon polarization, frequency, temperature and concentration of an adsorbable organic compound (pentanol-1) was conducted and the possibilities for inferring adsorption parameters from such measurements were considered.

In order to facilitate the investigation of adsorption phenomena by means if differential double layer capacitance measurements, an automatic impedance recording instrument was designed and constructed and the theory of the instrument response was developed. An unexpected frequency dispersion of the apparent capacity of the electrical double layer was observed experimentally at mercury-aqueous perchloric acid solution interfaces.

A theory of dielectric relaxation in the electrical double layer was proposed to account for this observed frequency dispersion of the double layer impedance. The assumption of two molecular species of solvent molecules within the compact region of the double layer was demonstrated to be sufficient to explain this behavior. Each of these molecular species was associated with a particular relaxation time which were found to be approximately 10^{-3} and 10^{-4} seconds, respectively, for the "bound" and "free" species of water molecules in the compact region of the

double layer. Using these values of the relaxation times, the observed frequency dispersion of the apparent capacity was quantitatively represented. Results of a similar study of double layer impedance measurements conducted on the mercury-aqueous potassium iodide solution interface reported by Bockris and Conway can be correlated by a similar treatment. It was also demonstrated that the effect of temperature upon the properties of the compact region of the electrical double layer can also be interpreted on this basis.

It was shown that the frequency dispersion of the double layer impedance in the presence of a capillary-active material in the neighborhood of the electrocapillary maximum can also be represented by an extension of the theory of dielectric relaxation within the electrical double layer. The relaxation time of adsorbed pentanol-1 molecules was found to be approximately 6.78×10^{-4} sec. Dielectric changes due to the concentration of adsorbate at the interface necessary for a representation of the data were correlated with the observed surface coverages obtained from equilibrium adsorption experiments and were found to be physically reasonable.

The pronounced frequency dispersion of the apparent capacity at high polarizations in the presence of adsorbable materials was discussed in the light of a kinetic treatment of adsorption processes proposed by Frumkin and Melik-Gaikazyan. Diagnostic criteria representative of various

rate controlling mechanisms were derived in terms of the instrument response and were applied to the inference of the rate controlling mechanism in the adsorption of pentanol-1. The criteria proved not to be definitive for resolving the kinetic mechanism of adsorption from results obtained in this work.

Conditions are discussed under which the electrical properties of the electrical double layer at a polarizable electrode interphase can be represented by an equivalent analog circuit. The equivalent circuit concept was found to be applicable only if the applied periodic field is a pure harmonic.

BIBLIOGRAPHY

1. Mackor, E. L. "Properties of the Electrical Double Layer," D. B. Centen's Uitgevers-Maatschappij N.V., Amsterdam (1951).

2. Woody, R. W. The Inference of Adsorption from Electrokinetic Data, Unpublished report. U.S. Atomic Energy Commission, Ames Laboratory, Ames Laboratory Document Library, Ames, Iowa (1958).

3. Grahame, D. C. Chem. Rev., 41, 441 (1947).

4. Parsons, R. Thermodynamics of Adsorption in Ionic Systems. In Symposium on Charge Transfer Processes, Toronto, Canada, Sept. 4-5, 1958. Paper No. 23. Chem. Inst. of Can., Phys. Chem. Div., (Ottawa, Canada.) (1958).

5. Blomgren, E. and Bockris, J. O'M. Adsorption of Organic Substances at the Mercury-Solution Interface. Ibid., Paper No. 25 (1958).

6. Los, J. M. and Tompkins, C. K. Adsorption of Methylene Blue on a Positively Charged Mercury Surface. Ibid., Paper No. 26 (1958).

7. Hansen, R. S. and Hickson, D. A. Adsorption Kinetics from Double-Layer Capacitance Measurements. Ibid., Paper No. 24 (1958).

8. Frumkin, A. and Melik-Gaikazyan, V. I. Zhur. Fix. Khim., 26, 560 (1952). (Original available in Russian. Privately translated from the Russian by E. Jarvesoo and edited by D. C. Grahame, Dept. of Chem., Amherst College, Amherst, Massachusetts. 1954).

9. Gouy, G. Ann. Chim. Phys., 29, 145 (1903).

10. Butler, J. A. V. "Electrocapillarity", Chemical Publishing Co., Inc., New York (1951).

11. Butler J. A. V. "Electrical Phenomena at Interfaces", Macmillan Co., New York (1954).

12. Bockris, J. O'M. "Modern Aspects of Electrochemistry", Academic Press, New York (1954).

13. Kruyt, H. R. "Colloid Science", Vol. 1, Elsevier Publishing Co., Amsterdam (1952).

14. Frumkin, A. Z. Physik, 35, 792 (1926).

15. Hansen, R. S., Minturn, R. E. and Hickson, D. A. J. Phys. Chem., 60, 1185 (1956).

16. _____, _____, _____. Ibid., 61, 953 (1957).

17. Minturn, R. E. The Inference of Adsorption from Differential Capacity Studies. Unpublished Ph.D. Thesis. Iowa State College Library, Ames, Iowa (1955).

18. Melik-Gaikazyan, V. I. Zhur. Fiz. Khim., 26, 1184 (1952). (Original available in Russian. Privately translated from the Russian by E. Jarvesoo and edited by D. C. Grahame, Dept. of Chem., Amherst College, Amherst, Massachusetts. 1953).

19. Laitenen, H. A. and Mosier, B. J. Am. Chem. Soc., 80, 2363 (1958).

20. Loveland, J. West and Elving, P. J. J. Phys. Chem., 56, 250 (1952).

21. _____, _____. Ibid., 56, 255 (1952).

22. _____, _____. Ibid., 56, 935 (1952.

23. _____, _____. Ibid., 56, 941 (1952).

24. _____, _____. Ibid., 56, 945 (1952).

25. _____, _____. Chem. Rev., 51, 67 (1952).

26. Breyer, B. and Hacobian, S. Aust. J. Sci. Res., A5, 500 (1952).

27. Frumkin, A. and Melik-Gaikazyan, V. I. Doklady Akad. Nauk. USSR. 77, 855 (1951). (Original not available. Privately translated from the Russian and distributed by the Department of Chemistry, Amherst College, Amherst, Massachusetts.)

28. Grahame, D. C. J. Am. Chem. Soc., 68, 301 (1946).

29. Lorentz, W. Z. Electrochem., 62, 192 (1958).

30. Lorentz, W. and Mockels, F., Ibid., 60, 507 (1956).

31. Delahay, P. and Trachenberg, I. J. Am. Chem. Soc., 71, 2355 (1957).

32. _____, _____. Ibid., 80, 2094 (1958).

33. _____ and Berzins, T. J. Phys. Chem., 59, 906 (1955).

34. Grahame, D. C. J. Am. Chem. Soc., 71, 2975 (1949).

35. _____. J. Phys. Chem., 61, 701 (1957).

36. Bowden, F. P. and Grew, K. E. W. Disc. Faraday Soc., 1, 86 (1947).

37. _____, _____. Ibid., 1, 91 (1947).

38. Hackerman, N. and Brodd, R. J. Capacity of the Electrical Double Layer at Metal Electrodes, Tech. Report to the Office of Naval Research Contract Nonr - 375(02) (University of Texas, Austin, Texas.) (Office of Naval Research, Washington, D.C.) August 30, 1955.

39. Hansen, R. S. and Clampitt, B. H. J. Phys. Chem., 58, 908 (1954).

40. Kolthoff, I. M. and Lingane, J. J. "Polarography", 2nd ed. Vol. 1, Interscience Publishers, New York. (1952).

41. Laitenen, H. A. Ann. Rev. Phys. Chem., 1, 309 (1950).

42. Grahame, D. C. Ibid., 6, 337 (1956).

43. Delahay, P. Ibid., 7, 229 (1957).

44. _____. "New Instrumental Methods in Electrochemistry", Interscience Publishers, Inc., New York (1954).

45. Sevcik, A. Coll. Czechoslov. Chem. Comm., 13, 349 (1948).

46. Barker, G. C. and Gardner, A. W. Square-Wave Polarography. Part 5. Organic Adsorption-Desorption Waves. Atomic Energy Research Establishment, C/R 1606, Harwell, Berkshire, England. (1957).

47. Breyer, B. and Gutmann, F. Disc. Faraday Soc., 1, 19 (1947).

48. Doss, K. S. G. and Kalyanasundarum, A. Indian Acad. Sci., Proc., 35A, 27 (1952).

49. Randles, J. E. B. Disc. Faraday Soc., 1, 11 (1947).

50. Kruger, F. Z. Physik. Chem. 45, 1 (1903).

51. Lange, N. A. "Handbook of Chemistry", 8th ed. Handbook Publishers, Sandusky, Ohio. (1952).

52. Delahay, P. and Berzins, T. J. Am. Chem. Soc., 77, 6448 (1955).

53. Hague, B. "Alternating Current Bridge Methods". 5th ed. Sir Isaac Pitman and Sons, Ltd., London (1943).

54. Kortüm, G. and Bockris, J. O'M. "Textbook of Electrochemistry", Vol. 2. Elsevier Publishing Co., London (1951).

55. Fröhlich, H. "Theory of Dielectrics", Clarendon Press, Oxford (1949).

56. Debye, P. "Polar Molecules", Dover Publications, Inc. New York. (1929).

57. Grahame, D. C. J. Chem. Phys., 23, 1725 (1955).

58. _____. J. Am. Chem. Soc., 79, 2093 (1957).

59. Bockris, J. O'M. and Conway, B. E. J. Chem. Phys., 28, 707 (1958).

60. Cole, K. S. and Cole, R. H. J. Chem. Phys., 9, 341 (1941).

61. Churchill, R. V. "Modern Operational Mathematics in Engineering", McGraw-Hill Book Co., Inc. New York (1944).

62. Crank, J. "The Mathematics of Diffusion", Clarendon Press, Oxford. (1956).

ACKNOWLEDGMENTS

To Dr. R. S. Hansen the author would like to express his heartfelt appreciation for the patience, guidance and immense assistance he has freely offered during the course of this investigation. His tremendous insight, perception and ability to solve some of the more difficult problems which arose were gratifying to observe.

The author would also like to acknowledge the assistance and suggestions of Mr. William Burkhard and the members of the electronic instrumentation group of the Ames Laboratory rendered in designing and constructing some of the electronic apparatus. To the many friends who encouraged and assisted the author in concluding this work successfully, many thanks.

APPENDIX

The Response of the Automatic Impedance Recording Instrument to an Applied Generalized Periodic Input Potential

Assuming the equivalent circuit of Figure 1E represents the impedance of the electrolytic cell containing an ideally polarizable electrode, the application of a periodic potential, V_s, across the terminals AB will result in a current flowing in the circuit. This current will generate a potential across the resistor, R, which determines the magnitude of the measured response of the automatic impedance recording instrument. The form and magnitude of this current will depend upon the magnitude of the circuit elements and upon the form and magnitude of the applied periodic potential. For the circuit under consideration, it is possible to derive an expression for the measured response in terms of a general periodic applied potential.

Let $V_s(t) = V_s(t + 2\pi/\omega)$ be the general periodic potential applied across the terminals of the circuit in Figure 1E. From Kirchhoff's loop rule, one obtains

$$V_s = V_c + i_t R \qquad (A.1)$$

where V_c is the potential drop across the parallel part of the circuit and i_t is the total current flowing through the

circuit. If $dQ_c(t)/dt$ and $dQ_p(t)/dt$ are the currents flowing through the capacitor, C, and the resistance, p, respectively, the total current, i_t, becomes

$$i_t = dQ_c(t)/dt + dQ_p(t)/dt \quad . \tag{A.2}$$

Now

$$V_c = Q_c(t)/C = p\, dQ_p(t)/dt \tag{A.3}$$

which when substituted into Equation A.1 results in the following boundary value problem:

$$d^2Q_p(t)/dt^2 + (p + R)/pRC\ dQ_p(t)/dt = V_s(t)/pRC \tag{A.4}$$

subject to

a. $dQ_p(0)/dt = 0$

b. $V_s(t) = V_s(t + 2\pi/\omega)$.

Let $a = 1/pRC$ and $b = -(p + R)$.

$v_s(s)$ = Laplace transform of $V_s(t)$

$q_p(s)$ = Laplace transform of $Q_p(t)$,

then the transform of Equation A.4 becomes

$$a\, v_s(s) = sq_p(s) - dQ_p(0)/dt - abq_s(s)$$

$$= q_s(s)(s - ab)$$

so that

$$q_s(s) = av_s(s)/(s - ab) \quad .$$

Inverting the transform,

$$dQ_p(t)/dt = aV_s(t) * \exp(abt)$$
$$= a\int_o^{\tau} \exp\left[ab(t - \tau)\right] \cdot V_s(\tau)\, d\tau. \quad (A.5)$$

Let $r = -ab = (p + R)/pRC$, then

$$dQ_p(t)/dt = a \exp(-rt) \int_o^t \exp(r\tau) V_s(\tau) d\tau . \quad (A.6)$$

Suppose

$$F(t) = \exp(-rt) \int_o^t \exp(r\tau)\, V_s(\tau)\, d\tau$$

and $t = \delta + 2n\pi/\omega$, one can now write

$$\exp(rt)\, F(t) = \int_o^t \exp(r\tau)\, V_s(\pi/\omega\ , \tau)\, d\tau$$
$$= \int_o^{2n\pi/\omega} \exp(r\tau)\, V_s(\pi/\omega, \tau)\, d\tau + \int_{2n\pi/\omega}^{\frac{2n\pi}{\omega}+\delta} \exp(r\tau)\, V_s$$
$$(\pi/\omega\ , \tau)\, d\tau = \sum_{j=o}^{n-1} \int_{2j\pi/\omega}^{\frac{2(j+1)\pi}{\omega}} \exp(r\tau)\, V_s(\pi/\omega\ , \tau)\, d\tau$$
$$+ \int_{2n\pi/\omega}^{2n\pi/\omega\ +\delta} \exp(r\tau)\, V_s(\pi/\omega\ , \tau)\, d\tau$$
$$= \sum_{j=o}^{n-1} I_j + \int_{2n\pi/\omega}^{2n\pi/\omega\ +\delta} \exp(r\tau)\, V_s(\pi/\omega\ , \tau)\, d\tau \quad (A.7)$$

where

$$I_j = \int_{2j\pi/\omega}^{2(j+1)\pi/\omega} \exp(r\tau)\, V_s(\pi/\omega\ ,\tau)\, d\tau . \qquad (A.8)$$

Let the following substitution be made in Equation A.8:

$$x = \tau - 2j\pi/\omega$$

$$dx = d\tau$$

$$= 2j\pi/\omega \text{ which implies } x = 0$$

$$= 2(j+1)\pi/\omega \text{ which implies } x = 2\pi/\omega$$

then

$$I_j = \exp(2j\pi r/\omega) \int_0^{2\pi/\omega} \exp(rx)\, V_s(\pi/\omega\ ,x)\, dx \qquad (A.9)$$

using the periodic property $V_s(t) = V_s(t + 2\pi/\omega)$. The integral in the last expression does not depend on the period. Consequently, one can write

$$\sum_{j=o}^{n=1} I_j = \int_o^{2\pi/\omega} \exp(rx)\, V_s(\pi/\omega\ ,x)dx \cdot \sum_{j=o}^{n-1} \exp(2j\pi r/\omega)$$

$$= \frac{(\exp(2n\pi r/\omega) - 1)}{(\exp(2\pi r/\omega) - 1)} \int_o^{2\pi/\omega} \exp(rx)\, V_s(\pi/\omega, x)dx \quad . \qquad (A.10)$$

To evaluate the second integral of Equation A.7, let

$$x = \tau - 2n\pi/\omega$$

$$dx = d\tau$$

$\tau = 2n\pi/\omega$ which implies $x = 0$

$\tau = 2n\pi/\omega + \delta$ which implies $x = \delta$

from which follows

$$\int_{2n\pi/\omega}^{2n\pi/\omega + \delta} \exp(r\tau)\, V_s(\pi/\omega, \tau)\, d\tau$$

$$= \exp(2n\pi r/\omega) \int_0^{\delta} \exp(rx)\, V_s(\pi/\omega, x)\, dx \quad . \qquad (A.11)$$

Assembling the last two results in Equation A.7 and dividing by exp(rt), the expression for the current flowing through the shunting resistance, p, becomes

$$dQ_p(t)/dt = aF(t)$$

$$= a \exp(2n\pi r/\omega - tr) \left\{ \left[\frac{1 - \exp(-2n\pi r/\omega)}{(\exp(2\pi r/\omega) - 1)} \right] \right.$$

$$\int_0^{2\pi/\omega} \exp(rx)\, V_s(\pi/\omega, x)\, dx$$

$$\left. + \int_0^{\delta} \exp(rx)\, V_s(\pi/\omega, x)\, dx \right\} \quad . \qquad (A.12)$$

Since the steady state current is desired, terms of the order $\exp(-2n\pi r/\omega)$ can be neglected for they are transients resulting from the initiation of the measurement and rapidly decay to zero. The steady state current now becomes

$$dQ_p(t)/dt = a \exp(-tr) \left[(\exp(2\pi r/\omega) - 1)^{-1} \int_0^{2\pi/\omega} \exp(rx)\, V_s(\pi/\omega, x)\, dx + \int_0^{t} \exp(rx)\, V_s(\pi/\omega, x)\, dx \right] \qquad (A.13)$$

where

$$0 < t < 2\pi/\omega \quad .$$

With the aid of Equation A.3 $Q_c(t)$ can be found and, hence, $dQ_c(t)/dt$.

$$dQ_c(t)/dt = pC\, d^2Q_p(t)/dt^2 = pCa\, dF(t)/dt \quad . \qquad (A.14)$$

Therefore, the total current flowing in the circuit can be found.

$$dQ_t(t)/dt = dQ_p(t)/dt + dQ_c(t)/dt = aF(t) + pC\, dF(t)/dt \qquad (A.15)$$

where

$$Q_t(t) = Q_t(t + 2\pi/\omega) \quad .$$

The instrument response depends on the magnitude of the potential which is developed across the series resistance, R, by the passage of the current given by the last equation. Actually, in the experimental arrangement used in this

investigation, this potential was converted into a d.c. output potential which was used to drive the recording instrument by means by a half-wave rectifier. Therefore, the response becomes

$$\overline{R} = \omega/\pi \int_{x=2n\pi/\omega}^{x=(2n+1)\pi/\omega} R \cdot i_t(x)\, dx \qquad (A.16)$$

which may be written

$$\overline{R} = \omega R/\pi \int_o^{\pi/\omega} i_t(t)dt$$

$$= \omega R \ /\pi \int_o^{\pi/\omega} F(t)dt$$

$$+ \frac{\omega R \quad p\ C}{\pi} \int_o^{\pi/\omega} \frac{d\ F(t)}{dt} \quad dt \qquad (A.17)$$

where

$$o < t < 2\pi/\omega \quad .$$

For the special case in which $V_s(t)$ is a periodic triangular potential given by $V^o \omega/\pi\ H(2\pi/\omega\ ,t)$ where $H(2\pi/\omega\ ,t)$ is the notation for a triangular function of unit amplitude and period $2\pi/\omega$, the total current given by Equation A.15 is

$$i_t = V^o\ \omega/\pi\ pRC/(p + R)^2 \left\{ (p + R)/pRC\ t + p/R \left[1 - \frac{2 \exp\left(-\frac{(P + R)t}{P\ R\ C}\right)}{1 + \exp - (P + R)\pi/\omega pRC} \right] \right\} \qquad (A.16)$$

from which the response is readily obtained from Equation A.17 and found to be

$$\bar{R} = V^{o}R/2(p + R) \left\{ 1 - \left[1/x - 1/x^{2} \tanh(x) \right] p/R \right\} \qquad A.18$$

where $x = (p + R)/2\omega pRC$.